The molecular dissection of the regulation of PGC-1α and the genome-wide activity of its transcriptional network in skeletal muscle cells

Inauguraldissertation

zur
Erlangung der Würde eines Doktors der Philosophie
vorgelegt der
Philosophisch-Naturwissenschaftlichen Fakultät
der Universität Basel

von

Mario Barešić
aus Kroatien / Schweiz (Schwyz SZ)

Basel, 2013

Genehmigt von der Philosophisch-Naturwissenschaftlichen Fakultät
auf Antrag von

Prof. Dr. Christoph Handschin und Prof. Dr. Markus A. Rüegg

Basel, den 12.11.2013

Prof. Dr. Jörg Schibler, Dekan

TABLE OF CONTENTS

ABBREVIATIONS

α-MSH	α-melanocyte stimulating hormone
β2-AR	β2-adrenergic receptor
cAMP	Cyclic adenosine monophosphate
AC	Adenylate cyclase
Akt (PKB)	Protein kinase B
AMP	Adenosine monophosphate
AMPK	AMP activated protein kinase
AP-1	Activator protein 1
AREs	Antioxidant response elements
ATP	Adenosine triphosphate
ATF-2	Activating transcription factor-2
BAF60a (SMARCD1)	BRG1-associated factor 60a
b.w.	Body weight
CaMKIV	Calcium /calmodulin-dependent protein kinase IV
cAMP	Cyclic adenosine monophosphate
cAMP-GEFs	cAMP-regulated guanine nucleotide exchange factors
CBP	cAMP response element binding protein-binding protein
Cdc4	Cell division control protein 4
CEBPB	CCAAT/enhancer-binding protein beta
cGMP	Cyclic guanosine monophosphate
ChIP	Chromatin immunoprecipitation
ChIP-on-chip	ChIP combined with arrays (chip)
ChIP-Seq	ChIP Sequencing
Clk2	Cdc2-like kinase 2
CnA	Calcineurin A
CREB	cAMP response element binding protein
ELAND	Efficient Large-Scale Alignment of Nucleotide Databases
eNOS	Endothelial nitric oxide synthase
Epac	Exchange proteins activated by cAMP
ERRα	Estrogen-related receptor α
ERRβ	Estrogen-related receptor β
ERRγ	Estrogen-related receptor γ
FDR	False discovery rate
FoxO1	Forkhead box protein O1
FXR	Farnesoid X receptor

GABA	γ-aminobutyric acid
Gabp	GA-binding protein
GCN5	General Control Non-repressed Protein 5
GLUT4	Glucose transporter 4
GPCR	G-protein coupled receptor
GPx1	Glutathione peroxidase 1
GR	Glucocorticoid receptor
GSK3β	Glycogen synthase kinase 3β
HAT	Histone acetyltransferase
HepG2	Human liver carcinoma cell-line
HIF	Hypoxia inducible factor
HNF4α	Hepatocyte nuclear factor 4
HSF1	Heat shock factor 1
kb	Kilobases
LXR	Liver X receptor
MACS	Model-based Analysis of ChIP-Seq
MAPK	Mitogen-activated protein kinase
MAQ	Mapping and Assembly with Quality
MARA	Motif activity response analysis
MEF	Myocyte enhancer factor
MEF2C	Myocyte enhancer factor 2C
mRNA	Messenger RNA (ribonucleic acid)
mTOR	Mammalian target of rapamycin
mtTFA	Mitochondrial transcription factor A
NAD+/NADH	Nicotinamide adenine dinucleotide
Nfe2l2	Nuclear factor erythroid 2-like 2
NMJ	Neuromuscular junction
NO	Nitric oxide
NRF-1	Nuclear respiratory factor-1
NRF-2	Nuclear respiratory factor-2
NT-PGC-1α	N-truncated PGC-1α
O-GlcNAc	O-lnked β-N-acetylglucosamine
OGT	O-lnked β-N-acetylglucosamine transferase
OXPHOS	Oxidative phosphorylation
$p160^{MBP}$	p160 myb binding protein
PARIS	Parkin interacting substrate
PCA	Principal component analysis

PDE	Phosphodiesterase
PGC-1α	Peroxisome proliferator-activated receptor γ coactivator 1α
PGC-1α-/-	PGC-1α gene knockout
PGC-1β	Peroxisome proliferator-activated receptor γ coactivator 1β
PKA	Protein kinase A
PPAR-α	Peroxisome proliferator-activated receptor α
PPAR-γ	Peroxisome proliferator-activated receptor γ
PRC	PGC-related coactivator
PRMT1	Protein arginine methyltransferase 1
Prox1	Prospero-related homeobox 1
RIP140	Receptor-interacting protein 140
RNF34	Ring-finger-containing protein 34
ROS	Reactive oxygen species
SHP	Small heterodimer partner
SCF	Skp1/Cullin/F-box
SCFCdc4	Skp1/Cullin/F-box - cell division control protein 4
SENP1	Sentrin/SUMO-specific protease 1
Sir2	Silent mating type information regulation 2
SIRT1	Silent mating type information regulation 2 homolog 1
SOD2	Superoxide dismutase 2
Sox9	SRY-related high mobility group-Box gene 9
Sp1	Specificity protein 1
SRC-1	Steroid receptor coactivator-1
Srxn1	Sulfiredoxin 1
SUMO	Small ubiquitin-like modifier
SWI/SNF	SWitch/Sucrose NonFermentable
TES	Transcription end site
TRAP/DRIP	Thyroid hormone receptor-associated protein/vitamin D receptor interacting protein
TSS	Transcription start site
TFBS	Transcription factor binding site
UCP1	Uncoupling protein 1
UV	Ultraviolet
VEGF	Vascular endothelial growth factor
Vmax	Maximal reaction rate

ABSTRACT

The transcriptional coactivator peroxisome proliferator-activated receptor γ coactivator 1α (PGC-1α) is a potent inducer of mitochondrial biogenesis and oxidative metabolism. Highest expression levels of PGC-1α are found in tissues with high energy demands like brain, skeletal muscle, heart, brown adipose tissue and kidney. In these tissues, PGC-1α can be induced by metabolic stress, like cold in brown fat, exercise in skeletal muscle or fasting in liver. Once activated, PGC-1α regulates the activity of transcription factors and is thus capable of inducing entire biological programs like mitochondrial biogenesis, fatty acid oxidation, angiogenesis or gluconeogenesis. PGC-1α does not possess an intrinsic histone acetylase activity (HAT), but instead binds proteins with HAT activity and recruits them to the site of transcription. Similarly, PGC-1α binds the mediator and to the SWI/SNF complexes and thereby serves as a platform to connect the transcription factors with transcription initiation complex, chromatin remodelling complex and proteins with HAT activity. Therefore, PGC-1α senses extracellular stimuli and metabolic stress and connects these events with gene transcription. In skeletal muscle, basically all pathways triggered by exercise at some point converge at PGC-1α and change the expression of *Ppargc1a* transcripts or stabilize the PGC-1α protein through posttranslational modifications. When expressed in skeletal muscle, PGC-1α induces mitochondrial biogenesis, glucose uptake, promotes angiogenesis, protects skeletal muscle from atrophy and leads to a muscle fibre type switch towards more oxidative fibres. Thus, PGC-1α acts as a master regulator of exercise-induced adaptations in skeletal muscle.

Some key transcription factors mediating these PGC-1α induced changes like ERRα, NRF-1 and MEF2C have been identified. However, a profound knowledge about the transcriptional network of transcription factors and other proteins mediating PGC-1α gene regulation is still missing. To reveal this transcriptional network and to be able to draw general conclusions about the role of PGC-1α as a coactivator, we have investigated the activity of PGC-1α on genome-wide scale. By combining ChIP-Seq studies with expression arrays, we have identified all interactions of PGC-1α with the genome in cultured skeletal muscle cells and gained knowledge about how PGC-1α regulates gene expression. PGC-1α induced expression of genes involved in oxidative metabolism and suppressed the expression of inflammatory response genes. Surprisingly, the induction of gene expression by PGC-1α was not only directly by binding to transcription factors in promoters, but also indirectly, without the need for PGC-1α to be present at the promoters of some induced genes. Inversely, the suppression of inflammatory genes was almost exclusively indirect because it did not require the recruitment of PGC-1α to the promoters of suppressed genes, indicating that PGC-1α does not act as a corepressor in skeletal muscle cells. We identified ERRα as a major mediator of PGC-1α induced gene expression. By performing ChIP-sequencing of ERRα, we have found that ERRα can be transcriptionally active and regulate gene expression with and without PGC-1α. In addition to ERRα, we predict several other transcription factors to cooperate with PGC-1α and directly regulate gene expression. By knocking

down some of these transcription factors, we validated our predictions and showed that these transcription factors are involved in the transcription of a subset of PGC-1α target genes. These results suggest that PGC-1α coactivates the transcription factor complex AP-1 to regulate the expression of genes involved in the response to hypoxia. Last, even though the inhibition of phosphodiesterases PDE1 and PDE4 led to induction of *Ppargc1a* expression in cultured skeletal muscle cells, this effect could not be shown *in vivo*. Because the activation of β2-AR signaling strongly induced *Ppargc1a* expression in skeletal muscle *in vivo*, the involvement of cAMP in the regulation of *Ppargc1a* expression is very likely. Therefore the involvement of other cAMP-specific PDEs in this regulation cannot be excluded.

In conclusion, in this thesis, we describe how the transcriptional coactivator PGC-1α controls gene expression in cultured skeletal muscle cells on a genome-wide scale. We identified and validated some key transcription factors as members of the PGC-1α transcriptional network. The large amount of data generated in this study and our predictions could serve as a starting point for future projects that aim to study PGC-1α.

1 GENERAL INTRODUCTION

1.1 PGC-1α, a powerful transcriptional coactivator

The Ppargc1a gene is located on chromosome 5 in the mouse genome and encodes a protein consisting of 797 amino acids (797 in mouse, 798 in humans) termed peroxisome proliferator-activated receptor γ coactivator 1α or briefly PGC-1α. Together with PGC-1β and the PGC-related coactivator (PRC) it forms the PGC-1 family of coactivators.

PGC-1α is a powerful transcriptional coactivator, capable to bind and coactivate numerous transcription factors including most members of the nuclear receptor superfamily of transcription factors (Puigserver and Spiegelman, 2003; Puigserver et al., 1998). Binding to the latter class of transcription factors is at least in part accomplished through the LLXXL and LXXLL motifs which are found close to the N terminus of the PGC-1α protein (Knutti et al., 2000; Puigserver et al., 1998). This motif is also found in other members of the PGC-1 family of coactivators as well as in other coregulators and was shown to serve for the interaction with nuclear receptors (Heery et al., 1997). The N terminus of PGC-1α itself is represented by an activation domain which interacts with proteins like cAMP response element binding protein-binding protein (CBP), p300 and the steroid receptor coactivator-1 (SRC-1) (Puigserver et al., 1999). Thus, although PGC-1α itself is not capable of acetylating histones, it binds to proteins with histone acetyltransferase (HAT) activity and brings them in the proximity of transcription factors and to the site of transcription. By modifying histones, these proteins make the chromatin accessible for the transcription factors and the transcription machinery. The C-terminal region of PGC-1α binds to the thyroid hormone receptor-associated protein/vitamin D receptor interacting protein (TRAP/DRIP) or simply mediator complex, allowing the interaction with the RNA polymerase and the transcription initiation machinery (Wallberg et al., 2003). The SWitch/Sucrose NonFermentable (SWI/SNF) chromatin remodelling complex was demonstrated to bind to PGC-1α through BAF60a, thus further increasing the PGC-1α coactivating capacity (Li et al., 2008b). Furthermore, in the C-terminal region of the PGC-1α protein, there are a serine- and arginine-rich domain and an RNA binding motif, linking PGC-1α to mRNA processing (Monsalve et al., 2000). Based on these findings, PGC-1α can be considered as a docking platform for proteins regulating gene transcription. PGC-1α binds to transcription factors and brings them together with the transcription initiation complex, proteins with HAT activity, chromatin remodelling complex and the proteins involved in mRNA processing.

Initially, PGC-1α was discovered as a coactivator of PPAR-γ in brown adipose tissue and therefore was termed PPAR-γ coactivator-1α (PGC-1α) (Puigserver et al., 1998). This and later studies revealed that PGC-1α coactivates other transcription factors as well and that it is not only present in brown fat, but in many tissues with high energy demands like skeletal muscle, heart, brown adipose tissue, kidney and brain (Lin et al., 2005; Puigserver et al., 1998). Generally, PGC-1α is a strong inducer of mitochondrial biogenesis and regulates many genes involved in energy metabolism (Lehman et al.,

2000; Lin et al., 2005; Mootha et al., 2004; Puigserver et al., 1998). In some of these tissues, the expression of PGC-1α can be induced by external stimuli. In liver, PGC-1α is strongly induced by fasting and boosts the expression of genes involved in hepatic gluconeogenesis and fatty acid oxidation (Herzig et al., 2001; Yoon et al., 2001). In brown adipose tissue, PGC-1α is induced by cold and regulates cold-induced thermogenesis by inducing biogenesis of mitochondria, increasing fatty acid oxidation and uncoupling of oxidative phosphorylation (Puigserver et al., 1998). PGC-1α mRNA is also found in skeletal muscle, especially in slow twitch muscle fibres, and its expression in this tissue can be induced by exercise training (Baar et al., 2002; Pilegaard et al., 2003; Russell et al., 2003).

To explore the function of PGC-1α *in vivo*, transgenic mice overexpressing PGC-1α as well as PGC-1α knockout mice have been generated and the role of PGC-1α in different tissues was studied (Leone et al., 2005; Lin et al., 2002; Lin et al., 2004). Mice lacking PGC-1α are viable, but a half of the pups die in the early postnatal period (Lin et al., 2004). These mice cannot maintain their body temperature when exposed to cold, show only a slight hypoglycaemia when fasted, have brain lesions and are hyperactive. Surprisingly, the PGC-1α$^{-/-}$ mice are lean and resistant to diet induced obesity (Lin et al., 2004). In another study however, PGC-1α$^{-/-}$ mice show an increased body fat with age (Leone et al., 2005). In contrast, transgenic PGC-1α expression in skeletal muscle induces mitochondrial biogenesis and drives a fibre type conversion in fast twitch muscle fibres towards a more oxidative, slow twitch phenotype (Lin et al., 2002). The muscles of these mice are redder in color, rich in mitochondria and resistant to contraction induced fatigue (Lin et al., 2002).

1.2 Upstream of PGC-1α - the regulation of PGC-1α expression and activity

1.2.1 Regulation of expression, protein stability and activity

Every living cell has to manage its energy needs, more precisely the cell needs to sense the current nutritional status and subsequently run biological programs which will allow the cell to keep a balance between energy intake, storage and expenditure. PGC-1α is thought to be such a metabolic sensor. The image of a coactivator which is constitutively expressed and passively recruited by transcription factors is wrong in the case of PGC-1α. The coactivator itself senses environmental changes and is an inducible regulator of energy metabolism. The expression and the activity of PGC-1α are regulated by external stimuli or nutritional status.

Liver

In liver, fasting strongly induces PGC-1α mRNA expression (Herzig et al., 2001; Yoon et al., 2001). The liver plays an important role in maintaining plasma glucose levels in fasting animals. It does so by breaking down glycogen (glycogenolysis) and by generating glucose from precursors (gluconeogenesis). In this way, the liver can replenish the glucose which was removed from the blood by the peripheral tissue. PGC-1α is central in regulating the hepatic fasting response (Handschin et al.,

2005; Herzig et al., 2001; Rhee et al., 2006; Yoon et al., 2001). The increased expression of PGC-1α mRNA following fasting is initiated by elevated blood glucagon levels and subsequently regulated by elevated cAMP levels (Herzig et al., 2001). This induction involves the binding of the cAMP response element binding protein (CREB) to the promoter of the Ppargc1a gene (Herzig et al., 2001). In this context, it was also shown that the activation of the p38 mitogen-activated protein kinase (MAPK) leads to a phosphorylation of PGC-1α and increases fasting induced PGC-1α expression (Figure 1) (Cao et al., 2005). In addition to hormonal regulation, the expression of the gluconeogenic gene program can be induced by free fatty acids. p38 and CREB are upstream of PGC-1α and regulate its expression which is important for the free fatty acid-induced gluconeogenesis in hepatocytes (Collins et al., 2006).

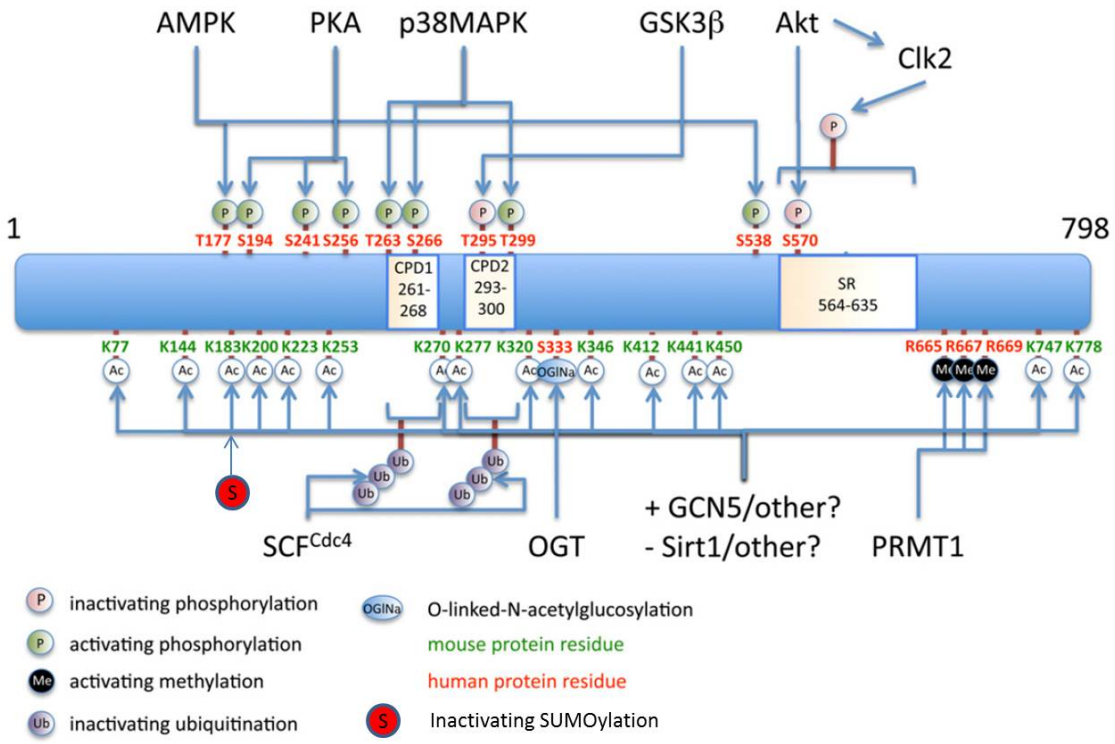

Figure 1. Posttranslational modifications of PGC-1α. Figure adapted from (Fernandez-Marcos and Auwerx, 2011).

In contrast to glucagon signalling, insulin triggers phosphorylation of PGC-1α by the protein kinase Akt2/protein kinase B (PKB)-β in the liver (Figure 1) (Li et al., 2007). This phosphorylation inhibits PGC-1α and thus attenuates the PGC-1α regulated gluconeogenesis and fatty acid oxidation in the liver (Li et al., 2007). Furthermore, another protein kinase Cdc2-like kinase 2 (Clk2) is regulated through the insulin/Akt pathway and phosphorylates PGC-1α to inhibit its cotranscriptional activity (Figure 1) (Rodgers et al., 2010). In addition to PGC-1α phosphorylation by Akt, this represents another mechanism by which insulin represses hepatic gluconeogenesis and glucose output through posttranslational modification of PGC-1α (Rodgers et al., 2010).

Acetylation represents yet another way to repress PGC-1α cotranscriptional activity in liver. The acetylation of PGC-1α by the acetyltransferase GCN5 leads to a translocation of PGC-1α to nuclear foci and prevents PGC-1α regulated expression of gluconeogenic genes and secretion of glucose (Figure 1) (Lerin et al., 2006). In contrast, the NAD+-dependent deacetylase SIRT1 deacetylates PGC-1α in response to fasting to control the gluconeogenic genes and thus represents a way to control PGC-1α activity by nutrient availability (Rodgers et al., 2005). Interestingly, SIRT1 is the mammalian homologue of Sir2 from *Saccharomyces cerevisiae* and *Caenorhabditis elegans*, which extends the lifespan in these organisms upon caloric restriction (Kaeberlein et al., 1999; Tissenbaum and Guarente, 2001). It is thus tempting to speculate that this link between metabolism and longevity might be functional in humans and extend the human lifespan as a result of caloric restriction.
Besides, the PGC-1α protein can be bound and modified by the *O*-lnked β-N-acetylglucosamine (*O*-GlcNAc) transerase (OGT) (Figure 1). This GlcNAcylation and interaction result in the targeting of OGT to FoxO1 to regulate its activity (Housley et al., 2009).

Brown fat

PGC-1α was discovered in brown fat and the brown fat was the first tissue in which the regulation of PGC-1α in response to environmental triggers was demonstrated. Cold-induced PGC-1α stimulates the expression of the uncoupling protein-1 (UCP1) in order to regulate thermogenesis by uncoupling the oxidative metabolism from ATP production, leading to dissipation of the proton gradient and thus heat generation (Puigserver et al., 1998). The expression of PGC-1α in brown fat is induced by cAMP, which is produced following cold exposure. Similarly, treating brown fat cells with β-adrenergic receptor agonists and thus mimicking cold exposure also leads to increased expression of PGC-1α mRNA (Puigserver et al., 1998). Similar to the regulation in the liver, p38 MAPK is involved in the regulation of PGC-1α expression and activity in the brown fat as well. P38 MAPK phosphorylates PGC-1α together with activating transcription factor-2 (ATF-2) to drive the expression of UCP1 (Figure 1). ATF-2 on the other hand induces the expression of PGC-1α. Thus in brown fat, p38 MAPK regulates PGC-1α by both phosphorylation and induction of mRNA expression (Cao et al., 2004). Besides, nitric oxide (NO) signalling induces mitochondrial biogenesis in brown adipose tissue by increasing expression of PGC-1α mRNA (Nisoli et al., 2003). Moreover, the mitochondrial biogenesis induced by cold in this tissue requires at least to some extent NO signalling, because the observed mitochondrial biogenesis is reduced when in absence of the endothelial nitric oxide synthase (eNOS) (Nisoli et al., 2003).
The transcriptional activity of PGC-1α is at least in part attenuated by direct interaction with the corepressor receptor-interacting protein 140 (RIP140) (Hallberg et al., 2008). RIP140 is a coregulator involved in energy homeostasis and interestingly, it represses the expression of genes which are typically induced by PGC-1α (Fritah et al., 2010). Whether this inhibition also affect all tissues in which PGC-1α is active remains to be yet investigated.

Skeletal muscle

Based on these observations that cold and fasting regulate PGC-1α in the brown fat and liver respectively, it becomes evident that PGC-1α is regulated by stress situations in metabolically active tissues. This is also true for the skeletal muscle because in this tissue, exercise training represents a stress situation. A working muscle uses up its energy stores and increases its needs for blood and oxygen supply to burn fuels. Accordingly, exercise training induces PGC-1α expression in skeletal muscle of rodents and humans (Baar et al., 2002; Pilegaard et al., 2003; Russell et al., 2003). This induction is transient but regular activity like in endurance exercise training results in higher basal PGC-1α transcription and a switch towards more oxidative muscle fibres (Pilegaard et al., 2003; Russell et al., 2003). In contrast, physical inactivity leads to lower PGC-1α expression and renders the muscle prone to atrophy (Sandri et al., 2006). Besides that fact, it is astonishing that nearly all signalling events which usually happen in an exercising muscle, at some step lead to modification of PGC-1α transcription or activity. Intracellular calcium levels are increased during exercise and important calcium effector proteins like the calcium /calmodulin-dependent protein kinase IV (CaMKIV) and calcineurin A (CnA) are upstream of PGC-1α and regulate its expression (Handschin et al., 2003; Olson and Williams, 2000). Analogous to the regulation in liver and brown fat, the PGC-1α regulation by CaMKIV and CnA in skeletal muscle involves cAMP signalling because CREB binds to the promoter of PGC-1α and regulates its transcription (Handschin et al., 2003). Furthermore, the members of the myocyte enhancer factor family of transcription factors (MEFs) bind to the PGC-1α promoter and are coactivated by PGC1α itself to regulate the expression at the PGC-1α promoter. This creates a positive autoregulatory loop and further increases PGC-1α expression (Handschin et al., 2003). Moreover, the activation of β2-adrenergic receptor (β2-AR) signalling triggers PGC-1α expression in skeletal muscle, again confirming the involvement of cAMP signalling in the regulation of PGC-1α expression (Miura et al., 2007). In muscle cell nuclei which are in the proximity of a neuromuscular junction (NMJ), PGC-1α is regulated through neuregulin boosted phosphorylation of PGC-1α and subsequent coactivation of the GA – binding protein (GABP) to control the expression of NMJ genes (Handschin et al., 2007).

The AMP activated protein kinase (AMPK) is an important intracellular metabolic sensor and becomes active after sensing the demand for ATP in a working muscle (Hardie and Hawley, 2001). Activated AMPK subsequently phosphorylates PGC-1α to activate the protein as well as increasing gene expression (Figure 1) (Jager et al., 2007). In addition to changing the AMP/ATP ratio, the increased energy demand in contracting muscle fibres also changes the ratio of the oxidized and reduced form of nicotinamide adenine dinucleotide (NAD+ / NADH). This ratio determines the activity of SIRT1, so that SIRT1 becomes active in an exercising muscle and deacetylates PGC-1α at several residues along the entire length of the PGC-1α protein (Figure 1) (Gerhart-Hines et al., 2007; Houtkooper et al., 2010). The deacetylation by SIRT1 increases the PGC-1α activity whereas the

acetylation of PGC-1α by GCN5 has the opposite effect and reduces the expression of PGC-1α target genes (Gerhart-Hines et al., 2007). Because NAD+ is a substrate for SIRT1 and active AMPK increases intracellular NAD+ levels, this AMP activity enhances the deacetylase activity of SIRT1 (Canto et al., 2009). Thus AMPK not only regulates PGC-1α by direct phosphorylation and induction of expression, but also through stimulation of deacetylation of PGC-1α by SIRT1. Moreover, the phosphorylation of PGC-1α by AMPK appears to be required for the subsequent deacetylation by SIRT1 (Figure 2) (Canto et al., 2009). It is possible that this phosphorylation induces conformational changes of PGC-1α protein which allow deacetylation by SIRT1. These observations reveal a coordinated regulation of PGC-1α activity by the two upstream enzymes SIRT1 and AMPK.

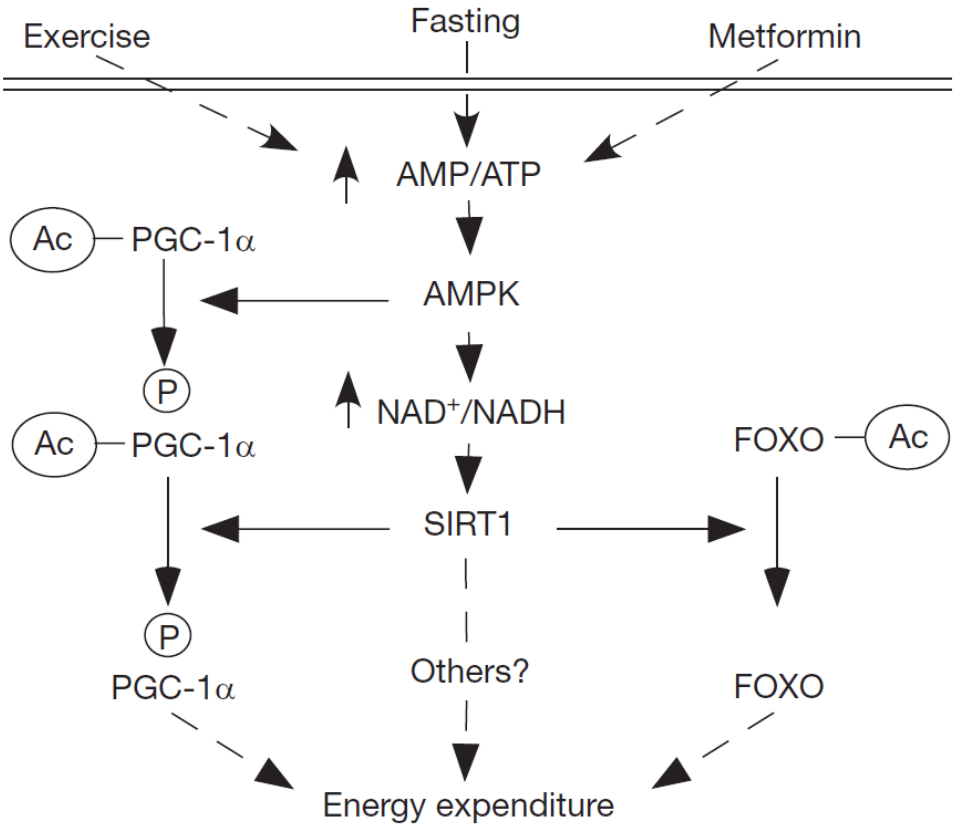

Figure 2. Schematic illustration of coordinated actions of AMPK and SIRT1 on PGC-1α. Figure adapted from (Canto et al., 2009).

An exercising muscle experiences a mechanical contraction stress which is sensed by the stress kinase p38 mitogen-activated protein kinase (MAPK) and results in the phosphorylation and stabilization of the PGC-1α protein which normally is susceptible to degradation (Puigserver et al., 2001). This stabilization of PGC-1α protein in exercising muscle appears to happen before the mRNA of PGC-1α is expressed, thus offering a fast way to provide the cell with active PGC-1α protein in the initial phase (Wright et al., 2007). However, the stabilization of the protein alone does not account for the observed increase in coregulatory activity. PGC-1α phosphorylation by p38 MAPK leads to the detachment of p160 myb binding protein ($p160^{MBP}$), a repressor which binds to the negative regulatory domain of

PGC-1α and represses its activity (Fan et al., 2004). This release of $p160^{MBP}$ further contributes to regulation of PGC-1α activity by p38 MAPK.

Another stress which is encountered in metabolically active tissues like the working skeletal muscle is the generation of reactive oxygen species (ROS) in active mitochondria which also has been shown to induce the expression of PGC-1α (St-Pierre et al., 2006).

In addition to an increased demand for nutrients, an exercising muscle increases its needs for oxygen, which are caused by the high metabolic activity and increased compression of the muscle during exercise, so that the muscle faces a transient hypoxia (Wagner, 2011). This hypoxic condition induces the expression of PGC-1α (Arany et al., 2008).

Similar to the regulation of PGC-1α by insulin and Akt/PKB signalling in liver, insulin represses expression of PGC-1α in skeletal muscles of healthy individuals but not of patients with type 2 diabetes (Southgate et al., 2005).

Last, the PGC-1α protein is phosphorylated by the glycogen synthase kinase 3β (GSK3β) and targeted to proteasomal degradation (Anderson et al., 2008). The physiological purpose of this regulation is not fully understood, but it is possible that this degradation of PGC-1α would limit the activation of PGC-1α by SIRT1 during oxidative stress (Fernandez-Marcos and Auwerx, 2011).

These observations together reveal that nearly all signalling pathways triggered by exercising muscle at some point converge on PGC-1α, and therefore suggest a role for PGC-1α in skeletal muscle as a sensor of changes induced by exercise in this tissue.

1.2.2 PGC-1α regulation in other tissues and by other mechanisms

Cardiac PGC-1α is strongly induced directly after birth after short term fasting (Lehman et al., 2000). This is when the neonatal heart changes the generation of its energy by shifting from glycolysis to fatty acid oxidation in mitochondria (Lehman et al., 2000). Thus, PGC-1α serves as a regulator of mitochondrial biogenesis and a molecular switch for the change in fuel usage in the heart.

The highest level of PGC-1α expression in rodent brain is reached two weeks after birth in different brain regions, especially in γ-aminobutyric acid (GABA)-positive neurons in the cortex, hippocampus and cerebellum (Cowell et al., 2007; Handschin, 2009). Because oxidative stress and mitochondrial dysfunction are associated with neurodegeneration, PGC-1α has been linked to disorders like Huntington, Parkinson or Alzheimer (Handschin, 2009). Indeed, the expression of PGC-1α appears to be reduced in brains of Alzheimer disease patients (Qin et al., 2009). PGC-1α also plays a role in the development of Parkinson disease. A transcriptional repressor termed parkin interacting substrate (PARIS) binds to the promoter of PGC-1α and inhibits its expression (Shin et al., 2011). It is suggested that in Parkinson disease, the reduction of parkin levels leads to higher availability of PARIS and thus suppression of PGC-1α expression and as a consequence reduced expression of PGC-1α target genes (Shin et al., 2011).

In mouse melanocytes, PGC-1α expression is regulated by ultraviolet (UV) light radiation (Shoag et al., 2013). When the skin cells experience damage by UV radiation, the keratinocytes start producing and releasing a peptide termed α-melanocyte stimulating hormone (α-MSH) and this hormone leads to induction of PGC-1α expression in melanocytes (Shoag et al., 2013). Nitric oxide (NO) modulates the expression of PGC-1α in endothelial cells (Borniquel et al., 2006). Short-term exposure to NO supresses PGC-1α expression, whereas long-term NO exposure up-regulates PGC-1α mRNA (Borniquel et al., 2006).

In addition to the previously mentioned posttranslational modifications, the PGC-1α protein is also subject to ubiquitinylation, methylation and SUMOylation (Olson et al., 2008; Rytinki and Palvimo, 2009; Teyssier et al., 2005). The ubiquitinylation of PGC-1α is performed by a member of the Skp1/Cullin/F-box (SCF) class of E3 ubiquitin ligases termed SCF^{Cdc4} (Olson et al., 2008). Cdc4 stands for cell division control protein 4 and represents the F-box component of the SCF^{Cdc4} complex. The ubiquitinylation targets PGC-1α for degradation and phosphorylation of PGC-1α by p38 and GSK3β might promote ubiquitinylation by SCF^{Cdc4} (Olson et al., 2008). Another E3 ubiquitin ligase known to modify PGC-1α and promote its degradation in brown adipose tissue is Ring-finger-containing protein 34 (RNF34) (Wei et al., 2012). Cold exposure however supresses RNF34 expression in brown fat, thereby allowing PGC-1α induction (Wei et al., 2012). Protein arginine methyltransferase 1 (PRMT1) methylates PGC-1α at three arginine residues and this modification is thought to promote the coactivator activity of PGC-1α (Teyssier et al., 2005).

PGC-1α can be SUMOylated at the lysine residue 183 and this is the same residue that can be acetylated by GCN5 (Rodgers et al., 2005; Rytinki and Palvimo, 2009). SUMOylation supresses the coactivator activity of PGC-1α and can be reversed by Sentrin/SUMO-specific protease 1 (SENP1) to promote PGC-1α activity and regulate mitochondrial biogenesis (Cai et al., 2012; Rytinki and Palvimo, 2009). Interestingly, SUMOylation does not attenuate PGC-1α by changing the stability of the protein, but promotes the interaction of PGC-1α with its repressor RIP140 (Fritah et al., 2010; Rytinki and Palvimo, 2009). The repressor RIP140 itself can also be SUMOylated, resulting in dislocation from small nuclear foci to a more dispersed distribution in the nucleus, allowing RIP140 to interact with other proteins and suppress their activity (Fritah et al., 2010; Rytinki and Palvimo, 2008).

Different isoforms of PGC-1α have been described and therefore, its activity and specificity for choosing its binding partners and regulating gene expression might also be regulated by alternative splicing (Baar et al., 2002; Tadaishi et al., 2011). Such an isoform is the truncated form of PGC-1α, termed NT-PGC-1α because it is contains the N terminus of the classical PGC-1α protein and harbours the transactivation and nuclear receptor interaction domain (Zhang et al., 2009). In contrast to the classical isoform, NT-PGC-1α is a relatively stable protein, which can localize in the cytoplasm. The export of NT-PGC-1α from nucleus to cytoplasm can be inhibited by protein kinase A (PKA) phosphorylation (Chang et al., 2010). Last, expression of PGC-1α shows a circadian rhythm and PGC-1α itself regulates mammalian clock genes (Liu et al., 2007).

These different modes of regulation prove that PGC-1α is not a constitutively expressed coactivator which is passively recruited by the transcriptional machinery. It is rather a tightly regulated sensor of environmental changes and connects these changes with transcription. Moreover, the multitude of possibilities to change its activity and expression indicates that PGC-1α is not only turned off or on, but can receive inputs through signals from different signalling pathways and initiate cellular changes which are adequate for the current environmental or metabolic conditions. It is also evident that some modifications of PGC-1α drastically change its activity or availability, whereas others can be seen as fine-tuning the current status of PGC-1α activity.

1.3 cAMP and cyclic nucleotide phosphodiesterases in the regulation of PGC-1α expression and activity

Generally, PGC-1α can be considered as a strong promoter of mitochondrial biogenesis (Wu et al., 1999). Nevertheless, PGC-1α also possesses tissue-specific functions like regulating hepatic response to fasting, inducing thermogenesis in brown adipose tissue or controlling a fibre type switch in skeletal muscle (Lin et al., 2002; Puigserver et al., 1998; Yoon et al., 2001). Therefore, it is not surprising that PGC-1α expression or activity was linked to different medical conditions in these tissues (Handschin, 2009). PGC-1α protects neural cells from oxidative stress and neurodegeneration (St-Pierre et al., 2006). Increased expression of PGC-1α in the bone might be beneficial for the treatment of osteoporosis (Nervina et al., 2006). Higher PGC-1α levels in skeletal muscle protect against atrophy and ameliorate Duchenne muscular dystrophy by up-regulating utrophin (Handschin et al., 2007; Sandri et al., 2006). Also, perturbations in PGC-1α expression have been linked to different pathological conditions. Reduced expression of PGC-1α is observed in the subcutaneous fat of morbidly obese people or in muscles of type 2 diabetes patients (Semple et al., 2004). Therefore, controlling PGC-1α levels by drug treatment might be beneficial for the treatment of these illnesses and the therapeutic potential of PGC-1α for different medical conditions is being investigated (Handschin, 2009).

Considering the different modes of regulation, which are described in chapter 1.2, it is clear that cAMP signalling or generally cyclic nucleotide signalling is involved in the regulation of PGC-1α expression and activity. This is based on the fact that molecules like CREB, PKA or β2-AR either bind to the PGC-1α promoter to induce its expression or phosphorylate either PGC-1α itself or proteins regulating PGC-1α. These proteins are either upstream or downstream of cAMP. β2-AR signalling promotes production of cAMP whereas CREB and PKA are directly regulated by cAMP (Omori and Kotera, 2007).

Cyclic adenosine monophosphate (cAMP) was discovered more than 50 years ago by Sutherland and colleagues and was found to be synthesized from ATP through adenylate cyclases (ACs) (Rall and Sutherland, 1958, 1962; Sutherland and Rall, 1958; Sutherland et al., 1962). cAMP is a second

messenger, meaning that extracellular signals which are received at the plasma membrane are transduced to generate a second, intracellular signal. In this way extracellular events can be communicated to intracellular structure. More precisely, hormones like epinephrine can activate membrane-resident G-protein coupled receptors (GPCRs) which in turn lead to activation of adenylate cyclase and subsequent synthesis of cAMP from ATP (Cooper, 2003; Sassone-Corsi, 2012). There are ten ACs in mammalian cells, nine of which are membrane-bound and a soluble AC which is not activated by GPCR signalling (Cooper, 2003). In 1971 Sutherland won a nobel prize in physiology/medicine for his work in this field and last year (2012), two other scientists, Robert Lefkowitz and Brian Kobilka, were awarded a nobel prize in chemistry for their work on GPCRs, reflecting the importance of this signalling pathway in biology (www.nobelprize.org).

Once generated, cAMP can disperse throughout the cell and control the activity of its effector proteins. These include cAMP gated ion channels, PKA and cAMP-regulated guanine nucleotide exchange factors (cAMP-GEFs) called exchange proteins activated by cAMP (Epac) (Omori and Kotera, 2007; Sassone-Corsi, 2012). After the second messenger has elicited cellular processes, the intracellular cAMP levels need to be lowered to the basal levels and thereby allow a new round of signalling events in future. Indeed, cyclic nucleotide phosphodiesterases (PDEs) have been described shortly after the discovery of cAMP (Butcher and Sutherland, 1962). PDEs play an important role by hydrolysing cAMP to AMP and thereby extinguishing the previously generated signal (Sassone-Corsi, 2012). The mammalian genome encodes 21 phosphodiesterase genes, which are subdivided into 11 gene families (Bender and Beavo, 2006). However, there are many more than 21 gene products. Due to expression from alternative promoters and alternative splicing there are estimates of 100 – 200 or more gene products (Bender and Beavo, 2006; Bingham et al., 2006). The nomenclature follows certain rules. In the name of the phosphodiesterase HsPDE1C2, “Hs” stands for *Homo sapiens*, “PDE1” indicates the gene family, followed by the letter “C” for the family member and finally with number “2” to specify the splice isoform. The members of the 11 PDE families share a conserved catalytic domain near the C terminus, but the amino acid sequences outside the catalytic domain show a high variation. This is seen when comparing the regulatory domains near the N terminus (Figure 3) (Francis et al., 2011).

PDE4, PDE7, PDE8 and are cAMP specific, PDE5, PDE6 and PDE9 are cGMP specific whereas PDE1, PDE2, PDE3, PDE10 and PDE11 hydrolyse both cAMP and cGMP (Francis et al., 2011; Omori and Kotera, 2007). However, PDEs show a tissue specific expression pattern and have tissue specific functions, thus the majority of the cAMP or cGMP activity depends on the most abundant PDE family in that specific tissue (Bingham et al., 2006; Omori and Kotera, 2007). PDE1C2 for example can be found in olfactory sensory neurons, PDE 6 plays an important role in vision and is therefore highly expressed in the retina and PDE4 has a more ubiquitous expression (Burns and Arshavsky, 2005; Houslay and Adams, 2003; Yan et al., 1995). This thesis focuses on skeletal muscle and the members of the PDE4, PDE5, PDE7A, PDE7B and PDE11 are highly expressed in the skeletal muscle tissue (Bender and Beavo, 2006). PDE1B is weakly expressed in skeletal muscle (Omori and

Kotera, 2007). PDE9 members show a wide tissue distribution and therefore, their expression in skeletal muscle tissue can be expected (Bender and Beavo, 2006).

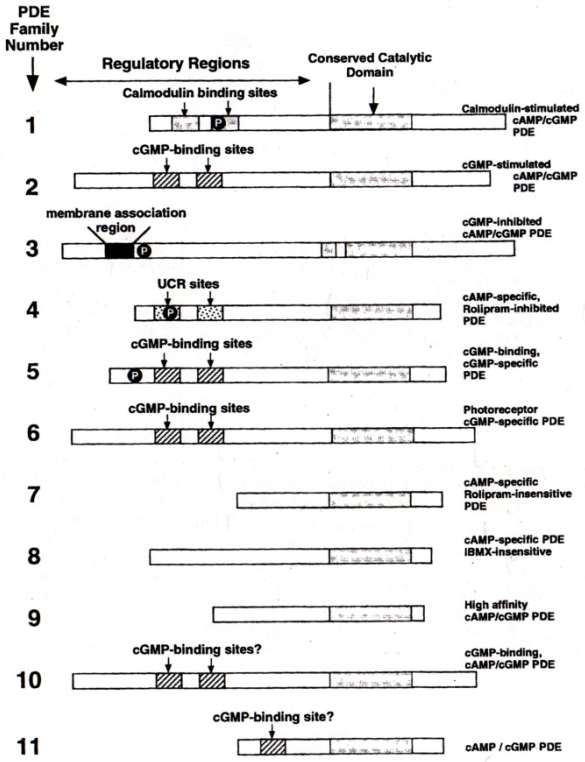

Figure 3. 11 phosphodiesterase families. Figure taken from (Francis et al., 2001).

This tissue specific distribution and the involvement in many important biological processes are only some of many reasons why PDEs are considered as important drug targets.

A selective PDE inhibitor would influence only those tissues in which the inhibited phosphodiesterase is expressed, thereby reducing the probability of side effects. Other reasons are the basic pharmacological principle that inhibiting degradation of a second messenger results often in a faster change than promoting the synthesis or that PDEs appear to have a higher maximal reaction rate (Vmax) than ACs (Bender and Beavo, 2006). A variety of selective and nonselective PDE inhibitors have been developed and are used to treat different medical conditions like asthma, depression or most prominently erectile dysfunction (Table 1) (Bender and Beavo, 2006; Coward and Carson, 2008; Hansen et al., 2000; Zhang et al., 2002).

Pharmacology of PDE family specific inhibitors

PDE	Inhibitors	Source	IC_{50}	Reference	Usage
PDE1	Vinpocetine	W-A	14 μM	Hagiwara et al. (1984)	Only recently have selective PDE1 inhibitors been developed; IC224 may be the most selective in intact cells
	IC224	ICOS	80 nM	Snyder et al. (2005)	
	SCH51866	Schering	13–100 nM	Watkins et al. (1995)	
PDE2	EHNA	W-A	1 μM	Podzuweit et al. (1995)	Inhibitors are being investigated for improving memory and decreasing endothelial permeability under inflammatory conditions
	BAY 60-7550	Bayer	4.7 nM	Boess et al. (2004)	
	PDP	Bayer	0.6 nM	Seybold et al. (2005)	
	IC933	ICOS	4 nM	Snyder et al. (2005)	
PDE3	Cilostamide	W-A	20 nM	Hidaka et al. (1979)	Milrinone is a currently approved treatment for short term congestive heart failure; cilastazol is a treatment for intermittent claudication
	Milrinone	W-A	150 nM	Harrison et al. (1986)	
	Trequinsin	W-A	300 pM	Ruppert and Weithmann (1982)	
	Cilastazol	Otsuka	200 nM	Tanaka et al. (1988)	
	OPC-33540	Otsuka	0.3–1.5 nM	Sudo et al. (2000)	
PDE4	Rolipram	W-A	1 μM	Schwabe et al. (1976)	Multiple compounds have undergone trials for treatment of chronic obstructive pulmonary disease but have experienced limited success because of side effects; compounds are also under investigation for several other inflammatory conditions; interest exists in using PDE4 inhibitors for CNS disorders, including depression and improvement of memory
	Roflumilast	Altana	0.8 nM	Hatzelmann and Schudt (2001)	
	Cilomilat	GlaxoSmithKline	120 nM	Barnette et al. (1998)	
	Ro 20-1724	W-A	2 μM	Sheppard and Tsien (1975)	
	AWD 12-281	Elbion A-G	9.7 nM	Schmidt et al. (2000)	
	SCH351591	Schering	58 nM	Billah et al. (2002)	
	V-11294A	Purdue Frederick	405 nM	Gale et al. (2002)	
PDE5	Zaprinast	W-A	0.13 μM	Lugnier et al. (1986)	Sildenafil, vardenafil, and tadalafil are in usage as erectile dysfunction drugs; these compounds are in trials for other indications such as pulmonary hypertension and benign prostatic hyperplasia
	Sildenafil	Pfizer	10 nM	Boolell et al. (1996)	
	Vardenafil	Bayer	1 nM	Bischoff et al. (2001)	
	Tadalafil	Lilly-ICOS	10 nM	Padma-Nathan et al (2001)	
	DA-8159	Dong-A	6 nM	Oh et al. (2000)	
PDE6					Inhibition of PDE6 may be a source of sildenafil side effects on vision; genetic mutations in PDE6 are the basis for several vision related diseases, but PDE6 has not been investigated as a therapeutic target
PDE7	BRL 50481	GSK	260 nM	Smith et al. (2004)	PDE7-selective inhibitors have been investigated as anti-inflammatory agents in vitro but so far have shown limited utility in vivo
	IC242	ICOS	370 nM	Lee et al. (2002)	
PDE8					No truly selective inhibitors are yet available
PDE9	BAY 73-6691	Bayer	55 nM	Wunder et al. (2005)	BAY 73-6691 is in preclinical development for Alzheimer's disease treatment
PDE10					No truly selective inhibitors are yet available
PDE11					PDE11 has received pharmacological interest because it is also inhibited by tadalafil and thus is a potential source for side effects

W-A, widely available; SCH51866, (+)-*cis*-5,6*a*,7,8,9,9*a*-hexahydro-2-[4-[trifluro-methyl] phenylmethyl]-5-methyl-cylopent[4,5]imidazo[2,1-*b*]purin-4(3*H*)one; EHNA, *erythro*-9-(2-hydroxy-3-nonyl)adenine; PDP, 9-(6-phenyl-2-oxohex-3-yl)-2-(3,4-dimethoxybenzyl)-purin-6-one; Ro 20-1724, 4-[(3-butoxy-4-methoxyphenyl)-methyl]-2-imidazolidinone; AWD 12-281; *N*-(3,5-dichloro-pyrid-4-yl)-[1-(4-fluorobenzyl)-5-hydroxy-indole-3-yl]-glyoxylic acid amide; SCH351591, 3,5-dichloro-4-[8-methoxy-2-(trifluoromethyl)-quinoline-5-ylcarboxamido]pyridine-1-oxide; V-11294A, 3-[3-(cyclopentyloxy)-4-methoxybenzyl]-6-(ethylamino)-8-isopropyl-3*H*-purine hydrochloride; DA-8159, 5-[2-propyloxy-5-(1-methyl-2-pyrollidinylethylamidosulfonyl)phenyl]-1-methyl-3-propyl-1,6-dihydro-7*H*-pyrazolo(4,3-*d*)pyrimidine-7-one.

Table 1. Specific PDE inhibitors. Table taken from (Bender and Beavo, 2006).

Because the activation of the PKA by forskolin and binding of CREB to the promoter of PGC-1α induces expression of the PGC-1α promoter in skeletal muscle cells, it might be expected that the inhibition of PDEs would also promote the expression of PGC-1α (Handschin et al., 2003). Moreover, because the induced expression of PGC-1α in skeletal muscle by triggers like exercise is transient, a successful regulation of PGC-1α by PDE combined with expression induction might delay the drop of PGC-1α expression. This would result in a long-lasting PGC-1α up-regulation and possibly a prominent induction of PGC-1α target genes.

1.4 Downstream of PGC-1α - biological pathways regulated by PGC-1α

As described above, external stimuli or metabolic changes trigger numerous signalling pathways which converge on PGC-1α. Typically, these events result in induced expression or protein modification of PGC-1α which can lead to either activation of PGC-1α or its degradation. Once PGC-1α is active, it binds to its transcriptional partners and regulates the expression of tissue-specific gene programs.

In response to fasting, PGC-1α coactivates Forkhead box protein O1 FoxO1, glucocorticoid receptor (GR) and hepatocyte nuclear factor 4 α (HNF4α) to promote the expression of gluconeogenic genes like phosphoenolpyruvate carboxykinase (PEPCK) and glucose-6-phosphatase (Puigserver et al., 2003; Yoon et al., 2001). Even though the requirement of the interaction of PGC-1α with FoxO1 has been disputed, PGC-1α cannot regulate hepatic gluconeogenesis without FoxO1. In addition to control gluconeogenesis, PGC-1α participates in the regulation of fatty acid β-oxidation, ketogenesis and bile-acid homeostasis in liver by coactivating several transcription factors like PPARα, FXR and LXR (Koo et al., 2004; Leone et al., 1999; Lin et al., 2005; Oberkofler et al., 2003; Shin et al., 2003; Zhang et al., 2004). Which transcription factors are involved in the regulation of oxidative phosphorylation genes in liver is not precisely known, but nuclear respiratory factor-1 (NRF-1) and estrogen-related receptor α (ERRα) are possible candidates (Schmidt and Mandrup, 2011). In heart, PGC-1α is induced after birth and following fasting and both events lead to increased utilization of fatty acids as major energy source. To induces genes which regulate mitochondrial respiratory function and fatty acid oxidation PGC-1α coactivates PPARα and ERRα (Finck and Kelly, 2006; Rowe et al., 2010). When expressed in heart cells, PGC-1α promotes mitochondrial biogenesis (Lehman et al., 2000). In neural cells, PGC-1α is induced by oxidative stress and increases the expression of ROS detoxifying enzymes superoxide dismutase 2 (SOD2) and glutathione peroxidase 1 (GPx1) thereby protecting these cells against oxidative stressors (St-Pierre et al., 2006). In mouse embryonic development, PGC-1α binds to SRY-related high mobility group-Box gene 9 (Sox9) enhancing its activity on the expression of chondrogenic genes in the embryonic limb buds (Kawakami et al., 2005).

Soon after the discovery that PGC-1α coactivates PPARγ in brown adipose tissue to run the thermogenic program, PGC-1α was found to induce the expression of the nuclear respiratory factors NRF-1 and NRF-2 and coactivate them (Wu et al., 1999). By coactivating NRF-1 in muscle cells, PGC-1α induces the expression of mitochondrial transcription factor A (mtTFA), which is an important regulator of mitochondrial DNA replication and transcription (Wu et al., 1999). In skeletal muscle, ERRα and GA repeat-binding protein α (Gabpa or NRF-2) are essential transcriptional partners and together with PGC-1α they regulate the expression of the entire genetic program for oxidative phosphorylation and mitochondrial biogenesis (Mootha et al., 2004; Schreiber et al., 2004). In addition to coactivating these transcription factors, PGC-1α also induces their expression (Mootha et al., 2004). The transcriptional complex consisting of ERRα and PGC-1α induces the expression of vascular endothelial growth factor (VEGF) to regulate angiogenesis in skeletal muscle (Arany et al.,

2008). Triggered by motor nerve activity, NRF-2 and PGC-1α together run the expression of the neuromuscular junction (NMJ) gene program (Handschin et al., 2007). By coactivating myocyte enhancer factor 2C (MEF2C), PGC-1α increases the expression of the insulin-sensitive glucose transporter (GLUT4), thus regulating glucose uptake in muscle (Michael et al., 2001). Therefore, by binding to chosen transcription factors and enhancing their expression, PGC-1α regulates nearly all adaptations of skeletal muscle to exercise. Likewise, as a result to stress situations in other tissues, PGC-1α can becomes active and regulate the expression of those gene programs which are necessary in that specific situation and help the cell to deal with that stress.

Based on these observations, PGC-1α can be considered as a master regulator, which responds to external stimuli and coactivates different transcription factors to induce entire gene programs. Although PGC-1α has been shown to coactivate numerous transcription factors, it is not likely that PGC-1α always coactivates all putative transcription factors. First, always inducing all potential target genes would be very inefficient, unspecific and a waste of energy and resources. Only inducing these genes that are required not only saves energy but also protects the cell from undesired consequences. The expression of a gene at wrong time or in wrong situation might even be deleterious for the cells. Second, different tissues express a different set of transcription factors, which subsequently become available for PGC-1α to bind to them. Third, some transcription factors are only available under specific conditions. Environmental stimuli or metabolic changes might result in increased expression of the mRNA for a certain transcription factor, its protein stabilization or translocation to nucleus, where it can interact with PGC-1α. Likewise, PGC-1α itself is target for numerous modes of regulation including regulated expression, protein stability, alternative splicing and posttranslational modifications. It can be assumed that these changes influence the preference of PGC-1α for its binding partners and modify its efficacy in performing its role as a coactivator (Figure 4). Indeed, an example of such a regulation mode can be observed in liver. The central role played by PGC-1α in hepatic fasting response is described in detail in previous chapters. Researchers have shown that S6 kinase becomes active in liver after feeding and subsequently phosphorylates PGC-1α (Lustig et al., 2011). Thereupon, PGC-1α is not anymore able to induce gluconeogenesis while the regulation of mitochondrial and fatty acid genes remains unchanged. This is because the S6 kinase phosphorylation blocks the interaction of PGC-1α with the gluconeogenesis regulator HN4α, whereas the interaction with mitochondrial biogenesis and fatty acid oxidation regulators ERRα and PPARα is not affected (Lustig et al., 2011). In this case, S6 kinase phosphorylation inhibits only one segment of the wide range of possible PGC-1α actions. It is very probable, that other posttranslational modifications, splicing or inhibition of PGC-1α by proteins like RIP140 or $p160^{MBP}$ operate in a similar way. Different posttranslational modifications derive from different signalling pathways and possibly influence the activity of PGC-1α in a unique way.

Considering that different modes of PGC-1α regulation can occur at the same time and theoretically can be combined in numerous ways, the combination of these events would allow an immense

combinatorial complexity. In such a model, the posttranslational modification status of PGC-1α can be considered as a "coactivator code", similar to the "phosphocode" suggested for the regulation of nuclear receptors (Wu et al., 2005). This coactivator code would direct and specify the PGC-1α activity (Figure 4).

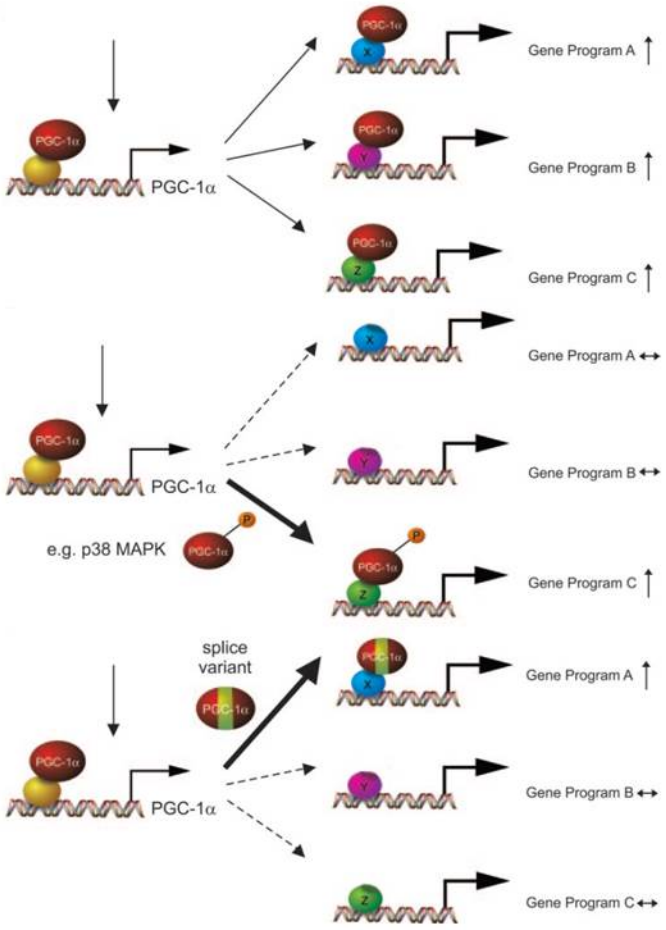

Figure 4. The regulation of PGC-1α specificity by posttranslational modifications or alternative splicing of PGC-1α. Figure adapted from (Handschin and Spiegelman, 2006).

Although the coactivator code regulation is possible, it is not proven yet that this regulation is really true. Nevertheless, it is clear that PGC-1α at any given time will coregulate several transcription factors and change the expression of many genes. Therefore, fully understanding the network of proteins which together with PGC-1α induce biological programs cannot be achieved by studying PGC-1α on individual gene promoters. Many studies focus their analysis on one promoter or a subset of promoters. Such approaches are not suitable to draw general conclusions, about how a transcription factor or coactivator regulates transcription. To understand the complex network and to get a global picture of the entire PGC-1α mediated gene regulation, a genome-wide approach is required. This approach should allow that the interaction of PGC-1α with the entire genome can be studied and this

knowledge should be used to understand genome-wide changes in gene expression induced by PGC-1α.

1.5 ChIP-Sequencing - detecting the interaction of PGC-1α with chromatin

The first step to study how a factor regulates gene expression is to investigate its interaction with the genome. Probably the best way to do so is by performing chromatin immunoprecipitation (ChIP) (Figure 5). In this approach, the cells or tissue are treated with formaldehyde to crosslink the protein of interest with the chromatin. In the next step the chromatin is sheared by sonication or digestion and the protein of interest is precipitated together with the DNA fragment bound to it by a specific antibody. The remaining chromatin is washed away, leaving only those chromatin pieces which were occupied by the protein of interest. Next, the crosslinking is reversed, protein and RNA are digested and the remaining DNA is precipitated. In this way, a DNA library is created which consist of only those parts of DNA which were initially bound by the protein of interest. This means that by identifying these DNA fragments, the researchers can deduce all parts of the genome that have been occupied by the protein of interest in the initial experiment. There are two common methods to identify all DNA fragment in the library generated by ChIP experiments (Euskirchen et al., 2007; Park, 2009). In one method, the goal is to hybridize DNA to tiling arrays which cover all promoters and thus detect all promoters bound by the protein of interest. Because this method combines chromatin immunoprecipitation with arrays (chip), it was termed ChIP-on-chip (Figure 5) (Blat and Kleckner, 1999; Ren et al., 2000). The other method utilizes ultrahigh-throughput DNA sequencing to identify the DNA fragments in the library and is therefore called ChIP-Sequencing or briefly ChIP-Seq (Figure 5) (Johnson et al., 2007; Robertson et al., 2007).

The coactivator PGC-1α does not bind DNA directly, but is rather recruited to DNA by transcription factors. Therefore the DNA library generated by chromatin immunoprecipitation of PGC-1α will contain DNA fragments which were bound by different transcription factors which were coactivated by PGC-1α.

ChIP-Seq has some advantages over ChIP-on-chip (Park, 2009). ChIP-Seq has a much greater resolution which is in best case a single nucleotide. In ChIP-on-chip the resolution is array-specific, but definitely lower. ChIP-on-chip only covers promoter regions whereas the coverage in ChIP-seq is basically not limited. Furthermore, arrays are only available for some organisms. The only restriction is limitations in alignability due to repeats, but with increasing DNA sequence fragment (read) length even repeat regions can be covered. The cost of ChIP-Seq is rapidly decreasing and the required amount of DNA for the library is much smaller. The disadvantage of ChIP-Seq is the complexity of data analysis and the lack of suitable analysis programs. In the last years, many ChIP-Seq analysis tools have been published, but most require profound skills in bioinformatics and the files generated by these tools often cannot be directly further analysed with other analysis tools without a time

consuming reformatting of the file (Furey, 2012). For our experiments, we decided to go with ChIP-Seq because of the numerous advantages of ChIP-Seq over ChIP-on-chip.

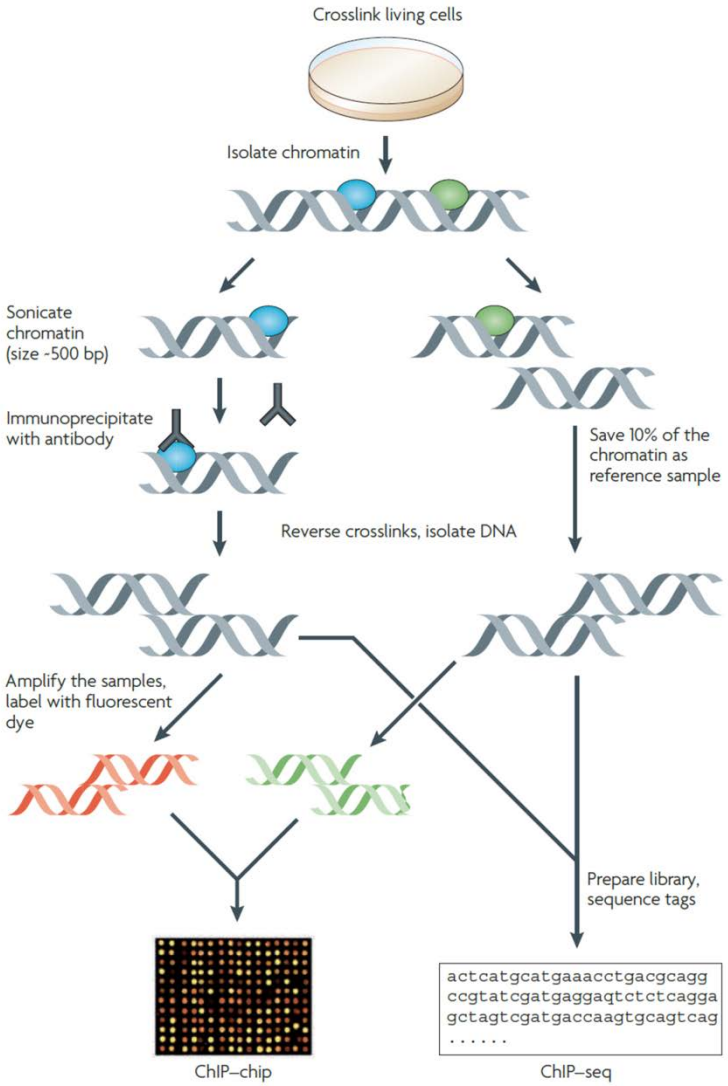

Figure 5. Schematic illustration of the methods ChIP-chip (ChIP-on-chip) and ChIP-Seq. Figure adapted from (Farnham, 2009).

The sequencing of the DNA library is performed by powerful genome analysers, which combine DNA amplification with scanning after every round of amplification. Because the DNA fragments are immobilised on the slides the obtained scan pictures can be used to retrieve sequences of millions of DNA fragments (Fields, 2007; Johnson et al., 2007; Park, 2009). The image processing and base calling depends on the sequencing platform and can introduce errors (Park, 2009). Another challenge is data management, because the files generated in ChIP-Seq experiments require big memory capacities (Park, 2009). The sequenced DNA fragments are also called reads and in a typical ChIP-Seq experiment many millions of reads are obtained.

The sequencing depth is rapidly increasing. In our first ChIP-Seq experiments, the number of reads obtained for one ChIP-Seq experiment was approximately 5-10 millions. A few years later, this number was ten times higher. To map the reads to a reference genome, several freely available tools

have been developed and are still being optimized (Furey, 2012). In the early years of ChIP-Seq however, there were very few alignment programs and other analysis tools available. This presented a major bottleneck in the ChIP-Seq analysis, because the researchers would relatively rapidly obtain the sequences, but did not have the proper programs or the computing capacities to run the analysis. Furthermore, many researchers were biologists and thus simply not qualified to develop new programs or analysis tool and were stuck with their data. One of the early aligners, ELAND, was developed by the company Illumina and was the standard aligner on their genome analysers (illumina.com). Researchers later developed freely available aligners like MAQ or Bowtie, just to mention a couple (Langmead et al., 2009; Li et al., 2008a). In general, the aligners are always a trade-off between accuracy on the one side and speed and memory usage on the other side (Park, 2009). Once the reads are mapped, the data can be visualized in a genome browser like the popular genome browser of the University of California at Santa Cruz (UCSC) (Meyer et al., 2013). The genome browser allows a visualisation of the data at individual sites in the genome and serves mainly to verify that the experiment has worked or to test the enrichment at individual sites. For an in-depth systemic analysis of enrichment, the reads are usually analysed with called peak finders. The programs like MACS or PeakSeq scan the data along the genome and identify areas of local read enrichment called peaks (Rozowsky et al., 2009; Zhang et al., 2008). Peaks are considered as genomic locations which were occupied by the protein of interest in the initial experiment. Alternatively, in ChIP-Seq experiments, which do not investigate the interaction of transcription factors with DNA but rather epigenetic modifications of the chromatin, a peak is considered as an area with histone modification. The width of a peak and its sharpness strongly depend on the experimental design and the phenomenon that is studied. In protein-DNA binding experiments the resulting peaks are mostly sharp and have a narrow range of peak width changes. In histone modification experiments, the peak width can vary (Park, 2009). Therefore, there cannot be one superior peak caller for all experiments.

By combining peaks with gene expression arrays, researcher can assign changes in gene expression to binding events (peaks) and thus verify if the binding of the protein of interest changes gene expression. If so, the protein of interest would directly regulate the expression of that specific gene by binding to its promoter or other adjacent regions. In the case of PGC-1α, this would mean that PGC-1α together with a transcription factor directly drives the expression of that gene. Conversely, a gene that is changing expression upon deletion or introduction of the protein of interest, but is not located in the proximity of a peak, would be indirectly regulated by the protein of interest. In addition, a gene ontology (GO) analysis can be applied on the induced and suppressed genes to reveal which biological pathways are directly and indirectly regulated by PGC-1α.

The genomic regions covered by the peaks can be searched for known transcription factor motifs or undergo a *de novo* motif search analysis. Motif search programs like MotEvo and PhyloGibbs developed by Arnold and colleagues or Siddharthan and colleagues respectively were used for the analysis of the data in this thesis (Arnold et al., 2012; Siddharthan et al., 2005). As mentioned

previously, PGC-1α does not bind DNA directly. Consequently, the motifs that could be found in PGC-1α occupation sites (peaks) would not represent the binding of PGC-1α to DNA, but the binding of transcription factors which are coactivated by PGC-1α. Therefore by identifying motifs in PGC-1α peaks, predictions about transcriptional partners of PGC-1α can be made. Moreover, gene ontology results might be combined with the findings from motif search. This would allow making predictions, which transcription factors are involved in the regulation of each biological pathway, that is regulated by PGC-1α.

Together these findings would provide an insight into the complex regulatory network of PGC-1α regulated gene programs. The described analysis procedure could also be applied after a posttranslational modification PGC-1α has been introduced. This would offer a possibility to identify which PGC-1α regulated gene programs are affected by each posttranslational modification of PGC-1α.

The question is, if a bioinformatics analysis would be sufficient to analyse the regulation of transcription by a protein of interest. First, the occurrence of a motif alone does not necessarily mean that the transcription factor bind *in vivo* to that site. In the case of PGC-1α there is no binding motif known, because it does not bind DNA directly. It is also not probable that all putative binding sites are occupied in all tissues and in under any condition. Conversely, transcription factors have been found to bind or to be active at sites which do not have a consensus motif for this transcription factor (Farnham, 2009). One possible explanation is that the factor binds at a distal site, which contains the motif and then loops to the site in question to interact with the transcriptional machinery (Farnham, 2009). Second, it is very likely that epigenetic modifications influence the binding of a transcription factor to DNA (Farnham, 2009). Third, it is not known if all binding events are really functional. It is imaginable that a transcription factor binds to a consensus motif in all tissues, but regulates the expression in only one (Farnham, 2009). Therefore, to obtain accurate studies of transcription, a prediction based on bioinformatics analysis alone is not sufficient. The physical interaction of the protein of interest with the chromatin has to be verified by biological experiments. Incidentally, much of the knowledge how transcription works and how the genomic information translates to gene expression has been gained from genome-wide studies (Birney et al., 2007).

1.6 PGC-1α in genome-wide studies

PGC-1α was discovered in 1998 and its role as a coactivator and a potent inducer of mitochondrial biogenesis, oxidative phosphorylation, gluconeogenesis and thermogenesis has been described in numerous studies (Handschin and Spiegelman, 2006; Puigserver et al., 1998). Nevertheless, only few studies investigated the activity of PGC-1α on genome-wide scale. In a study published in 2004, Mootha, Handschin and colleagues analysed PGC-1α induced genome-wide expression in cultured skeletal muscle cells (Mootha et al., 2004). They developed motifADE, a motif analysis tool, and applied it to analyse the expression array. MotifADE first ranks differentially expressed genes and

searches then in the promoters of the ranked genes for known transcription factor motifs. MotifADE then tests whether the genes containing a motif tend to rank higher or not. If a motif is found in promoters of genes, which rank high, it can be assumed that the corresponding transcription factor regulates the expression of this subset of PGC-1α induced genes (Mootha et al., 2004). In this study they identified the motifs for ERRα and NRF-2 as top scoring transcription factors motifs, suggesting that these two transcription factors are major binding partners for PGC-1α induced genes in skeletal muscle cells (Mootha et al., 2004). When the interaction of PGC-1α with ERRα was inhibited with the synthetic inverse agonist XCT790, the induction of PGC-1α induced genes with an ERRα binding site in the promoter was diminished. Conversely, PGC-1α genes without ERRα binding site in the promoter were not affected by the inhibitor treatment (Mootha et al., 2004). Schreiber and colleagues demonstrated in another study that PGC-1α requires ERRα expression to induce mitochondrial genes and to increase the content of mitochondrial DNA (Schreiber et al., 2004). A constitutively active form of ERRα induced these pathways even without PGC-1α. These studies suggest that PGC-1α requires ERRα to regulate at least a subset of its target genes. However, it is not precisely known which genes PGC-1α and ERRα regulate together and which independently. It is also not known which PGC-1α target genes are regulated by the direct recruitment of the coactivator to the promoter and which genes are regulated in an indirect manner. The latter issue also concerns the ERRα target genes. The occurrence of an ERRα motif in the promoter does not necessarily mean that ERRα really binds there. This promoter might serve for the regulation of that gene by ERRα but in another tissue or eventually only under certain conditions.

Charest-Marcotte studied the gene regulation by the PGC-1α/ERRα complex in liver and cultured liver cells (Charest-Marcotte et al., 2010). The identified a transcription factor called prospero-related homeobox 1 (Prox1) as a negative regulator of the PGC-1α/ERRα regulated transcription. Prox1 appears to attach to ERRα and repress its transcriptional activity. To study the interaction of these proteins on a genome-wide scale they conducted ChIP-on-chip studies with ERRα and Prox1, but not with PGC-1α (Charest-Marcotte et al., 2010). Therefore the role of PGC-1α on a genome-wide scale cannot be completely delineated from the finding in this study.

The only genome-wide analysis of PGC-1α recruitment to DNA was conducted in cultured liver cells (Charos et al., 2012). ChIP-Seq was performed in human liver carcinoma cells (HepG2), which were treated with forskolin, an activator of PKA, to induce PGC-1α expression. They identified 1886 genomic sites which were occupied by PGC-1α using a false discovery rate (FDR) of 1%. However, this number varies strongly if the value for FDR changes, thus the number of peaks with FDR=5% goes up to 9366 (Charos et al., 2012). Therefore it is hard to estimate which peaks represent real binding events. The motif search of top 250 PGC-1α peaks discovered only three motifs with statistical significance. Top scoring motif was the one for heat shock factor 1 (HSF1), followed by ERRα and CCAAT/enhancer-binding protein beta (CEBPB). However the role of the coactivation of HSF1 by PGC-1α is not clear, because it is not known which biological pathways are regulated by the

two factors together. It is also not known, if the induction of a subset of PGC-1α target gene is diminished if HSF1 is absent. Therefore the role of HSF1 for the regulation of PGC-1α induced genes in liver needs to be further investigated. It is surprising that the motif for HNF4α was not detected in PGC-1α peaks, considering that this factor is important for the PGC-1α regulated hepatic fasting response (Charos et al., 2012; Yoon et al., 2001). When the expression of genes in HepG2 cells was compared PGC-1α peak occurrence, PGC-1α was detected in the proximity of up-regulated and down-regulated genes. It appears that recruitment of PGC-1α to repressed genes is even stronger than to induced genes (Charos et al., 2012). This is surprising, because PGC-1α is mainly known as a coactivator and less as a repressor.

Together, these genome-wide approaches indicate that ERRα appears to be a very important effector of PGC-1α regulated gene expression. But it is not to which extent the PGC-1α regulated gene expression requires ERRα. Other transcription factors like HSF1 might be novel transcriptional partners, but this interaction might be tissue-specific. Are there transcription factors which are active with PGC-1α in all tissues? Which PGC-1α partners are tissue-specific? To answer these questions, the complete transcriptional network still needs to be revealed.

1.7 Aims of the thesis

The work in this thesis focuses on the role of PGC-1α in skeletal muscle. As described above, different signalling events in skeletal muscle converge at some time point on PGC-1α and affect its expression or lead to its posttranslational modification. In this way, extracellular events, activity and metabolic changes influence the availability and activity of PGC-1α in skeletal muscle cells. The combination of these events allows an immense combinatorial complexity of PGC-1α regulation. Following activation, PGC-1α masters the expression of entire gene programs by coactivating key transcription factors. Therefore PGC-1α represents a junction between environmental changes and transcription. Therefore, to fully understand how PGC-1α regulates gene expression in response to metabolic changes, pathways upstream and downstream of PGC-1α have to be studied.

The aims of this thesis can be summarized as follows:

- Upstream: Because cAMP regulates PGC-1α gene expression, we want to discover if the manipulation of intracellular cAMP levels by cyclic nucleotide phosphodiesterase inhibition changes PGC- 1α gene expression or protein levels. If so, which precise phosphodiesterase is involved in this regulation? Does the combined activation of cAMP synthesis together with suppressed hydrolysis by PDE inhibition lead to a long lasting PGC-1α expression in skeletal muscle?

- Downstream: We want to get a global picture of the PGC-1α mediated regulation of gene expression in skeletal muscle cells. To which and to how many genomic locations is PGC-1α recruited? Is this recruitment in the proximity of genes and is it functional? Which biological pathways are regulated by PGC-1α in skeletal muscle cells? Which are the key transcription factors that act together with PGC-1α to regulate this expression changes? Does PGC-1α regulate gene expression directly by binding transcription factors in promoters of these genes or indirectly, or both? Can PGC-1α act as a corepressor?

- Downstream: Based on studies described previously, ERRα appears to be the major effector of PGC-1α induced gene expression. Is that true on a genome-wide scale? To which extent is ERRα required for PGC-1α mediated gene expression changes? In other words, which genes require ERRα to be regulated by PGC-1α? Which biological pathways do these genes regulate? Does ERRα suppress gene expression? Which biological pathways does PGC-1α regulate without ERRα and which transcription factors partner PGC-1α in this case?

1.8 References

Anderson, R.M., Barger, J.L., Edwards, M.G., Braun, K.H., O'Connor, C.E., Prolla, T.A., and Weindruch, R. (2008). Dynamic regulation of PGC-1alpha localization and turnover implicates mitochondrial adaptation in calorie restriction and the stress response. Aging Cell *7*, 101-111.

Arany, Z., Foo, S.Y., Ma, Y., Ruas, J.L., Bommi-Reddy, A., Girnun, G., Cooper, M., Laznik, D., Chinsomboon, J., Rangwala, S.M.*, et al.* (2008). HIF-independent regulation of VEGF and angiogenesis by the transcriptional coactivator PGC-1alpha. Nature *451*, 1008-1012.

Arnold, P., Erb, I., Pachkov, M., Molina, N., and van Nimwegen, E. (2012). MotEvo: integrated Bayesian probabilistic methods for inferring regulatory sites and motifs on multiple alignments of DNA sequences. Bioinformatics *28*, 487-494.

Baar, K., Wende, A.R., Jones, T.E., Marison, M., Nolte, L.A., Chen, M., Kelly, D.P., and Holloszy, J.O. (2002). Adaptations of skeletal muscle to exercise: rapid increase in the transcriptional coactivator PGC-1. Faseb J *16*, 1879-1886.

Bender, A.T., and Beavo, J.A. (2006). Cyclic nucleotide phosphodiesterases: molecular regulation to clinical use. Pharmacol Rev *58*, 488-520.

Bingham, J., Sudarsanam, S., and Srinivasan, S. (2006). Profiling human phosphodiesterase genes and splice isoforms. Biochem Biophys Res Commun *350*, 25-32.

Birney, E., Stamatoyannopoulos, J.A., Dutta, A., Guigo, R., Gingeras, T.R., Margulies, E.H., Weng, Z., Snyder, M., Dermitzakis, E.T., Thurman, R.E.*, et al.* (2007). Identification and analysis of functional elements in 1% of the human genome by the ENCODE pilot project. Nature *447*, 799-816.

Blat, Y., and Kleckner, N. (1999). Cohesins bind to preferential sites along yeast chromosome III, with differential regulation along arms versus the centric region. Cell *98*, 249-259.

Borniquel, S., Valle, I., Cadenas, S., Lamas, S., and Monsalve, M. (2006). Nitric oxide regulates mitochondrial oxidative stress protection via the transcriptional coactivator PGC-1alpha. Faseb J *20*, 1889-1891.

Burns, M.E., and Arshavsky, V.Y. (2005). Beyond counting photons: trials and trends in vertebrate visual transduction. Neuron *48*, 387-401.

Butcher, R.W., and Sutherland, E.W. (1962). Adenosine 3',5'-phosphate in biological materials. I. Purification and properties of cyclic 3',5'-nucleotide phosphodiesterase and use of this enzyme to characterize adenosine 3',5'-phosphate in human urine. J Biol Chem *237*, 1244-1250.

Cai, R., Yu, T., Huang, C., Xia, X., Liu, X., Gu, J., Xue, S., Yeh, E.T., and Cheng, J. (2012). SUMO-specific protease 1 regulates mitochondrial biogenesis through PGC-1alpha. J Biol Chem *287*, 44464-44470.

Canto, C., Gerhart-Hines, Z., Feige, J.N., Lagouge, M., Noriega, L., Milne, J.C., Elliott, P.J., Puigserver, P., and Auwerx, J. (2009). AMPK regulates energy expenditure by modulating NAD+ metabolism and SIRT1 activity. Nature *458*, 1056-1060.

Cao, W., Collins, Q.F., Becker, T.C., Robidoux, J., Lupo, E.G., Jr., Xiong, Y., Daniel, K.W., Floering, L., and Collins, S. (2005). p38 Mitogen-activated protein kinase plays a stimulatory role in hepatic gluconeogenesis. J Biol Chem *280*, 42731-42737.

Cao, W., Daniel, K.W., Robidoux, J., Puigserver, P., Medvedev, A.V., Bai, X., Floering, L.M., Spiegelman, B.M., and Collins, S. (2004). p38 mitogen-activated protein kinase is the central regulator of cyclic AMP-dependent transcription of the brown fat uncoupling protein 1 gene. Mol Cell Biol *24*, 3057-3067.

Chang, J.S., Huypens, P., Zhang, Y., Black, C., Kralli, A., and Gettys, T.W. (2010). Regulation of NT-PGC-1alpha subcellular localization and function by protein kinase A-dependent modulation of nuclear export by CRM1. J Biol Chem *285*, 18039-18050.

Charest-Marcotte, A., Dufour, C.R., Wilson, B.J., Tremblay, A.M., Eichner, L.J., Arlow, D.H., Mootha, V.K., and Giguere, V. (2010). The homeobox protein Prox1 is a negative modulator of ERR{alpha}/PGC-1{alpha} bioenergetic functions. Genes Dev *24*, 537-542.

Charos, A.E., Reed, B.D., Raha, D., Szekely, A.M., Weissman, S.M., and Snyder, M. (2012). A highly integrated and complex PPARGC1A transcription factor binding network in HepG2 cells. Genome Res *22*, 1668-1679.

Collins, Q.F., Xiong, Y., Lupo, E.G., Jr., Liu, H.Y., and Cao, W. (2006). p38 Mitogen-activated protein kinase mediates free fatty acid-induced gluconeogenesis in hepatocytes. J Biol Chem *281*, 24336-24344.

Cooper, D.M. (2003). Regulation and organization of adenylyl cyclases and cAMP. Biochem J *375*, 517-529.

Coward, R.M., and Carson, C.C. (2008). Tadalafil in the treatment of erectile dysfunction. Ther Clin Risk Manag *4*, 1315-1330.

Cowell, R.M., Blake, K.R., and Russell, J.W. (2007). Localization of the transcriptional coactivator PGC-1alpha to GABAergic neurons during maturation of the rat brain. J Comp Neurol *502*, 1-18.

Euskirchen, G.M., Rozowsky, J.S., Wei, C.L., Lee, W.H., Zhang, Z.D., Hartman, S., Emanuelsson, O., Stolc, V., Weissman, S., Gerstein, M.B.*, et al.* (2007). Mapping of transcription factor binding regions in mammalian cells by ChIP: comparison of array- and sequencing-based technologies. Genome Res *17*, 898-909.

Fan, M., Rhee, J., St-Pierre, J., Handschin, C., Puigserver, P., Lin, J., Jaeger, S., Erdjument-Bromage, H., Tempst, P., and Spiegelman, B.M. (2004). Suppression of mitochondrial respiration through recruitment of p160 myb binding protein to PGC-1alpha: modulation by p38 MAPK. Genes Dev *18*, 278-289.

Farnham, P.J. (2009). Insights from genomic profiling of transcription factors. Nat Rev Genet *10*, 605-616.

Fernandez-Marcos, P.J., and Auwerx, J. (2011). Regulation of PGC-1alpha, a nodal regulator of mitochondrial biogenesis. Am J Clin Nutr *93*, 884S-890.

Fields, S. (2007). Molecular biology. Site-seeing by sequencing. Science *316*, 1441-1442.

Finck, B.N., and Kelly, D.P. (2006). PGC-1 coactivators: inducible regulators of energy metabolism in health and disease. J Clin Invest *116*, 615-622.

Francis, S.H., Blount, M.A., and Corbin, J.D. (2011). Mammalian cyclic nucleotide phosphodiesterases: molecular mechanisms and physiological functions. Physiol Rev *91*, 651-690.

Francis, S.H., Turko, I.V., and Corbin, J.D. (2001). Cyclic nucleotide phosphodiesterases: relating structure and function. Prog Nucleic Acid Res Mol Biol *65*, 1-52.

Fritah, A., Christian, M., and Parker, M.G. (2010). The metabolic coregulator RIP140: an update. Am J Physiol Endocrinol Metab *299*, E335-340.

Furey, T.S. (2012). ChIP-seq and beyond: new and improved methodologies to detect and characterize protein-DNA interactions. Nat Rev Genet *13*, 840-852.

Gerhart-Hines, Z., Rodgers, J.T., Bare, O., Lerin, C., Kim, S.H., Mostoslavsky, R., Alt, F.W., Wu, Z., and Puigserver, P. (2007). Metabolic control of muscle mitochondrial function and fatty acid oxidation through SIRT1/PGC-1alpha. Embo J *26*, 1913-1923.

Hallberg, M., Morganstein, D.L., Kiskinis, E., Shah, K., Kralli, A., Dilworth, S.M., White, R., Parker, M.G., and Christian, M. (2008). A functional interaction between RIP140 and PGC-1alpha regulates the expression of the lipid droplet protein CIDEA. Mol Cell Biol *28*, 6785-6795.

Handschin, C. (2009). The biology of PGC-1alpha and its therapeutic potential. Trends Pharmacol Sci *30*, 322-329.

Handschin, C., Kobayashi, Y.M., Chin, S., Seale, P., Campbell, K.P., and Spiegelman, B.M. (2007). PGC-1alpha regulates the neuromuscular junction program and ameliorates Duchenne muscular dystrophy. Genes Dev *21*, 770-783.

Handschin, C., Lin, J., Rhee, J., Peyer, A.K., Chin, S., Wu, P.H., Meyer, U.A., and Spiegelman, B.M. (2005). Nutritional regulation of hepatic heme biosynthesis and porphyria through PGC-1alpha. Cell *122*, 505-515.

Handschin, C., Rhee, J., Lin, J., Tarr, P.T., and Spiegelman, B.M. (2003). An autoregulatory loop controls peroxisome proliferator-activated receptor gamma coactivator 1alpha expression in muscle. Proc Natl Acad Sci U S A *100*, 7111-7116.

Handschin, C., and Spiegelman, B.M. (2006). Peroxisome proliferator-activated receptor gamma coactivator 1 coactivators, energy homeostasis, and metabolism. Endocr Rev *27*, 728-735.

Hansen, G., Jin, S., Umetsu, D.T., and Conti, M. (2000). Absence of muscarinic cholinergic airway responses in mice deficient in the cyclic nucleotide phosphodiesterase PDE4D. Proc Natl Acad Sci U S A *97*, 6751-6756.

Hardie, D.G., and Hawley, S.A. (2001). AMP-activated protein kinase: the energy charge hypothesis revisited. Bioessays *23*, 1112-1119.

Heery, D.M., Kalkhoven, E., Hoare, S., and Parker, M.G. (1997). A signature motif in transcriptional co-activators mediates binding to nuclear receptors. Nature *387*, 733-736.

Herzig, S., Long, F., Jhala, U.S., Hedrick, S., Quinn, R., Bauer, A., Rudolph, D., Schutz, G., Yoon, C., Puigserver, P.*, et al.* (2001). CREB regulates hepatic gluconeogenesis through the coactivator PGC-1. Nature *413*, 179-183.

Houslay, M.D., and Adams, D.R. (2003). PDE4 cAMP phosphodiesterases: modular enzymes that orchestrate signalling cross-talk, desensitization and compartmentalization. Biochem J *370*, 1-18.

Housley, M.P., Udeshi, N.D., Rodgers, J.T., Shabanowitz, J., Puigserver, P., Hunt, D.F., and Hart, G.W. (2009). A PGC-1alpha-O-GlcNAc transferase complex regulates FoxO transcription factor activity in response to glucose. J Biol Chem *284*, 5148-5157.

Houtkooper, R.H., Canto, C., Wanders, R.J., and Auwerx, J. (2010). The secret life of NAD+: an old metabolite controlling new metabolic signaling pathways. Endocr Rev *31*, 194-223.

Jager, S., Handschin, C., St-Pierre, J., and Spiegelman, B.M. (2007). AMP-activated protein kinase (AMPK) action in skeletal muscle via direct phosphorylation of PGC-1alpha. Proc Natl Acad Sci U S A *104*, 12017-12022.

Johnson, D.S., Mortazavi, A., Myers, R.M., and Wold, B. (2007). Genome-wide mapping of in vivo protein-DNA interactions. Science *316*, 1497-1502.

Kaeberlein, M., McVey, M., and Guarente, L. (1999). The SIR2/3/4 complex and SIR2 alone promote longevity in Saccharomyces cerevisiae by two different mechanisms. Genes Dev *13*, 2570-2580.

Kawakami, Y., Tsuda, M., Takahashi, S., Taniguchi, N., Esteban, C.R., Zemmyo, M., Furumatsu, T., Lotz, M., Izpisua Belmonte, J.C., and Asahara, H. (2005). Transcriptional coactivator PGC-1alpha regulates chondrogenesis via association with Sox9. Proc Natl Acad Sci U S A *102*, 2414-2419.

Knutti, D., Kaul, A., and Kralli, A. (2000). A tissue-specific coactivator of steroid receptors, identified in a functional genetic screen. Mol Cell Biol *20*, 2411-2422.

Koo, S.H., Satoh, H., Herzig, S., Lee, C.H., Hedrick, S., Kulkarni, R., Evans, R.M., Olefsky, J., and Montminy, M. (2004). PGC-1 promotes insulin resistance in liver through PPAR-alpha-dependent induction of TRB-3. Nat Med *10*, 530-534.

Langmead, B., Trapnell, C., Pop, M., and Salzberg, S.L. (2009). Ultrafast and memory-efficient alignment of short DNA sequences to the human genome. Genome Biol *10*, R25.

Lehman, J.J., Barger, P.M., Kovacs, A., Saffitz, J.E., Medeiros, D.M., and Kelly, D.P. (2000). Peroxisome proliferator-activated receptor gamma coactivator-1 promotes cardiac mitochondrial biogenesis. J Clin Invest *106*, 847-856.

Leone, T.C., Lehman, J.J., Finck, B.N., Schaeffer, P.J., Wende, A.R., Boudina, S., Courtois, M., Wozniak, D.F., Sambandam, N., Bernal-Mizrachi, C.*, et al.* (2005). PGC-1alpha deficiency causes multi-system energy metabolic derangements: muscle dysfunction, abnormal weight control and hepatic steatosis. PLoS Biol *3*, e101.

Leone, T.C., Weinheimer, C.J., and Kelly, D.P. (1999). A critical role for the peroxisome proliferator-activated receptor alpha (PPARalpha) in the cellular fasting response: the PPARalpha-null mouse as a model of fatty acid oxidation disorders. Proc Natl Acad Sci U S A *96*, 7473-7478.

Lerin, C., Rodgers, J.T., Kalume, D.E., Kim, S.H., Pandey, A., and Puigserver, P. (2006). GCN5 acetyltransferase complex controls glucose metabolism through transcriptional repression of PGC-1alpha. Cell Metab *3*, 429-438.

Li, H., Ruan, J., and Durbin, R. (2008a). Mapping short DNA sequencing reads and calling variants using mapping quality scores. Genome Res *18*, 1851-1858.

Li, S., Liu, C., Li, N., Hao, T., Han, T., Hill, D.E., Vidal, M., and Lin, J.D. (2008b). Genome-wide coactivation analysis of PGC-1alpha identifies BAF60a as a regulator of hepatic lipid metabolism. Cell Metab *8*, 105-117.

Li, X., Monks, B., Ge, Q., and Birnbaum, M.J. (2007). Akt/PKB regulates hepatic metabolism by directly inhibiting PGC-1alpha transcription coactivator. Nature *447*, 1012-1016.

Lin, J., Handschin, C., and Spiegelman, B.M. (2005). Metabolic control through the PGC-1 family of transcription coactivators. Cell Metab *1*, 361-370.

Lin, J., Wu, H., Tarr, P.T., Zhang, C.Y., Wu, Z., Boss, O., Michael, L.F., Puigserver, P., Isotani, E., Olson, E.N.*, et al.* (2002). Transcriptional co-activator PGC-1 alpha drives the formation of slow-twitch muscle fibres. Nature *418*, 797-801.

Lin, J., Wu, P.H., Tarr, P.T., Lindenberg, K.S., St-Pierre, J., Zhang, C.Y., Mootha, V.K., Jager, S., Vianna, C.R., Reznick, R.M.*, et al.* (2004). Defects in adaptive energy metabolism with CNS-linked hyperactivity in PGC-1alpha null mice. Cell *119*, 121-135.

Liu, C., Li, S., Liu, T., Borjigin, J., and Lin, J.D. (2007). Transcriptional coactivator PGC-1alpha integrates the mammalian clock and energy metabolism. Nature *447*, 477-481.

Lustig, Y., Ruas, J.L., Estall, J.L., Lo, J.C., Devarakonda, S., Laznik, D., Choi, J.H., Ono, H., Olsen, J.V., and Spiegelman, B.M. (2011). Separation of the gluconeogenic and mitochondrial functions of PGC-1{alpha} through S6 kinase. Genes Dev *25*, 1232-1244.

Meyer, L.R., Zweig, A.S., Hinrichs, A.S., Karolchik, D., Kuhn, R.M., Wong, M., Sloan, C.A., Rosenbloom, K.R., Roe, G., Rhead, B.*, et al.* (2013). The UCSC Genome Browser database: extensions and updates 2013. Nucleic Acids Res *41*, D64-69.

Michael, L.F., Wu, Z., Cheatham, R.B., Puigserver, P., Adelmant, G., Lehman, J.J., Kelly, D.P., and Spiegelman, B.M. (2001). Restoration of insulin-sensitive glucose transporter (GLUT4) gene expression in muscle cells by the transcriptional coactivator PGC-1. Proc Natl Acad Sci U S A *98*, 3820-3825.

Miura, S., Kawanaka, K., Kai, Y., Tamura, M., Goto, M., Shiuchi, T., Minokoshi, Y., and Ezaki, O. (2007). An increase in murine skeletal muscle peroxisome proliferator-activated receptor-gamma coactivator-1alpha (PGC-1alpha) mRNA in response to exercise is mediated by beta-adrenergic receptor activation. Endocrinology *148*, 3441-3448.

Monsalve, M., Wu, Z., Adelmant, G., Puigserver, P., Fan, M., and Spiegelman, B.M. (2000). Direct coupling of transcription and mRNA processing through the thermogenic coactivator PGC-1. Mol Cell *6*, 307-316.

Mootha, V.K., Handschin, C., Arlow, D., Xie, X., St Pierre, J., Sihag, S., Yang, W., Altshuler, D., Puigserver, P., Patterson, N.*, et al.* (2004). Erralpha and Gabpa/b specify PGC-1alpha-dependent oxidative phosphorylation gene expression that is altered in diabetic muscle. Proc Natl Acad Sci U S A *101*, 6570-6575.

Nervina, J.M., Magyar, C.E., Pirih, F.Q., and Tetradis, S. (2006). PGC-1alpha is induced by parathyroid hormone and coactivates Nurr1-mediated promoter activity in osteoblasts. Bone *39*, 1018-1025.

Nisoli, E., Clementi, E., Paolucci, C., Cozzi, V., Tonello, C., Sciorati, C., Bracale, R., Valerio, A., Francolini, M., Moncada, S.*, et al.* (2003). Mitochondrial biogenesis in mammals: the role of endogenous nitric oxide. Science *299*, 896-899.

Oberkofler, H., Schraml, E., Krempler, F., and Patsch, W. (2003). Potentiation of liver X receptor transcriptional activity by peroxisome-proliferator-activated receptor gamma co-activator 1 alpha. Biochem J *371*, 89-96.

Olson, B.L., Hock, M.B., Ekholm-Reed, S., Wohlschlegel, J.A., Dev, K.K., Kralli, A., and Reed, S.I. (2008). SCFCdc4 acts antagonistically to the PGC-1alpha transcriptional coactivator by targeting it for ubiquitin-mediated proteolysis. Genes Dev *22*, 252-264.

Olson, E.N., and Williams, R.S. (2000). Calcineurin signaling and muscle remodeling. Cell *101*, 689-692.

Omori, K., and Kotera, J. (2007). Overview of PDEs and their regulation. Circ Res *100*, 309-327.

Park, P.J. (2009). ChIP-seq: advantages and challenges of a maturing technology. Nat Rev Genet *10*, 669-680.

Pilegaard, H., Saltin, B., and Neufer, P.D. (2003). Exercise induces transient transcriptional activation of the PGC-1alpha gene in human skeletal muscle. J Physiol *546*, 851-858.

Puigserver, P., Adelmant, G., Wu, Z., Fan, M., Xu, J., O'Malley, B., and Spiegelman, B.M. (1999). Activation of PPARgamma coactivator-1 through transcription factor docking. Science *286*, 1368-1371.

Puigserver, P., Rhee, J., Donovan, J., Walkey, C.J., Yoon, J.C., Oriente, F., Kitamura, Y., Altomonte, J., Dong, H., Accili, D.*, et al.* (2003). Insulin-regulated hepatic gluconeogenesis through FOXO1-PGC-1alpha interaction. Nature *423*, 550-555.

Puigserver, P., Rhee, J., Lin, J., Wu, Z., Yoon, J.C., Zhang, C.Y., Krauss, S., Mootha, V.K., Lowell, B.B., and Spiegelman, B.M. (2001). Cytokine stimulation of energy expenditure through p38 MAP kinase activation of PPARgamma coactivator-1. Mol Cell *8*, 971-982.

Puigserver, P., and Spiegelman, B.M. (2003). Peroxisome proliferator-activated receptor-gamma coactivator 1 alpha (PGC-1 alpha): transcriptional coactivator and metabolic regulator. Endocr Rev *24*, 78-90.

Puigserver, P., Wu, Z., Park, C.W., Graves, R., Wright, M., and Spiegelman, B.M. (1998). A cold-inducible coactivator of nuclear receptors linked to adaptive thermogenesis. Cell *92*, 829-839.

Qin, W., Haroutunian, V., Katsel, P., Cardozo, C.P., Ho, L., Buxbaum, J.D., and Pasinetti, G.M. (2009). PGC-1alpha expression decreases in the Alzheimer disease brain as a function of dementia. Arch Neurol *66*, 352-361.

Rall, T.W., and Sutherland, E.W. (1958). Formation of a cyclic adenine ribonucleotide by tissue particles. J Biol Chem *232*, 1065-1076.

Rall, T.W., and Sutherland, E.W. (1962). Adenyl cyclase. II. The enzymatically catalyzed formation of adenosine 3',5'-phosphate and inorganic pyrophosphate from adenosine triphosphate. J Biol Chem *237*, 1228-1232.

Ren, B., Robert, F., Wyrick, J.J., Aparicio, O., Jennings, E.G., Simon, I., Zeitlinger, J., Schreiber, J., Hannett, N., Kanin, E.*, et al.* (2000). Genome-wide location and function of DNA binding proteins. Science *290*, 2306-2309.

Rhee, J., Ge, H., Yang, W., Fan, M., Handschin, C., Cooper, M., Lin, J., Li, C., and Spiegelman, B.M. (2006). Partnership of PGC-1alpha and HNF4alpha in the regulation of lipoprotein metabolism. J Biol Chem *281*, 14683-14690.

Robertson, G., Hirst, M., Bainbridge, M., Bilenky, M., Zhao, Y., Zeng, T., Euskirchen, G., Bernier, B., Varhol, R., Delaney, A.*, et al.* (2007). Genome-wide profiles of STAT1 DNA association using chromatin immunoprecipitation and massively parallel sequencing. Nat Methods *4*, 651-657.

Rodgers, J.T., Haas, W., Gygi, S.P., and Puigserver, P. (2010). Cdc2-like kinase 2 is an insulin-regulated suppressor of hepatic gluconeogenesis. Cell Metab *11*, 23-34.

Rodgers, J.T., Lerin, C., Haas, W., Gygi, S.P., Spiegelman, B.M., and Puigserver, P. (2005). Nutrient control of glucose homeostasis through a complex of PGC-1alpha and SIRT1. Nature *434*, 113-118.

Rowe, G.C., Jiang, A., and Arany, Z. (2010). PGC-1 coactivators in cardiac development and disease. Circ Res *107*, 825-838.

Rozowsky, J., Euskirchen, G., Auerbach, R.K., Zhang, Z.D., Gibson, T., Bjornson, R., Carriero, N., Snyder, M., and Gerstein, M.B. (2009). PeakSeq enables systematic scoring of ChIP-seq experiments relative to controls. Nat Biotechnol *27*, 66-75.

Russell, A.P., Feilchenfeldt, J., Schreiber, S., Praz, M., Crettenand, A., Gobelet, C., Meier, C.A., Bell, D.R., Kralli, A., Giacobino, J.P.*, et al.* (2003). Endurance training in humans leads to fiber type-specific increases in levels of peroxisome proliferator-activated receptor-gamma coactivator-1 and peroxisome proliferator-activated receptor-alpha in skeletal muscle. Diabetes *52*, 2874-2881.

Rytinki, M.M., and Palvimo, J.J. (2008). SUMOylation modulates the transcription repressor function of RIP140. J Biol Chem *283*, 11586-11595.

Rytinki, M.M., and Palvimo, J.J. (2009). SUMOylation attenuates the function of PGC-1alpha. J Biol Chem *284*, 26184-26193.

Sandri, M., Lin, J., Handschin, C., Yang, W., Arany, Z.P., Lecker, S.H., Goldberg, A.L., and Spiegelman, B.M. (2006). PGC-1alpha protects skeletal muscle from atrophy by suppressing FoxO3 action and atrophy-specific gene transcription. Proc Natl Acad Sci U S A *103*, 16260-16265.

Sassone-Corsi, P. (2012). The cyclic AMP pathway. Cold Spring Harb Perspect Biol *4*.

Schmidt, S.F., and Mandrup, S. (2011). Gene program-specific regulation of PGC-1{alpha} activity. Genes Dev *25*, 1453-1458.

Schreiber, S.N., Emter, R., Hock, M.B., Knutti, D., Cardenas, J., Podvinec, M., Oakeley, E.J., and Kralli, A. (2004). The estrogen-related receptor alpha (ERRalpha) functions in PPARgamma coactivator 1alpha (PGC-1alpha)-induced mitochondrial biogenesis. Proc Natl Acad Sci U S A *101*, 6472-6477.

Semple, R.K., Crowley, V.C., Sewter, C.P., Laudes, M., Christodoulides, C., Considine, R.V., Vidal-Puig, A., and O'Rahilly, S. (2004). Expression of the thermogenic nuclear hormone receptor coactivator PGC-1alpha is reduced in the adipose tissue of morbidly obese subjects. Int J Obes Relat Metab Disord *28*, 176-179.

Shin, D.J., Campos, J.A., Gil, G., and Osborne, T.F. (2003). PGC-1alpha activates CYP7A1 and bile acid biosynthesis. J Biol Chem *278*, 50047-50052.

Shin, J.H., Ko, H.S., Kang, H., Lee, Y., Lee, Y.I., Pletinkova, O., Troconso, J.C., Dawson, V.L., and Dawson, T.M. (2011). PARIS (ZNF746) repression of PGC-1alpha contributes to neurodegeneration in Parkinson's disease. Cell *144*, 689-702.

Shoag, J., Haq, R., Zhang, M., Liu, L., Rowe, G.C., Jiang, A., Koulisis, N., Farrel, C., Amos, C.I., Wei, Q.*, et al.* (2013). PGC-1 coactivators regulate MITF and the tanning response. Mol Cell *49*, 145-157.

Siddharthan, R., Siggia, E.D., and van Nimwegen, E. (2005). PhyloGibbs: a Gibbs sampling motif finder that incorporates phylogeny. PLoS Comput Biol *1*, e67.

Southgate, R.J., Bruce, C.R., Carey, A.L., Steinberg, G.R., Walder, K., Monks, R., Watt, M.J., Hawley, J.A., Birnbaum, M.J., and Febbraio, M.A. (2005). PGC-1alpha gene expression is down-regulated by Akt- mediated phosphorylation and nuclear exclusion of FoxO1 in insulin-stimulated skeletal muscle. Faseb J *19*, 2072-2074.

St-Pierre, J., Drori, S., Uldry, M., Silvaggi, J.M., Rhee, J., Jager, S., Handschin, C., Zheng, K., Lin, J., Yang, W.*, et al.* (2006). Suppression of reactive oxygen species and neurodegeneration by the PGC-1 transcriptional coactivators. Cell *127*, 397-408.

Sutherland, E.W., and Rall, T.W. (1958). Fractionation and characterization of a cyclic adenine ribonucleotide formed by tissue particles. J Biol Chem *232*, 1077-1091.

Sutherland, E.W., Rall, T.W., and Menon, T. (1962). Adenyl cylase. I. Distribution, preparation, and properties. J Biol Chem *237*, 1220-1227.

Tadaishi, M., Miura, S., Kai, Y., Kawasaki, E., Koshinaka, K., Kawanaka, K., Nagata, J., Oishi, Y., and Ezaki, O. (2011). Effect of exercise intensity and AICAR on isoform-specific expressions of murine skeletal muscle PGC-1alpha mRNA: a role of beta(2)-adrenergic receptor activation. Am J Physiol Endocrinol Metab *300*, E341-349.

Teyssier, C., Ma, H., Emter, R., Kralli, A., and Stallcup, M.R. (2005). Activation of nuclear receptor coactivator PGC-1alpha by arginine methylation. Genes Dev *19*, 1466-1473.

Tissenbaum, H.A., and Guarente, L. (2001). Increased dosage of a sir-2 gene extends lifespan in Caenorhabditis elegans. Nature *410*, 227-230.

Wagner, P.D. (2011). The critical role of VEGF in skeletal muscle angiogenesis and blood flow. Biochem Soc Trans *39*, 1556-1559.

Wallberg, A.E., Yamamura, S., Malik, S., Spiegelman, B.M., and Roeder, R.G. (2003). Coordination of p300-mediated chromatin remodeling and TRAP/mediator function through coactivator PGC-1alpha. Mol Cell *12*, 1137-1149.

Wei, P., Pan, D., Mao, C., and Wang, Y.X. (2012). RNF34 is a cold-regulated E3 ubiquitin ligase for PGC-1alpha and modulates brown fat cell metabolism. Mol Cell Biol *32*, 266-275.

Wright, D.C., Han, D.H., Garcia-Roves, P.M., Geiger, P.C., Jones, T.E., and Holloszy, J.O. (2007). Exercise-induced mitochondrial biogenesis begins before the increase in muscle PGC-1alpha expression. J Biol Chem *282*, 194-199.

Wu, R.C., Smith, C.L., and O'Malley, B.W. (2005). Transcriptional regulation by steroid receptor coactivator phosphorylation. Endocr Rev *26*, 393-399.

Wu, Z., Puigserver, P., Andersson, U., Zhang, C., Adelmant, G., Mootha, V., Troy, A., Cinti, S., Lowell, B., Scarpulla, R.C*., et al.* (1999). Mechanisms controlling mitochondrial biogenesis and respiration through the thermogenic coactivator PGC-1. Cell *98*, 115-124.

Yan, C., Zhao, A.Z., Bentley, J.K., Loughney, K., Ferguson, K., and Beavo, J.A. (1995). Molecular cloning and characterization of a calmodulin-dependent phosphodiesterase enriched in olfactory sensory neurons. Proc Natl Acad Sci U S A *92*, 9677-9681.

Yoon, J.C., Puigserver, P., Chen, G., Donovan, J., Wu, Z., Rhee, J., Adelmant, G., Stafford, J., Kahn, C.R., Granner, D.K*., et al.* (2001). Control of hepatic gluconeogenesis through the transcriptional coactivator PGC-1. Nature *413*, 131-138.

Zhang, H.T., Huang, Y., Jin, S.L., Frith, S.A., Suvarna, N., Conti, M., and O'Donnell, J.M. (2002). Antidepressant-like profile and reduced sensitivity to rolipram in mice deficient in the PDE4D phosphodiesterase enzyme. Neuropsychopharmacology *27*, 587-595.

Zhang, Y., Castellani, L.W., Sinal, C.J., Gonzalez, F.J., and Edwards, P.A. (2004). Peroxisome proliferator-activated receptor-gamma coactivator 1alpha (PGC-1alpha) regulates triglyceride metabolism by activation of the nuclear receptor FXR. Genes Dev *18*, 157-169.

Zhang, Y., Huypens, P., Adamson, A.W., Chang, J.S., Henagan, T.M., Boudreau, A., Lenard, N.R., Burk, D., Klein, J., Perwitz, N*., et al.* (2009). Alternative mRNA splicing produces a novel biologically active short isoform of PGC-1alpha. J Biol Chem *284*, 32813-32826.

Zhang, Y., Liu, T., Meyer, C.A., Eeckhoute, J., Johnson, D.S., Bernstein, B.E., Nusbaum, C., Myers, R.M., Brown, M., Li, W*., et al.* (2008). Model-based analysis of ChIP-Seq (MACS). Genome Biol *9*, R137.

2 MANUSCRIPT-1: Transcriptional network analysis in muscle reveals AP-1 as a partner of PGC-1α in the hypoxic gene program

(Manuscript submitted for publication)

SHORT TITLE: PGC-1α-regulated transcriptional network in muscle

Mario Baresic[1,*], Silvia Salatino[1,2,3,*], Erik van Nimwegen[2,3,#], and Christoph Handschin[1,#]

[1]Focal Area Growth & Development and [2]Focal Area Computational & Systems Biology, Biozentrum, University of Basel, Basel, Switzerland

[3]Swiss Institute of Bioinformatics, Basel, Switzerland

[*]These authors contributed equally to this manuscript

[#]Correspondence to: Christoph Handschin, Biozentrum, University of Basel, Klingelbergstrasse 70, CH-4056 Basel, Switzerland, email: christoph.handschin@unibas.ch +41 (0)61 267 23 78 or Erik van Nimwegen, Biozentrum, University of Basel, Klingelbergstrasse 70, CH-4056 Basel, Switzerland, email: erik.vannimwegen@unibas.ch +41 (0) 61 267 15 76.

In this study I:

- contributed to the planning and design of this project.
- performed all the wet-lab experiments: cell culture, chromatin immunoprecipitation (including optimization of the entire protocol to be applied for ChIP-Seq), expression arrays, knockdown of transcription factors by siRNA and the validation of the knockdown by real-time PCR.
- contributed to the analysis and the interpretation of the results.
- Contributed to the writing of the manuscript.

KEYWORDS: PGC-1α; transcriptional coactivators; skeletal muscle; transcriptional network; ChIP-Seq; transcription factor binding site prediction; motif activity response analysis; transcriptional regulation

2.1 Abstract

Skeletal muscle tissue shows an extraordinary cellular plasticity, but the underlying molecular mechanisms are still poorly understood. Here we use a combination of experimental and computational approaches to unravel the complex transcriptional network of muscle cell plasticity centered on the peroxisome proliferator-activated receptor γ coactivator 1α (PGC-1α), a regulatory nexus in endurance training adaptation. By integrating data on genome-wide binding of PGC-1α and gene expression upon PGC-1α over-expression with comprehensive computational prediction of transcription factor binding sites (TFBSs), we uncover a hitherto underestimated number of transcription factor partners involved in mediating PGC-1α action. In particular, principal component analysis of TFBSs at PGC-1α binding regions predicts that, besides the well-known role of the estrogen-related receptor α (ERRα), the activator protein-1 complex (AP-1) plays a major role in regulating the PGC-1α-controlled gene program of hypoxia response. Our findings thus reveal the complex transcriptional network of muscle cell plasticity controlled by PGC-1α.

Significance statement

PGC-1α coordinates the adaptations of skeletal muscle to endurance exercise by regulating the transcription of the entire gene program required for this enormous cellular remodeling. By acting as a transcriptional coactivator, PGC-1α modulates the activity of numerous transcription factors. In the present study, we identified the genomic locations to which PGC-1α is recruited in skeletal muscle cells. Moreover, we linked the recruitment data with functional outcome in terms of gene expression as well as prediction and validation of transcription factor binding partners involved in the genome-wide control of PGC-1α-regulated muscle gene expression. In doing so, we identified AP-1 as a novel transcriptional partner of PGC-1α in the regulation of the gene program for hypoxia in muscle.

2.2 Introduction

A sedentary life style can lead to an imbalance between energy intake and expenditure and favors the development of a number of chronic diseases like obesity and type 2 diabetes. Regular exercise on the other hand is an effective way to reduce the risk for these lifestyle-related pathologies (1). The health benefits of exercise are at least in part induced by changes in skeletal muscle tissue. Muscle cells exhibit a high plasticity and thus a remarkably complex adaptation to increased contractile activity. For example, endurance training induces mitochondrial biogenesis, increases capillary density and improves insulin sensitivity (1, 2). To achieve such a complex plastic response, a number of different signaling pathways are activated in an exercising muscle, for example p38 MAPK-mediated protein phosphorylation events, increased intracellular calcium levels or the activation of the metabolic sensors AMP-dependent protein kinase (AMPK) and sirtuin-1 (SIRT1) (3). While the temporal coordination of the numerous inputs is not clear, all of the major signaling pathways converge on the peroxisome proliferator-activated receptor γ coactivator 1α (PGC-1α) to either induce *Ppargc1a* gene expression, promote post-translational modifications of the PGC-1α protein, or by doing both (4, 5). Upon activation, PGC-1α mediates the muscular adaptations to endurance exercise by coactivating various transcription factors (TFs) involved in the regulation of diverse biological programs such as mitochondrial biogenesis, angiogenesis, ROS detoxification or glucose uptake (3). Accordingly, transgenic expression of PGC-1α in mouse skeletal muscle at physiological levels not only induces mitochondrial biogenesis but also drives a fiber type conversion towards a more oxidative, slow-twitch phenotype (6) while muscle-specific *Ppargc1a* knockout animals exhibit several symptoms of pathological inactivity (7, 8).

Coregulators are part of multicomponent regulatory protein complexes that are well suited to translate external stimuli into changes in promoter and enhancer activities by combining various enzymatic activities to modulate histones and chromatin structure, and recruit other TFs (9). Thus, dynamic assembly of distinct coregulator complexes enables the integration of many different signaling pathways leading to a coordinated and specific regulation of entire biological programs by multiple TFs (10, 11). For example, PGC-1α not only recruits histone acetylases (12), the TRAP/DRIP/Mediator (13) as well as the SWI/SNF protein complexes (14), but also binds to and coactivates a myriad of different transcription factors, even though a systematic inventory of TF binding partners has not been compiled yet (15). Thus, the specific control exerted by the PGC-1α-dependent transcriptional network might provide an explanation for the dynamic and coordinated muscle adaptation to exercise. Since PGC-1α in skeletal muscle not only confers a trained phenotype, but also ameliorates several different muscle diseases (16), the unraveling of the PGC-1α-controlled transcriptional network in skeletal muscle would be of great interest to identify putative therapeutic targets within this pathway.

Therefore, we aimed at obtaining a global picture of the co-regulatory activity of PGC-1α in skeletal muscle cells. More precisely, by combining data on the genome-wide binding locations of PGC-1α

and the gene expression profiles in response to PGC-1α over-expression with comprehensive computational prediction of transcription factor binding site (TFBS) occurrence, we sought to unveil the biological processes that are regulated by PGC-1α, to identify the transcription factors that partner with PGC-1α, and to determine the mechanistic details of PGC-1α-regulated transcription. We not only mapped the locations on the DNA where PGC-1α was bound, but also delineated the target genes whose expression is either directly or indirectly affected by PGC-1α and identified novel putative transcription factor partners that mediated PGC-1α's action. In particular, our results strongly suggest that the activator protein-1 (AP-1) complex is a major regulatory partner of PGC-1α, with AP-1 and PGC-1α together regulating the hypoxic response gene program in muscle cells.

2.3 Results

2.3.1 Broad recruitment of PGC-1α to the mouse genome

PGC-1α-dependent gene transcription has been studied in many different experimental contexts. In isolation, gene expression arrays however are unable to distinguish direct from indirect targets, or to reveal the genomic sites where PGC-1α is recruited to enhancer and promoter elements, i.e. by coactivating TFs that directly bind to the DNA. Thus, we first performed chromatin immunoprecipitation followed by deep sequencing (ChIP-Seq) of PGC-1α in differentiated C2C12 mouse myotubes to identify the locations where PGC-1α is bound to the genome. To identify genomic regions that are significantly enriched in the ChIP, we slid a 200 bp window across the genome comparing the local ChIP read density with the read density from a background whole cell extract sample. We selected all regions with a Z-statistic larger than 4.5 as significantly enriched (FDR 0.6%, Suppl. Fig. S1A). Using this stringent cutoff, we identified 7512 binding regions for PGC-1α via interaction with a TF genome-wide, which include binding regions in the promoters of known PGC-1α target genes (Fig. 1A) such as medium-chain specific acyl-CoA dehydrogenase (*Acadm*) and cytochrome c (*Cycs*) (17, 18). The enrichment of immunoprecipitated DNA fragments from the ChIP-Seq was validated for these and other PGC-1α target genes by semiquantitative real-time PCR (Fig. 1B). In absolute terms, the distribution of the ChIP-Seq peaks revealed that PGC-1α is mostly recruited at distal sites from the assigned targets and, to a lesser extent, to proximal regions of the gene or within an intronic sequence (Fig. 1C). However, when compared to randomly selected DNA regions of equal size and number, PGC-1α binding peaks occur twice as often within 10 kb upstream of the transcription start site (TSS).

In parallel to the ChIP-Seq experiment, we furthermore analyzed gene expression patterns in differentiated muscle cells both in control condition and under PGC-1α over-expression. Using a reference set of mouse promoters (19) and associating microarray probes to promoters by mapping to known transcripts, we found 1566 promoters (corresponding to 984 genes) to be significantly up-regulated (log2 fold change >= 1; Z score >= 3) and 1165 promoters (corresponding to 727 genes) to be significantly down-regulated (log2 fold change <= -1; Z score <= -3). Thus, similar to previous reports, PGC-1α induced and repressed the transcription of almost the same number of genes, respectively, indicating that the physiological function of PGC-1α includes both the activation and inhibition of substantial numbers of genes.

To combine the DNA binding results from the ChIP-Seq with the data of the gene expression arrays, we then assigned ChIP-Seq peaks to the closest promoter (and the associated gene) within a maximum distance of 10 kb. In this way, about 30% of all peaks (2295 of 7512) could be associated with a target promoter. Inversely, for about 35% of all significantly up-regulated genes (341 of 984), a PGC-1α binding peak is found within 10 kb of the promoter. Since some of the up-regulated promoters may be regulated by more distal peaks, this is only a lower bound on the fraction of genes that are directly regulated.

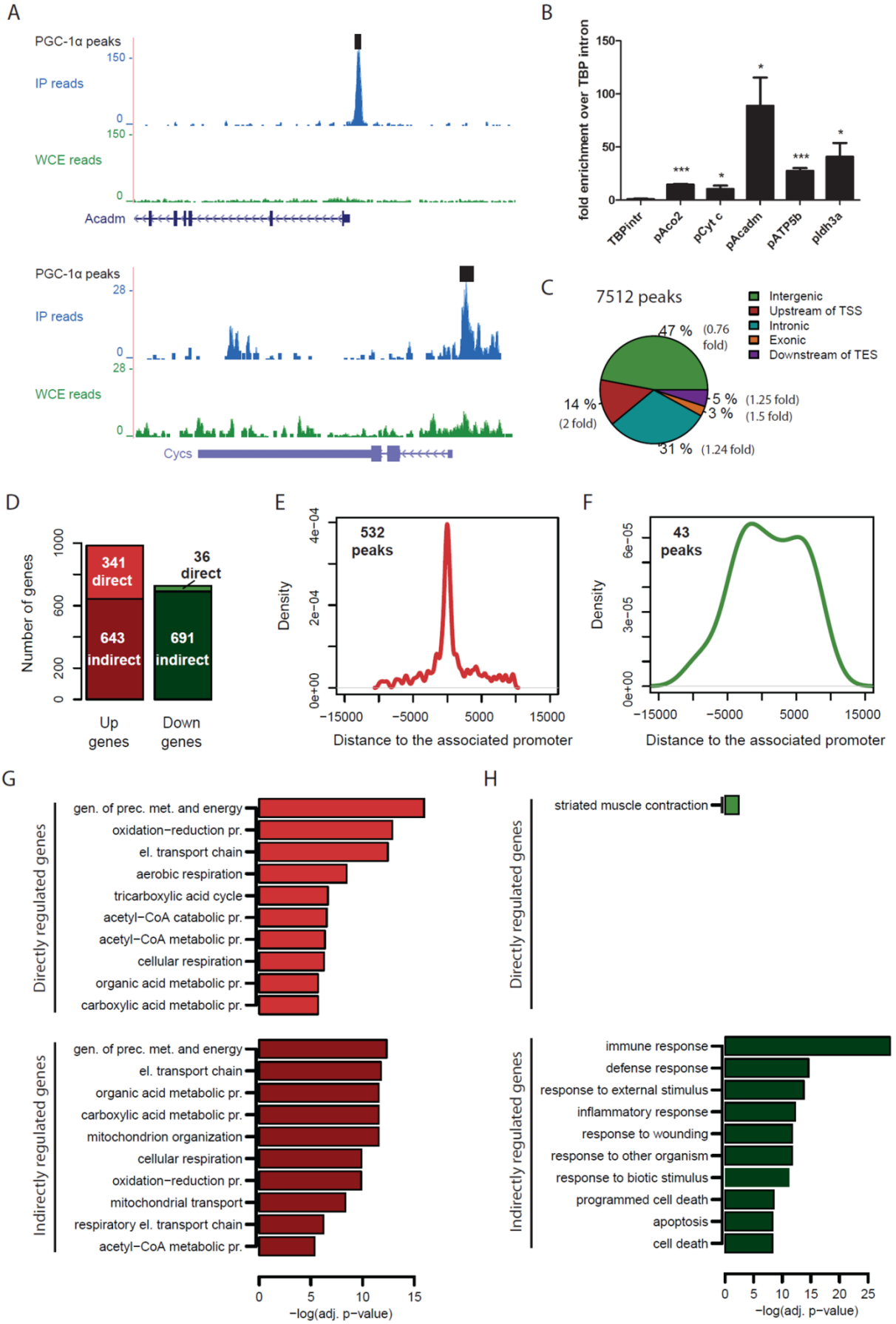
A
PGC-1α peaks
IP reads
WCE reads
Acadm
PGC-1α peaks
IP reads
WCE reads
Cycs
B
fold enrichment over TBP intron
TBPintr
pAco2
pCyt c
pAcadm
pATP5b
pldh3a
C
7512 peaks
Intergenic
Upstream of TSS
Intronic
Exonic
Downstream of TES
47 % (0.76 fold)
5 % (1.25 fold)
3 % (1.5 fold)
31 % (1.24 fold)
14 % (2 fold)
D
Number of genes
341 direct
643 indirect
36 direct
691 indirect
Up genes
Down genes
E
532 peaks
Density
Distance to the associated promoter
F
43 peaks
Density
Distance to the associated promoter
G
Directly regulated genes
gen. of prec. met. and energy
oxidation−reduction pr.
el. transport chain
aerobic respiration
tricarboxylic acid cycle
acetyl−CoA catabolic pr.
acetyl−CoA metabolic pr.
cellular respiration
organic acid metabolic pr.
carboxylic acid metabolic pr.
Indirectly regulated genes
gen. of prec. met. and energy
el. transport chain
organic acid metabolic pr.
carboxylic acid metabolic pr.
mitochondrion organization
cellular respiration
oxidation−reduction pr.
mitochondrial transport
respiratory el. transport chain
acetyl−CoA metabolic pr.
−log(adj. p−value)
H
Directly regulated genes
striated muscle contraction
Indirectly regulated genes
immune response
defense response
response to external stimulus
inflammatory response
response to wounding
response to other organism
response to biotic stimulus
programmed cell death
apoptosis
cell death
−log(adj. p−value)

Figure 1. Genome-wide DNA recruitment of PGC-1α in mouse muscle cells.

(A) PGC-1α ChIP-Seq binding peaks (read densities) around the TSS of the genes *Acadm* and *Cycs* obtained from the UCSC Genome Browser.

(B) Real-time PCR validation of the ChIP enrichment measured at the promoter of a set of PGC-1α target genes. Bars represent fold enrichment over that of the *Tbp* intron, error bars represent SEM. *p < 0.05; **p < 0.01; ***p < 0.001.

(C) Mapping ChIP-Seq PGC-1α peaks across the genome. Transcription Start Site (TSS) and Transcription End Site (TES) are relative to mm9 RefSeq transcripts. "Intergenic": ≥ 10 kb from the nearest transcript; "Upstream of TSS": -10 to 0 kb from the TSS; "Downstream of TES": 0 to 10 kb from the TES. Numbers between brackets indicate, for each category, the ratio between the percentage of PGC-1α peaks and the percentage of the same number of randomly distributed peaks.

(D) Histogram illustrating the number of direct and indirect genes either up- or down-regulated by over-expression of PGC-1α in muscle cells. Direct genes are those associated to promoters found within ±10 kb relative to the nearest peak.

(E) Distribution of the distances of 532 peaks from their associated up-regulated gene promoters.

(F) Distribution of the distances of 43 peaks from their associated down-regulated gene promoters.

(G-H) Subset of the top significantly enriched GO Biological Process terms identified for directly and indirectly up-regulated (G) and down-regulated (H) PGC-1α target genes.

In stark contrast, only about 5% of all repressed genes harbor one or more PGC-1α DNA recruitment peaks in their vicinity (36 of 727) opposed to 95% indirectly down-regulated PGC-1α target genes (691 genes) (Fig. 1D). Moreover, the distribution of the distances between PGC-1α peaks and their associated promoters revealed a tight cluster of 532 peaks close to promoter regions for up-regulated, direct PGC-1α target genes (Fig. 1E) whereas the distribution of the 43 peaks associated to down-regulated genes was much wider, raising the possibility that the association of peaks to transcriptionally repressed genes might be spurious (Fig. 1F). In summary, the strong enrichment of binding peaks near up-regulated genes and the almost complete absence of binding peaks near down-regulated genes suggest that direct regulation of transcription by PGC-1α is almost exclusively activating. We note that there is a large fraction of binding peaks (75%) that are associated to target genes that do not significantly alter their expression. These peaks may have been wrongly assigned, their functionality may be dependent on additional factors not active in these cells, or they may simply be spurious binding events that are not functional.

We next used this stratification of peaks and genes to study whether direct (i.e. with an associated binding peak) and indirect PGC-1α target genes exert different biological function and identified Gene Ontology (GO) terms that were over-represented in any of the four categories. First, we observed that the most significantly enriched functional categories for directly and indirectly up-regulated genes were those related to mitochondria, oxidative phosphorylation and energy production (Fig. 1G and Suppl. Fig. S1B). In contrast, GO analysis of indirectly down-regulated PGC-1α target genes revealed a high prevalence of terms related to inflammation and immune response (Fig. 1H and Suppl. Fig.

S1C). Assuming that the assignment of peaks to repressed genes is not spurious, the few directly repressed PGC-1α targets exhibit an enrichment in functions related to muscle contraction, in particular for genes that are linked to contractile and metabolic properties of glycolytic, fast-twitch muscle fibers (Fig. 1H and Suppl. Fig. S1D), as would be expected from the observed shift from glycolytic to oxidative fibers mediated by PGC-1α in muscle (6).

2.3.2 Modeling the direct and indirect gene regulatory effects of PGC-1α

As a next step, we rigorously modeled the effects of PGC-1α on its target genes in terms of the occurrence of TFBSs for a large collection of mammalian regulatory motifs. We previously introduced a general framework, called Motif Activity Response Analysis (MARA) (20), for modeling the gene expression profiles as a linear function of the TFBSs occurring in the promoters and unknown regulatory "activities" of each of the regulators. As detailed in the Methods, we here extended MARA to incorporate information from the PGC-1α ChIP-Seq data, with the aim of identifying which other TFs are involved in mediating both the direct and indirect regulatory effects of PGC-1α. Specifically, for all "direct target" promoters that were associated with a PGC-1α binding peak, we modeled the expression of the promoter in terms of the predicted TFBSs in the neighborhood of the binding peak, while for "indirect target" promoters we modeled the promoter's expression in terms of the predicted TFBSs in the proximal promoter region, according to the conventional MARA approach (Fig. 2A and 2B).

First, further supporting our analysis above, direct target promoters were almost exclusively up-regulated and only in a few exceptional cases reached statistical significance for PGC-1α-repressed transcripts (Fig. 2C). Among the direct motif activities, the ESRRA position weight matrix was the top ranking motif with a Z score of 6.04 (Suppl. Fig. 2). The corresponding TF estrogen-related receptor α (ERRα), an orphan nuclear receptor, has been extensively studied as a central binding partner for PGC-1α in the regulation of mitochondrial gene expression (17, 18, 21). To stratify the different motifs according to their predicted function, we then divided all motifs into groups according to the behavior of both their direct and indirect activity changes. Strikingly, all motifs exhibited one of only four different motif activity patterns. First, 6 TFs (Suppl. Fig. S2) were predicted to positively regulate PGC-1α target genes only in the presence of PGC-1α (Fig. 2D). Second, we found 6 motifs (Suppl. Fig. S2) with significantly up-regulated direct and indirect motif activities upon PGC-1α over-expression (Fig. 2E). To our surprise, ERRα was predicted to regulate PGC-1α target genes in this manner, even though in previous reports gene regulation by ERRα in the context of activated PGC-1α was suggested to be dependent on PGC-1α coactivation (17, 18, 21). Third, we found 13 motifs (Suppl. Fig. S2) that were predicted to regulate PGC-1α target genes, however only in the absence of PGC-1α (Fig. 2F). Fourth, there was a group of 28 motifs (Suppl. Fig. S2) that showed a significant decrease of indirect motif activity upon PGC-1α over-expression, but no significant change of their direct motif activity, including NFκB (Fig. 2G), a central regulator of inflammation which is indirectly

repressed by PGC-1α (22). Intriguingly however, no motif was found that showed significant direct repression of target genes, reinforcing the hypothesis that PGC-1α-dependent gene repression is an indirect event.

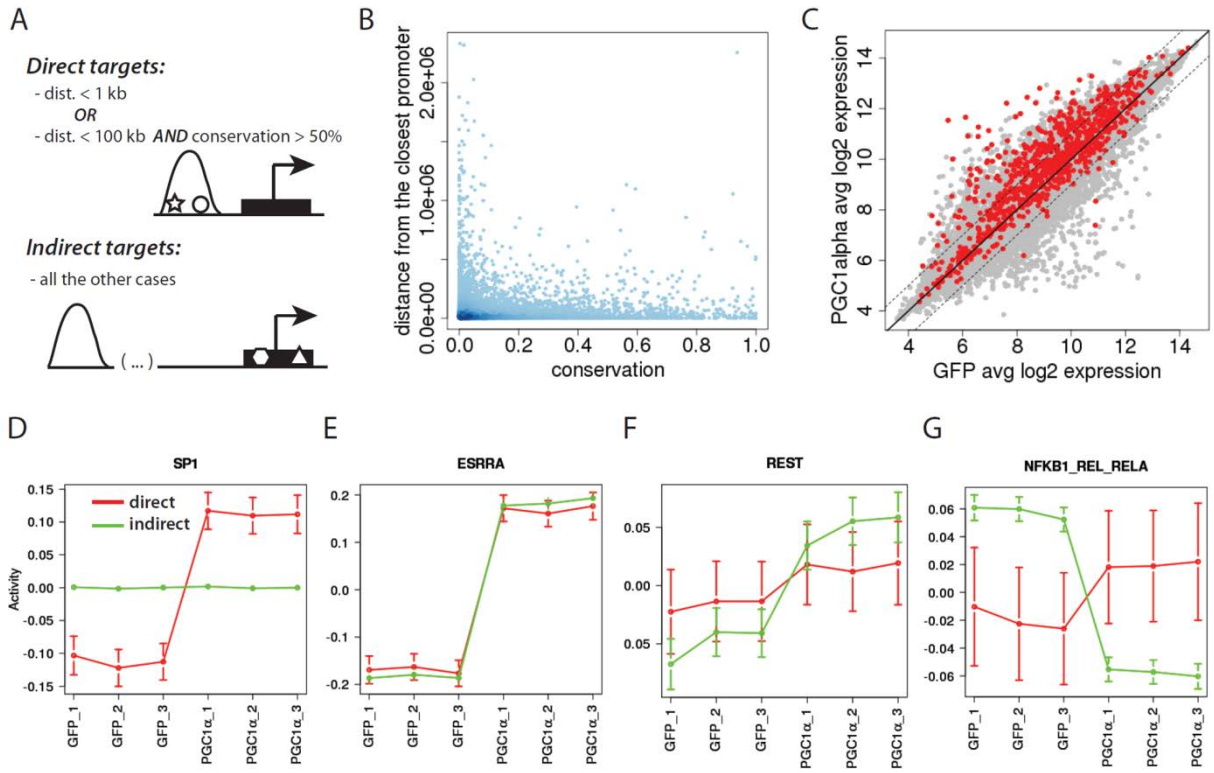

Figure 2. Three distinct mechanistic modes of action for gene expression regulated by PGC-1α and TF partners.

(A) Classification of direct and indirect target genes in MARA (see Methods)

(B) Distribution of peak distance from the closest promoter and phastCons conservation score of the peak.

(C) Distribution of log2 expression values for all mouse promoters. Expression values were averaged across the 3 GFP and the 3 PGC-1α samples. Direct targets are depicted in red, indirect targets in grey.

(D-G) Activity plot of the motifs SP1 (D), ESRRA (E), REST (F) and NFKB1_REL_RELA (G) as predicted by MARA (Motif Activity Response Analysis). Red: direct targets; green: indirect targets.

2.3.3 Nuclear receptors and activator protein-1-like leucine zipper proteins are the main functional partners of PGC-1α in muscle cells

As a next step, we analyzed the occurrence of TF DNA-binding motifs in the PGC-1α peaks identified by ChIP-Seq. We first performed *de novo* motif prediction on the top 200 peaks, using PhyloGibbs (23). As shown in Figure 3A, the motif that PhyloGibbs identified matches significantly (E-value = 7.7834e-10, as calculated by STAMP (24)) the canonical ESRRA motif. In addition to the *de novo* prediction, we also used the same collection of 190 mammalian regulatory motifs used by MARA (19) to check which known TF DNA-binding motifs were significantly over-represented in the PGC-1α peaks relative to a set of background regions. Many of the most significantly enriched motifs represent

variations of nuclear receptor binding sequences that are based on the "AG$^{T}/_{G}$TCA" core hexamer and occur either alone or in direct, inverted or everted repeats with variable spacing (Fig. 3B). Of these, the most significantly enriched motif was ESRRA, which is present in ~20% of all peaks. Moreover, among all genes with at least one associated binding peak within 10Kb, ~28% are associated with a peak containing a predicted ERRα site. Interestingly, besides the nuclear receptor motifs, we also found the DNA-binding element of the insulator protein CCCTC-binding factor (CTCF), and a set of highly similar DNA elements sharing the FOS-JUN-like recognition sequence "TGA$^{G}/_{C}$TCA" bound by the TFs BACH2, FOS, FOSB, FOSL1, JUN, JUNB, JUND, FOSL2, NFE2, and NFE2L2 among the top 15 motifs enriched in PGC-1α peaks (Fig. 3B).

The identity of the exact nuclear receptor binding partner that is bound at each peak is difficult to deduce from DNA-binding motifs, since considerable promiscuity exists between receptors and DNA-binding elements in different configurations of hexameric repeats (25). Moreover, non-nuclear receptor-like TFs are less well studied in the context of PGC-1α-controlled gene expression. Thus, to identify which regulatory motifs are most over-represented among peaks that do not contain nuclear receptor-like sites, we first manually grouped all of the motifs with a sequence logo very similar to that of ESRRA. Next, we discarded all peaks that had one or more predicted TFBSs for any of the motifs in this set. With the remaining 3856 DNA sequences (51.33% of the peaks), we then again assessed the over-representation of each of the 190 mammalian regulatory motifs. In this analysis, "TGA$^{G}/_{C}$TCA" recognition elements, hence FOS-JUN-like motifs, were the most significantly enriched among these peaks (Suppl. Fig. S3A). This result suggests that PGC-1α peaks naturally fall into two classes: those containing ESRRA-like sites, and those containing sites for FOS-JUN-like motifs.

We then constructed a matrix N, whose elements N_{pm} contain the number of predicted TFBSs for each motif m in each peak region p. We then performed principal component analysis (PCA) on this site-count matrix to identify linear combinations of regulatory motifs that explain most of the variation in site-counts across the PGC-1α peaks. The first two components (out of 190 in total) clearly proved to be the most relevant ones, accounting for 10% and 9.6 % of the total variation in our dataset, respectively (Fig. 3C). Figure 3D shows the projection of all motifs on these first two principal components, with the names of the motifs with the largest projection indicated in the figure. Whereas most motifs have projections close to zero along the first component, there is one group of motifs with strong negative projections (ESRRA, NR1H4, NR5A1,2, NR6A1) and one group of motifs with strong positive projections (BACH2, FOS_FOS(B,L1)_JUN(B,D), FOSL2, NFE2, NFE2L1, NFE2L2). These two sets of sites correspond precisely to the two classes of motifs identified above, confirming that the most significant variation in TFBSs across PGC-1α peaks is caused by the occurrence of either ESRRA-like motifs, or FOS-JUN-like motifs. Most interestingly, these two clusters of motifs reflect structurally distinct classes of TFs; the negatively scoring eigenmotifs are characterized by binding of

nuclear receptor-type zinc finger domains, while the eigenmotifs with a positive score correspond to activator protein-1 (AP-1)-like leucine zipper domains.

The second principal component corresponds to the strength of the binding signal for these 10 motifs, as confirmed by the robust negative correlation (r=-0.92) between the TFBSs posterior sum per peak and the peak's projection along the second principal component (Suppl. Fig. S3B).

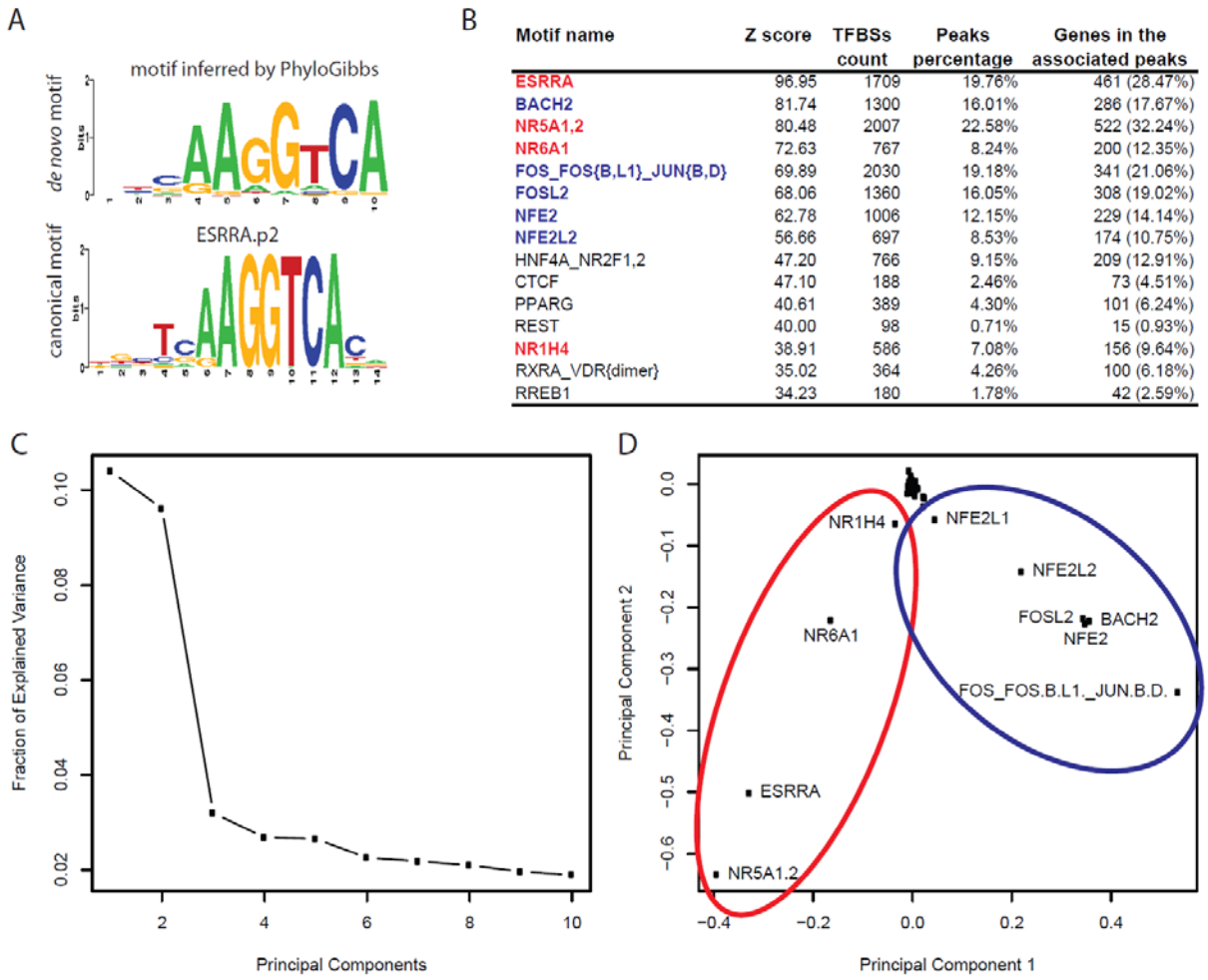

Motif name	Z score	TFBSs count	Peaks percentage	Genes in the associated peaks
ESRRA	96.95	1709	19.76%	461 (28.47%)
BACH2	81.74	1300	16.01%	286 (17.67%)
NR5A1,2	80.48	2007	22.58%	522 (32.24%)
NR6A1	72.63	767	8.24%	200 (12.35%)
FOS_FOS{B,L1}_JUN{B,D}	69.89	2030	19.18%	341 (21.06%)
FOSL2	68.06	1360	16.05%	308 (19.02%)
NFE2	62.78	1006	12.15%	229 (14.14%)
NFE2L2	56.66	697	8.53%	174 (10.75%)
HNF4A_NR2F1,2	47.20	766	9.15%	209 (12.91%)
CTCF	47.10	188	2.46%	73 (4.51%)
PPARG	40.61	389	4.30%	101 (6.24%)
REST	40.00	98	0.71%	15 (0.93%)
NR1H4	38.91	586	7.08%	156 (9.64%)
RXRA_VDR{dimer}	35.02	364	4.26%	100 (6.18%)
RREB1	34.23	180	1.78%	42 (2.59%)

Figure 3. PCA reveals FOS-JUN-like leucine zippers as a new class of putative functional PGC-1α partners.

(A) Sequence logo of the top position weight matrix discovered *de novo* by PhyloGibbs in the top 200 scoring peaks and of the corresponding canonical motif of ERRα as predicted by STAMP.

(B) Top scoring results of motif search performed on all 7512 PGC-1α peaks with MotEvo. Motifs depicted in red and blue correspond to the clusters identified by PCA in panel D.

(C) Fraction of explained variance of the top 10 PCA components.

(D) PCA analysis of the 7512 PGC-1α peaks. Eigenmotif scores across Principal Component 1 (PC1) and Principal Component 2 (PC2) are shown. Red and blue ellipses highlight motif clusters, as identified by PC1, of nuclear hormone receptor-like zinc finger and FOS-JUN-like leucine zipper proteins, respectively.

2.3.4 Validation of top scoring motifs reveals novel functional partners of PGC-1α

Our analysis identified a number of so-far uncharacterized TFs as potentially functional partners for PGC-1α-controlled gene expression in skeletal muscle cells. In order to experimentally validate some of these candidates, we sorted all TFs by a number of criteria including TFBS over-representation in binding peaks, MARA activity upon PGC-1α over-expression, and the expression pattern of the TFs themselves. Table 1 shows the top 15 ranked TFs according to this selection. As expected, the well-known PGC-1α partner ERRα was identified as the most important factor. For our validation experiments, we chose the next two motifs (FOS_FOS(B,L1)_JUN(B,D) and ZNF143, which is also known as ZFP143) as well as three motifs from further down the list of the top 15 motifs (GTF2I, NFE2L2 and NFYC).

FOS, the most up-regulated TF (log2 fold change = 1.78) among the TFs associated with the motif FOS_FOS(B,L1)_JUN(B,D), is a basic leucine zipper transcription factor known to heterodimerize with other leucine zipper proteins in order to form the AP-1 complex (26). The AP-1 complex furthermore contains JUN as well as ATF proteins. Thus, to dissect the function of the AP-1 protein complex, we also included JUN and ATF3, the most highly expressed isoforms of their respective protein families in muscle cells.

For each of these 7 TFs (ATF3, FOS, GTF2I, JUN, NFE2L2, NFYC and ZFP143), we selected a dozen target genes based on the Chi^2 score of the MARA prediction, presence of a PGC-1α binding peak with at least one predicted binding site for the factor of interest, and at least a 2-fold induction upon over-expression of PGC-1α. As summarized in Fig. 4 and Suppl. Fig. S4, siRNA-based knockdown of all TFs resulted in a robust reduction of the target mRNAs from -40% to -75%. With the exception of NFYC and JUN, we found that the large majority of predicted target genes were down-regulated upon knockdown of the factor, confirming our predictions (Fig. 4). The most consistent effects were observed for FOS and ZFP143 (all targets down-regulated), followed by GTF2I (11 out of 12 down-regulated) and NFE2L2 and ATF3 (10 out of 12 down-regulated). Interestingly, distinct target genes of the AP-1 complex showed differential responsiveness to knockdown of the three AP-1 complex components FOS, JUN and ATF3 (Fig. 4B, Fig. 4C and Fig. 4D). Similarly, PGC-1α-mediated induction of a majority of the predicted target genes for NFE2L2 (Fig. 4E), ZFP143 (Fig. 4F) and GTF2I (Fig. 4G) was reduced upon knockdown of the respective TF when compared to the expression in cells with overexpressed PGC-1α and a scrambled siRNA control. Surprisingly, only 1 of the 11 predicted target genes for NFYC that have been chosen for validation was significantly repressed by siRNA-induced reduction of this TF (Fig. 4H), suggesting that other TFs may be involved in mediating the regulatory effects of the NFY regulatory motif.

Tables

Table 1. Global summary of all analyses performed on PGC-1α peaks.

The final score is the count of all analyses where a certain motif passed the defined cutoffs. The motifs chosen for validation and their corresponding values which satisfied the cutoffs are shown in bold.

Motif name	PCA[1]	Over-repr. in all PGC-1α	Over-repr. in "non ESRRA-	MARA activity Z score		Log2FC in expr. array[4]	Abs. expr. in PGC-1α	**Final ranking**
				Direct[3]	Indirect[3]			
ESRRA	Yes	1	182	6.04 (14.78)	15.49	2.31	1829.45	6
FOS_FOS(B,L1)_JUN(B,D)	**Yes**	**5**	**2**	0.88 (2.14)	1.81 (-4.34)	**1.78**	**1508.85**	**5**
ZNF143		**27**	**28**	**2.48 (6.05)**	**4.65 (9.68)**	0.38	**384.36**	**5**
BPTF		21	12	1.38 (3.37)	2.56 (-6.25)	-0.56	333.34	4
ESR1		17	50	2.33 (5.69)	4.53 (11.04)	-0.47	232.42	4
FOSL2	Yes	6	3	0.88 (2.14)	1.51 (3.65)	-0.98	717.09	4
GTF2I		34	**13**	**2.09 (5.10)**	**2.38 (-5.80)**	-0.55	**1207.81**	**4**
NFE2L2	**Yes**	**8**	**5**	0.57 (1.38)	1.01 (-2.37)	-0.38	**3673.63**	**4**
NFY(A,B,C)		96	116	**2.37 (5.80)**	**3.56 (7.62)**	**1.07**	**2409.48**	**4**
NR5A1,2	Yes	3	188	3.53 (8.66)	7.73 (17.00)	-0.08	80.97	4
REST		12	6	0.48 (1.15)	2.41 (5.70)	-0.89	328.04	4
RREB1		15	10	1.56 (3.82)	2.39 (-5.42)	0.05	678.44	4
SP1		24	22	3.99 (9.76)	0.61 (0.33)	-0.32	751.98	4
STAT2,4,6		29	23	0.35 (0.52)	4.81 (-9.67)	-2.72	380.12	4
TLX1..3_NFIC(dimer)		19	17	0.84 (-2.05)	4.91 (-	-0.34	2339.33	4

[1] Requirement for PCA: being among the top 10 most contributing motifs to PC1 and PC2.
[2] Requirement for motifs over-representation: being among the top 30 significant motifs; ranking position shown.
[3] Requirement for MARA: have a Z-score ≥ 2.0. Numbers between brackets show the difference between the PGC-1α state and the GFP state, representing the direction in which the motif activity changes following PGC-1α over-expression.
[4] Requirement for the expression array (1): having a log2 fold change value ≥ 1.0 (corresponding to 2 folds up-regulation)
[5] Requirement for the expression array (2): having an absolute expression in the PGC-1α sample ≥ 100

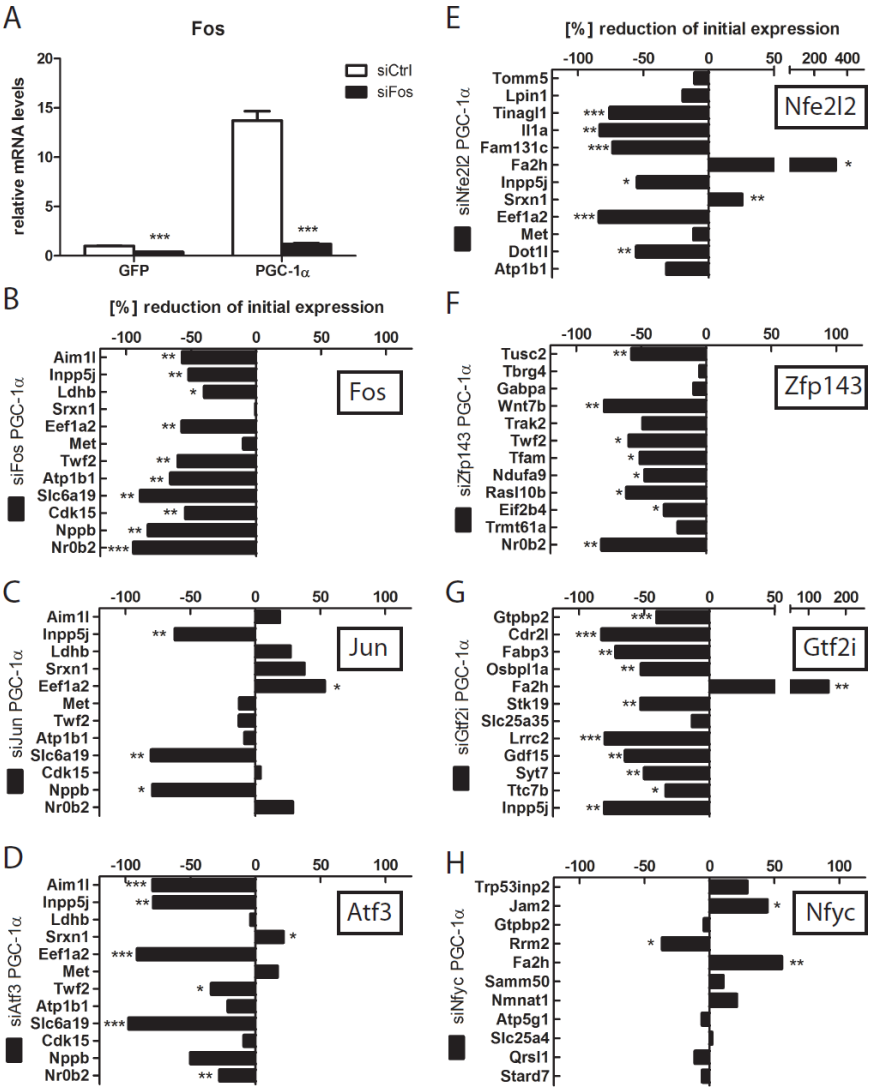

Figure 4. Validation of TFs associated with top scoring motifs reveals novel functional PGC-1α partners.

(A) siRNA-mediated knock-down efficiency for FOS. Bars represent fold induction over GFP/siCtrl value, error bars represent SEM. *p < 0.05; **p < 0.01; ***p < 0.001. See also Figure S4.

(B-H) qRT-PCR analysis of PGC-1α target genes whose associated peak contains at least one binding site for the motif: FOS_FOS(B,L1)_JUN(B,D) (B-D), NFE2L2 (E), ZNF143 (F), GTF2I (G), NFY(A,B,C) (H). Bars represent % change compared to PGC-1α/siCtrl values. Error bars represent SEM. *p < 0.05; **p < 0.01; ***p < 0.001.

2.3.5 Functional interaction between PGC-1α and different compositions of the AP-1 protein complex

Our targeted validation strategy revealed that PGC-1α target genes predicted to be regulated by the FOS-JUN-like motif react in distinct manners to siRNA-mediated knockdown of individual components of the AP-1 transcription factor protein complex. For example, some genes only reacted to reduction of FOS (Fig. 5A), while others were responsive to the knock-down of two (Fig. 5B) or even all three AP-1 protein partners (Fig. 5C) that we have tested using the siRNA-based approach. To further dissect the responsiveness of PGC-1α target genes to different AP-1 protein complexes, we

performed global gene expression arrays upon knockdown of each of the three TF components of the AP-1 complex. Fig. 5D depicts the number of genes that were induced by PGC-1α and that were, at the same time, down-regulated by the siRNA knockdown of any of the three AP-1 complex members. Amongst a total of 477 genes, 89% responded to FOS knockdown, 52% to ATF3 knockdown, and 31% to JUN knockdown. Moreover, while 37% of all targets responded exclusively to FOS, the fraction of targets responding exclusively to either JUN or ATF3 was at most 5%. This analysis shows that, whereas different target genes respond differently to the knock-down of distinct AP-1 components, FOS is the dominant factor in determining AP-1 function in these conditions.

As shown in Fig. 3B, 341 genes were associated to a PGC-1α binding peak containing a predicted site for the FOS-JUN-like motif bound by the AP-1 complex. Of these genes, the expression of 55 was significantly induced by PGC-1α over-expression in muscle cells. In our siRNA-based validation experiment, we found that 47 out of these 55 PGC-1α-induced/AP-1 predicted targets were significantly down-regulated by knockdown of the AP-1 complex components and we called these genes “direct PGC-1α/AP-1 targets”. The remaining 430 genes out of 477 (Fig. 5D) were defined accordingly as “indirect PGC-1α/AP-1 targets” that lack a PGC-1α peak containing a FOS-JUN-like motif, but still are regulated by PGC-1α and the AP-1 protein components (Fig. 5E). To reveal whether these gene categories exert distinct functions, GO and KEGG enrichment analyses were performed. Surprisingly, the 47 direct PGC-1α/AP-1 target genes showed a distinct and significant over-representation of the terms “response to hypoxia” (GO ID: 0001666; adjusted p-value: 0.0247542) and “mTOR signaling pathway” (KEGG ID: mmu04150; adjusted p-value: 0.030674) that were absent in the GO analysis of the remaining PGC-1α/AP-1 targets (Fig. 5F). These results suggest that AP-1, when coactivated by PGC-1α, drives a synergic effect of response to hypoxia; on the other hand, when AP-1 and PGC-1α act separately, and furthermore through downstream intermediate TFs, they regulate the expression of genes involved in mitochondrial organization and energy metabolism (Figure 5G).

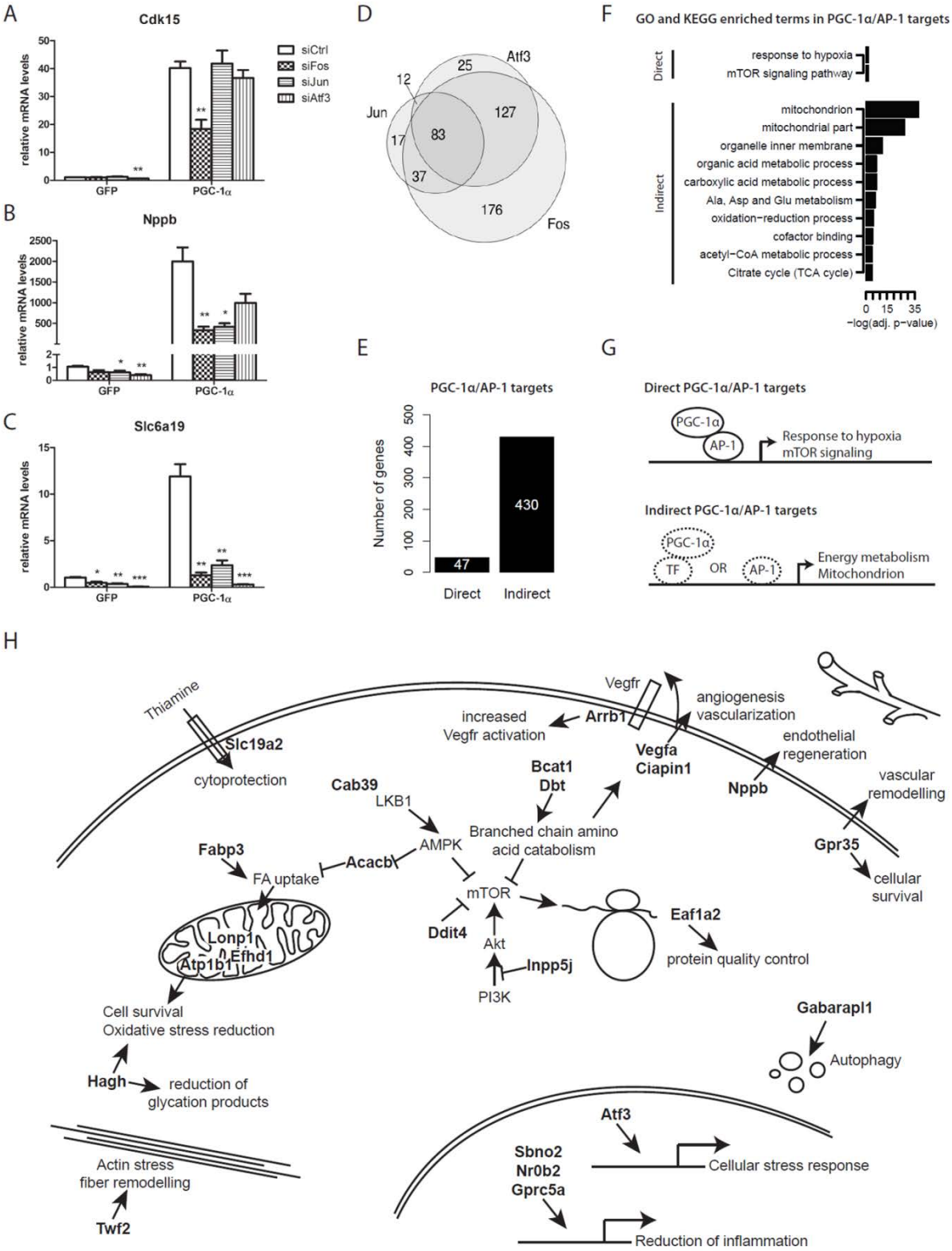
A
Cdk15
relative mRNA levels
siCtrl
siFos
siJun
siAtf3
GFP
PGC-1α
B
Nppb
C
Slc6a19
D
Atf3
Jun
Fos
25
12
127
17
83
37
176
E
PGC-1α/AP-1 targets
Number of genes
47
430
Direct
Indirect
F
GO and KEGG enriched terms in PGC-1α/AP-1 targets
Direct
response to hypoxia
mTOR signaling pathway
Indirect
mitochondrion
mitochondrial part
organelle inner membrane
organic acid metabolic process
carboxylic acid metabolic process
Ala, Asp and Glu metabolism
oxidation−reduction process
cofactor binding
acetyl−CoA metabolic process
Citrate cycle (TCA cycle)
−log(adj. p−value)
G
Direct PGC-1α/AP-1 targets
PGC-1α
AP-1
Response to hypoxia
mTOR signaling
Indirect PGC-1α/AP-1 targets
TF
OR
Energy metabolism
Mitochondrion
H
Thiamine
Slc19a2
cytoprotection
Vegfr
increased
Vegfr activation
Arrb1
angiogenesis
vascularization
Vegfa
Ciapin1
endothelial
regeneration
Nppb
vascular
remodelling
Gpr35
cellular
survival
Cab39
LKB1
AMPK
Bcat1
Dbt
Branched chain amino
acid catabolism
Fabp3
FA uptake
Acacb
mTOR
Ddit4
Akt
Inpp5j
PI3K
Eaf1a2
protein quality control
Lonp1
Efhd1
Atp1b1
Cell survival
Oxidative stress reduction
Hagh
reduction of
glycation products
Gabarapl1
Autophagy
Actin stress
fiber remodelling
Twf2
Atf3
Sbno2
Nr0b2
Gprc5a
Cellular stress response
Reduction of inflammation

Figure 5. PGC-1α controls the hypoxia gene program via a functional interaction with different configurations of the AP-1 protein complex.

(A-C) qRT-PCR analysis of *Cdk15*, *Nppb* and *Slc6a19* mRNA levels in response to PGC-1α over-expression and either siFos, siJun or siAtf3 knock-down. Data are normalized to mRNA levels in GFP infected cells. Error bars represent ± SEM. *p < 0.05; **p < 0.01; ***p < 0.001.

(D) Venn diagram illustrating the overlap in number of genes up-regulated by PGC-1α and down-regulated by either FOS, JUN or ATF3 knock-down.

(E) Histogram illustrating the number of direct and indirect PGC-1α/AP-1 target genes.

(F) Subset of the top significantly enriched Gene Ontology and KEGG terms identified for the two gene groups illustrated in panel (E).

(G) Schematic representation highlighting the functional link between PGC-1α and AP-1 in terms of directly and indirectly regulated signaling pathways. Dashed lines indicate that the protein might or might not be present at the site.

(H) Schematic representation depicting the downstream effects of the functional interaction between PGC-1α and the AP-1 complex in the context of the hypoxia gene program. Direct targets of PGC-1α and AP-1 are indicated in bold.

2.4 Discussion

Exercise-induced skeletal muscle cell plasticity is a highly complex biological program that involves the remodeling of a number of fundamental cellular properties. Since PGC-1α function has been strongly linked to the induction of an endurance-trained muscle phenotype, we here dissected the PGC-1α-controlled transcriptional network in muscle cells. First, our results reveal a broad recruitment of PGC-1α to many different sites in the mouse genome (7512 peaks), the majority of which were either not located within 10 kb distance of a TSS or close to a gene that was not regulated by PGC-1α over-expression at the time of harvest of the cells, as has analogously been observed in many other ChIP-Seq experiments (e.g. see (19)). Apart from the fact that PGC-1α could mediate long-range enhancer effects that were excluded in our peak-gene assignment, it is conceivable that PGC-1α recruitment is transcriptionally silent in some binding peaks because it requires the recruitment of additional cofactors for activation, which are not present in the conditions or cell type in which our experiments were performed. In addition, it is possible that a large fraction of PGC-1α binding peaks may be "neutral" in the sense of not having any direct role in regulating gene expression.

Second, while an almost equally strong effect of PGC-1α on gene induction and repression has been reported (18), our analysis now indicates that direct PGC-1α-mediated gene expression is restricted almost exclusively to positively regulated PGC-1α target genes, whereas the vast majority of gene repression is indirect, i.e. not associated with PGC-1α recruitment within a 10 kb distance to their promoters. Thus, the fact that almost 95% of all repressed genes were not linked to PGC-1α recruitment strongly implies that this coregulator primarily acts as a coactivator, and not as a corepressor as suggested by the data of some studies (27-29). Importantly, indirect repression of PGC-1α target genes was also supported by the MARA prediction. The strong indirect inhibition of genes, many of which are involved in inflammatory processes, is predicted by MARA to be mediated by TFs such as NFκB and IRF factors. Such an indirect inhibition of NFκB and pro-inflammatory genes by PGC-1α in muscle cells has been reported previously (22).

One of the main functions of PGC-1α in all cells and organs is to boost mitochondrial gene transcription and oxidative metabolism. Accordingly, we observed that Gene Ontology terms related to these pathways were highly enriched when analyzing positively regulated PGC-1α target genes in muscle cells. Based on previous studies, the regulation of this core function could have been assigned to the direct interaction of PGC-1α and ERRα binding to regulatory elements of these genes (18, 21). Surprisingly, our data indicate that many of the genes that are involved in oxidative metabolic pathways are indirectly controlled by PGC-1α and, hence, do not require PGC-1α recruitment to enhancer and promoter elements. Likewise unexpectedly, the MARA analysis implies ERRα action on direct and indirect PGC-1α-induced target genes, i.e. in the presence or absence of PGC-1α coactivation. Thus, while these observations might obviously reflect a temporally distinct control of different PGC-1α target genes that is not represented in our simultaneous analysis of DNA binding and gene expression at one time point, it is conceivable that PGC-1α acts primarily as an upstream

regulator of other factors that are subsequently controlling more downstream PGC-1α target genes without direct involvement of PGC-1α itself.

In skeletal muscle, PGC-1α has been reported to interact with ERRs, PPARs and other nuclear receptors, as well as myocyte enhancer and nuclear respiratory factors to mediate transcriptional regulation (3). Accordingly, ERRα and other nuclear receptor binding motifs were amongst the most highly significant binding elements in our present report. Importantly however, we also predict a number of so-far unknown TFs to functionally interact with PGC-1α and thereby contribute to PGC-1α-controlled gene expression in skeletal muscle. Since a complete functional validation of all new putative TF partners is beyond the scope of this manuscript, we combined the high-throughput results with several computational analyses (see Table 1) to select and test some of the potentially most important factors together with predicted target genes. Notably, in siRNA-based knockdown experiments, we could show that depletion of FOS and its putative AP-1 multimerization partners JUN and ATF3 as well as NFE2L2, ZFP143 and GTF2I in muscle cells reduced the ability of PGC-1α to positively regulate target genes, confirming a functional interaction between these TFs and PGC-1α. Thus, our results indicate that the coactivation repertoire of PGC-1α in muscle exceeds the prediction of previous studies by far. For example, even in our list of the top 15 motifs, several predicted TFs have not yet been investigated in the context of PGC-1α-controlled gene expression, including BPTF, FOSL2, REST or RREB1. Future studies will aim at a more detailed dissection of the global functional consequences of PGC-1α coactivation of these TFs in muscle cells.

Curiously, almost all of our analyses, and in particular the principal component analysis, highlighted the relevance of FOS-JUN-like motifs. In fact, the largest amount of variation in TFBS occurrence within PGC-1α binding peaks results from either ESRRA-like or FOS-JUN-like motifs. The FOS-JUN-like motif, in particular, embodies the main binding elements of the AP-1 complex, which consists of different configurations of FOS, JUN, ATF and MAF proteins (26, 30). Our data comparing gene expression in cells with reduced FOS, JUN and ATF3 levels indicate that PGC-1α functionally interacts with the AP-1 complex in different configurations in the regulation of specific genes. The differential requirement observed for distinct AP-1 components might provide an additional layer of control for specific PGC-1α target gene regulation.

AP-1 function itself is regulated by a variety of stimuli, including cytokines, growth factors and stress, and subsequently controls a number of cellular processes including apoptosis, cell proliferation and differentiation, stress response and hypoxia (30, 31). Mechanistically, we classified PGC-1α-induced/AP-1-knocked-down targets in either direct or indirect genes. Most interestingly, functional analysis of these two groups of genes revealed that when AP-1 and PGC-1α act disjointedly, they are involved in the regulation of mitochondrial and other metabolic genes while, when coactivated by PGC-1α, AP-1 distinctly alters the expression of genes that are enriched in the ontology terms “response to hypoxia” and “mTOR signaling” (Fig. 5G). Intriguingly, a closer analysis of all 47 direct AP-1/PGC-1α target genes revealed 24 genes that are induced by hypoxia, are effectors of hypoxia or

attenuate the detrimental consequences of hypoxia (Fig. 5H). For example, several inhibitors of the mTOR signaling pathways are included in this group of genes and hypoxia has been described as a suppressor of mTORC1 activity (32). Another group of genes contributes to the reduction of cellular stress, detrimental metabolites, reactive oxygen species and increase in cellular survival to reduce potential harmful consequences of prolonged hypoxia (33). Furthermore, several genes promote endothelial regeneration, vascular remodeling and vascularization (34). In this context, PGC-1α has previously been shown to promote vascular endothelial growth factor (VEGF)-induced angiogenesis in skeletal muscle in a hypoxia-inducible factor 1α (HIF-1α)-independent, ERRα-dependent manner (35). Similarly, PGC-1α regulates the hypoxic response of brown fat (36), neuronal and endothelial cells (37) even though the mechanisms of cellular protection exerted by PGC-1α in these experimental contexts have not been elucidated. Our findings now indicate that, to ensure adequate oxygen and nutrient supplies for oxidative metabolism in skeletal muscle cells, PGC-1α might coordinate metabolic needs through ERRα-induced *Vegf* expression with a broad, stress-induced AP-1-dependent hypoxia program.

In summary, our data provide a first insight into the transcriptional network controlled by PGC-1α in muscle cells. While one other study of global DNA recruitment of PGC-1α has been performed in the human hepatoma cell line HepG2 (38), our results highlight the importance of combining ChIP-Seq experiment, transcriptional data together with a comprehensive computational modeling approach and experimental validation of predicted key regulators, in order to be able to discover mechanistic as well as functional outcomes of such a network. Combined with the knowledge of transcriptional regulation, posttranslational modifications, alternative splicing and recruitment of different chromatin remodeling protein complexes, a scenario can thus be conceived in which PGC-1α is able to control and integrate different signaling pathways using a multitude of different transcription factor binding partners (10, 11). A better understanding of such regulatory networks will eventually allow the targeting of whole biological programs or specific sub-modules in pathological states of disregulation.

2.5 Methods

Cell culture and siRNA transfection

C2C12 cells were grown in Dulbecco's modified Eagle's medium (DMEM) supplemented with 10% fetal bovine serum (FBS), 100 Units/ml penicillin and 100ug/ml streptomycin. To obtain myotubes, the C2C12 myoblasts were allowed to reach 90% confluence and the medium was changed to DMEM supplemented with 2% horse serum (differentiation medium) for 72 hours.

The siRNAs for the knock-down of NFE2L2, FOS, JUN, ATF3, NFYC, ZFP143, GTF2I, the non-targeting siRNA pool and the DharmaFECT1 transfection reagent were purchased from Dharmacon (Fisher Scientific) and the siRNA transfection was performed according to the Thermo Scientific DharmaFECT Transfection Reagents siRNA Transfection Protocol. Briefly, after three days of differentiation, the respective siRNAs (50nM final concentration) was added to the medium. 24h after siRNA transfection, the cells were infected with either the PGC-1α or GFP adenovirus. Then, 48h after adenoviral infection, the cells were harvested.

ChIP and ChIP Sequencing

ChIP was performed according to the Agilent Mammalian ChIP-on-chip Protocol version 10.0. For detailed protocol see Supplemental Information.

Identification of bound regions

To identify regions that were significantly enriched in the ChIP, we passed a 200 bps long sliding window along the genome, sliding by 25 bps between consecutive windows, and estimated the fraction of all ChIP reads f_{IP} that fall within the window, as well as the fraction f_{WCE} of reads from the whole cell extract that fall in the same window (which we estimate from a 2000 bps long window centered on the same genomic location). A Z-score quantifying the enrichment in the ChIP of each window was computed as:

$$Z = \frac{f_{IP} - f_{WCE}}{\sqrt{\sigma^2{}_{IP} + \sigma^2{}_{WCE}}}$$

where $\sigma^2{}_{IP}$ and $\sigma^2{}_{WCE}$ are the variances of the IP and WCE read frequencies, which are given by:

$$\sigma^2{}_{IP} = \frac{f_{IP} * (1 - f_{IP})}{N_{IP}} \text{ and } \sigma^2{}_{WCE} = \frac{f_{WCE} * (1 - f_{WCE})}{N_{WCE}}$$

respectively.

The enrichments were reproducible across biological replicates. Using only the first sequencing dataset, we called peaks at a Z cutoff of 4.5; we then compared these with the Z scores from the corresponding regions of the second dataset and the Pearson correlation coefficient was found to be 0.778. Similarly, we called peaks at a Z cutoff of 4.5 using only the second sequencing dataset; when we compared these peaks with the Z scores of the corresponding regions from the first dataset, the Pearson correlation coefficient was found to be 0.782.

To obtain a final set of binding peaks, we combined the reads from the two biological replicates computing the Z score of each window was computed as:

$$Z = \frac{f_{IP1} + f_{IP2} - f_{WCE1} - f_{WCE2}}{\sqrt{\sigma^2_{IP1} + \sigma^2_{IP2} + \sigma^2_{WCE1} + \sigma^2_{WCE2}}}.$$

We conservatively considered all windows with a Z-score larger than 4.5 as were considered significantly enriched (False Discovery Rate 0.6%). The final binding peaks were obtained by merging consecutive windows that all passed the cut-off and by considering the "peak" to correspond to the top scoring window, i.e. corresponding to the summit of the ChIP-Seq signal. To determine the PGC-1α distribution genome-wide, peaks were annotated according in relation to their closest Mus musculus RefSeq transcripts. We defined peaks as: "Intronic" (peak center lying inside an intron); "Exonic" (peak center lying inside an exon); "Upstream of TSS" (peak center lying within -10 to 0 kb from the closest TSS); "Downstream of TES" (peak center lying within 0 to 10 kb from the closest TES); "Intergenic" (peak center located farer than 10 kb from the nearest transcript). Moreover, we computed the ratio between observed and expected peak location distributions, obtained by generating 100 peak sets composed of 7512 random peaks each.

Motif finding and TFBSs over-representation

The binding peak regions were aligned to orthologous regions from other 6 mammalian species – human (hg18), rhesus macaque (rheMac2), dog (canFam2), horse (equCab1), cow (bosTau3) and opossum (monDom4) – using T-Coffee (39). A collection of 190 mammalian regulatory motifs (position weight matrices or WMs) representing the binding specificities of approximate 350 mouse TFs (in many cases, sequence specificities of multiple closely-related TFs were represented with the same WM) were downloaded from the SwissRegulon website (19). TFBSs for all known motifs were predicted using the MotEvo algorithm (40) on the alignments of all the 7512 peak sequences. Only binding sites with a posterior probability >= 0.1 were considered for the further steps of the analysis. In order to create a background set of regions to assess the overrepresentation of binding sites within our regions, we created randomized alignments by shuffling the multiple alignment columns, maintaining both the gap patterns and the conservation patterns of the original alignments. TFBSs were predicted on the shuffled alignments using the same MotEvo settings as for the original peak alignments. Over-representation of motifs in the PGC-1α binding peaks was calculated by comparing total predicted TFBS occurrence within binding peaks with the predicted TFBS occurrence in the shuffled alignments. We evaluated the enrichment of TFBSs for each motif *x* by collecting the sum n_x of the posterior probabilities of its predicted sites in the peak alignments as well as the corresponding sum n'_x in the shuffled alignments, and computed a Z-score:

$$Z = \frac{f_x - f'_x}{\sqrt{\frac{f_x * (1 - f_x)}{L_x} + \frac{f'_x * (1 - f'_x)}{L'_x}}}$$

where L_x and L'_x are the total lengths of the original and shuffled alignments, respectively, while f_x and f'_x are given by the equations:

$$n_x * l_x = f_x * L_x \text{ and } n'_x * l_x = f'_x * L'_x$$

with l_x the length of motif x.

Principal Component Analysis of TFBS occurrence in binding peaks

The input matrix N for the Principal Component Analysis (PCA) contained the total number of predicted binding sites N_{pm} in each of the 7512 binding peaks p (rows) for each of the 190 mammalian regulatory motifs m (columns). After mean centering the columns of this matrix, $\widetilde{N}_{pm} = N_{pm} - \langle N_m \rangle$, i.e. subtracting the average site count for each motif), Singular Value Decomposition (SVD) was used to factorize this matrix: $\widetilde{N} = U \cdot S \cdot V^T$, where U is an $P \times M$ matrix whose columns are the left singular vectors of $\widetilde{N}$; S is a $M \times M$ diagonal matrix containing the singular values, and V^T (the transpose of V) is an $M \times M$ matrix whose rows are the right singular vectors, with P the number of peaks, and M the number of motifs. The SVD was performed using the "svd" package of the "R" programming language.

Gene expression arrays

Whole-gene expression after 48 hours of transfection with adenovirus was measured in C2C12 cells with Affymetrix GeneChip® Mouse Gene 1.0 ST microarrays at the Life Science Training core facility of the University of Basel. Raw probe intensities were corrected for background and unspecific binding using the Bioconductor package "affy" (41). Subsequently, probes were classified as expressed or non-expressed by using the "Mclust" R package (42) and, after removal of non-expressed probes, the intensity values were quantile normalized across all samples. Using mapping of the probes to the UCSC collection of mouse mRNAs, probes were then associated to a comprehensive collection of mouse promoters available from the SwissRegulon database (19). The log2 expression level of a given promoter was calculated as the weighted average of the expression levels of all probes associated to it. Log2 expression levels were then compared between over-expressed PGC-1α and the control GFP sample; for each promoter, the change in expression level across the two conditions was measured by log2 fold change (log2FC), computed as the difference between the mean of the log2 values in PGC-1α and the mean of the log2 values in GFP. The significance of the expression change was assessed by a Z score, which was computed as:

$$Z = \frac{\bar{E}_{PGC1\alpha} - \bar{E}_{GFP}}{\sqrt{\frac{{\sigma^2}_{PGC1\alpha}}{n} + \frac{{\sigma^2}_{GFP}}{n}}}$$

where $n = 3$ was the number of replicate samples, $\bar{E}_{PGC1\alpha}$ is the mean log2 expression across the PGC-1α samples, $\bar{E}_{GFP}$ is the mean log2 expression across the GFP samples, and ${\sigma^2}_{PGC1\alpha}$ and ${\sigma^2}_{GFP}$ are the variances of log2 expression levels across the replicates for the PGC-1α and control samples,

respectively. Promoters were considered significantly up-regulated when log2FC >= 1 and Z >= 3, and significantly down-regulated when log2FC <= -1 and Z <= -3.

Peaks were assigned to promoters by proximity. To assign each peak to a promoter, we calculated the distance from the center of the peak to the center of neighboring promoters; whenever the peak was closer than 10 kb from at least one promoter, it was assigned to the nearest promoter and, thus, to its associated gene.

Gene Ontology enrichment analysis

Gene IDs were extracted from differentially regulated promoters and divided in four groups: up-regulated promoters with an assigned binding peak, up-regulated promoters without an assigned binding peak, down-regulated promoters with an assigned peak, and down-regulated promoters without an assigned peak. These four gene sets were used as input for the functional analysis tool FatiGO (43) to identify significantly over-represented Gene Ontology (GO) categories compared to all Mus musculus genes. Only GO terms having an FDR-adjusted p-value <= 0.05 were considered significant.

Motif activity at direct and indirect targets of PGC-1α

To integrate the information from the PGC-1α binding peaks, we extended MARA (20) to model the direct and indirect regulatory effects of PGC-1α. Given the input expression data and the computationally predicted binding sites, MARA infers, for each of 190 regulatory motifs *m*, the activity A_{ms} of the motif in each sample *s* when the motif occurs *outside* of a region of PGC-1α, and the activities A^*_{ms} of the motifs when they occur *within* a PGC-1α binding peak. That is, changes in the motif activities A_{ms} upon over-expression of PGC-1α indicate indirect regulatory effects of PGC-1α on each motif *m*, whereas changes in the motif activities A^*_{ms} reflect direct regulatory effects of PGC-1α as mediated by each motif *m*. For each promoter *p* that was not associated with any PGC-1α binding peak (which we denote indirect targets), we modeled its log-expression in sample *s,* e_{ps}, in terms of the predicted number of TFBSs N_{pm} that occur in the proximal promoter region (running from -500 to +500 relative to TSS) for each regulatory motif *m.* That is, MARA assumes the linear model:

$$e_{ps} = c_p + \tilde{c}_s + \sum_m N_{pm} A_{ms}$$

where c_p is the basal expression of promoter *p*, $\tilde{c}_s$ is a sample-dependent normalization constant, and A_{ms} is the regulatory activity of motif *m* in sample *s*, which is inferred by the model. Formally, A_{ms} quantifies amount by which the expression of promoter *p* in sample *s* would be reduced if a binding site for motif *m* were to be deleted from the promoter.

For each “direct target” promoter *p* that has that has an associated PGC-1α binding peak, which we defined as promoters with a peak within 1 kb or with a peak within 100 kb that was highly conserved

according to PhastCons score of the region (44), we model its expression in terms of the predicted TFBSs in the binding peak, i.e.:

$$e_{ps} = c_p + \tilde{c}_s + \sum_m N^*_{pm} A^*_{ms}$$

where N^*_{pm} is the number of predicted TFBSs for motif *m* in *the peak* associated with promoter *p*, and A^*_{ms} is the motif activity of regulator *m* in sample *s* when this motif occurs in the context of PGC-1α binding. That is, the inferred motif activities A_{ms} quantify the activities of regulatory motifs when they occur independent of PGC-1α binding, and the motif activities A^*_{ms} quantify the activities of motifs when they occur in a PGC-1α binding peak, i.e. the latter activities reflect direct effects of a PGC-1α while the former reflect indirect effects.

MARA predicts activities for 190 different mammalian regulatory motifs, associated with roughly 350 mouse TFs. Besides motif activities MARA also calculates error-bars δ_{ms} for each motif *m* in each sample *s*. Using these, MARA calculates, for each motif *m*, an overall significance measure for the variation in motif activities across the samples analogous to a z-statistic:

$$z_m = \sqrt{\frac{1}{S}\sum_m (A_{ms})^2}$$

For each motif we calculate both a z-score z_m associated with its indirect activity changes, and a z-score z^*_m associated with its direct activity changes. MARA also ranks the confidence on predicted target promoters of each motif by a Bayesian procedure that quantifies the contribution of that factor to explaining the promoter's expression variation by a Chi-squared value (for details, see (20)). The parameters used for motif stratification were: (i) the Z score z^*_m for direct activity changes, (ii) the Z score z_m for indirect motif activity changes, (iii) the Z score $\bar{z}^*_m$ for direct motif activity changes, computed by averaging the sample replicates and (iv) the Z score $\bar{z}_m$ for indirect motif activity changes, computed by averaging the sample replicates. The latter two measures were used to show which direction the motif activity changes when over-expressing PGC-1α with respect to the control condition. All motifs *m* for which either the direct or indirect motif activities were changing significantly ($z \geq 2$) were subsequently selected.

***De novo* motif finding**

PhyloGibbs (23) was used to identify *de novo* motifs across the 200 top enriched PGC-1α peaks. The parameters used were -D 1 -z 1 -y 200 -m 10, corresponding to searching on multiple alignments for a single motif of length 10 with a total of 200 sites. The resulting motif was scanned for similarity to the other known motifs from our dataset using STAMP (24), with settings: Pearson Correlation Coefficient for column comparison metric, Smith-Waterman for the alignment method, penalty of 0.5 and 0.25 for gap opening and gap extension, respectively.

Real-time PCR and target gene validation

Putative target genes of distinct transcription factor-PGC-1α combinations were chosen according to three criteria: first, positive transcriptional regulation by PGC-1α by more than 2 fold, second, presence of a PGC-1α binding peak within a 10 kb distance from the TSS and third, prediction of targeting by MARA with a positive Chi-squared score. The sequences of the primers used in real-time PCR experiments are depicted in Suppl. Table 1. The values are presented as the mean +/- SEM. A Student's t-test was performed and a p-value < 0.05 was considered as significant (*$p<0.05$, **$p<0.01$, ***$p<0.001$).

DATA ACCESS: The ChIP-seq and gene expression array data described in this manuscript are accessible at the Gene Expression Omnibus (GEO) under the accession no. GSE51191.

Acknowledgments

This project was funded by the Swiss National Science Foundation (31003A_135397 to EvN, 310030_132900 to CH), SystemsX.ch (CellPlasticity, StoNets, and BrainstemX research projects to EvN), the Muscular Dystrophy Association USA (MDA), the SwissLife "Jubiläumsstiftung für Volksgesundheit und medizinische Forschung", the Swiss Society for Research on Muscle Diseases (SSEM), the Swiss Diabetes Association, the Roche Research Foundation, the United Mitochondrial Disease Foundation (UMDF), the Association Française contre les Myopathies (AFM), the Neuromuscular Research Association Basel (NeRAB), the Gebert-Rüf Foundation "Rare Diseases" Program, the University of Basel and the Biozentrum. SS was supported by an IPhD fellowship of the SystemsX.ch Swiss Initiative in Systems Biology. We are thankful of the [BC]2 Basel Computational Biology Center for providing computational resources.

Disclosure declaration: The authors have no conflict of interest in regard to this manuscript.

2.6 References

1. Handschin C & Spiegelman BM (2008) The role of exercise and PGC1alpha in inflammation and chronic disease. *Nature* 454(7203):463-469.
2. Pedersen BK & Febbraio MA (2012) Muscles, exercise and obesity: skeletal muscle as a secretory organ. *Nat Rev Endocrinol* 8(8):457-465.
3. Handschin C (2010) Regulation of skeletal muscle cell plasticity by the peroxisome proliferator-activated receptor gamma coactivator 1alpha. *J Recept Signal Transduct Res* 30(6):376-384.
4. Handschin C & Spiegelman BM (2006) Peroxisome proliferator-activated receptor gamma coactivator 1 coactivators, energy homeostasis, and metabolism. *Endocr Rev* 27(7):728-735.
5. Finck BN & Kelly DP (2006) PGC-1 coactivators: inducible regulators of energy metabolism in health and disease. *J Clin Invest* 116(3):615-622.
6. Lin J*, et al.* (2002) Transcriptional co-activator PGC-1 alpha drives the formation of slow-twitch muscle fibres. *Nature* 418(6899):797-801.
7. Handschin C*, et al.* (2007) Skeletal muscle fiber-type switching, exercise intolerance, and myopathy in PGC-1alpha muscle-specific knock-out animals. *J Biol Chem* 282(41):30014-30021.
8. Handschin C*, et al.* (2007) Abnormal glucose homeostasis in skeletal muscle-specific PGC-1alpha knockout mice reveals skeletal muscle-pancreatic beta cell crosstalk. *J Clin Invest* 117(11):3463-3474.
9. Lonard DM & O'Malley BW (2006) The expanding cosmos of nuclear receptor coactivators. *Cell* 125(3):411-414.
10. Lonard DM & O'Malley B W (2007) Nuclear receptor coregulators: judges, juries, and executioners of cellular regulation. *Mol Cell* 27(5):691-700.
11. Spiegelman BM & Heinrich R (2004) Biological control through regulated transcriptional coactivators. *Cell* 119(2):157-167.
12. Puigserver P*, et al.* (1999) Activation of PPARgamma coactivator-1 through transcription factor docking. *Science* 286(5443):1368-1371.
13. Wallberg AE, Yamamura S, Malik S, Spiegelman BM, & Roeder RG (2003) Coordination of p300-mediated chromatin remodeling and TRAP/mediator function through coactivator PGC-1alpha. *Mol Cell* 12(5):1137-1149.
14. Li S*, et al.* (2008) Genome-wide coactivation analysis of PGC-1alpha identifies BAF60a as a regulator of hepatic lipid metabolism. *Cell Metab* 8(2):105-117.
15. Lin J, Handschin C, & Spiegelman BM (2005) Metabolic control through the PGC-1 family of transcription coactivators. *Cell Metab* 1(6):361-370.
16. Handschin C (2009) The biology of PGC-1alpha and its therapeutic potential. *Trends Pharmacol Sci* 30(6):322-329.
17. Huss JM, Torra IP, Staels B, Giguere V, & Kelly DP (2004) Estrogen-related receptor alpha directs peroxisome proliferator-activated receptor alpha signaling in the transcriptional control of energy metabolism in cardiac and skeletal muscle. *Mol Cell Biol* 24(20):9079-9091.
18. Mootha VK*, et al.* (2004) Erralpha and Gabpa/b specify PGC-1alpha-dependent oxidative phosphorylation gene expression that is altered in diabetic muscle. *Proc Natl Acad Sci U S A* 101(17):6570-6575.
19. Pachkov M, Balwierz PJ, Arnold P, Ozonov E, & van Nimwegen E (2013) SwissRegulon, a database of genome-wide annotations of regulatory sites: recent updates. *Nucleic Acids Res* 41(Database issue):D214-220.
20. Suzuki H*, et al.* (2009) The transcriptional network that controls growth arrest and differentiation in a human myeloid leukemia cell line. *Nat Genet* 41(5):553-562.
21. Schreiber SN*, et al.* (2004) The estrogen-related receptor alpha (ERRalpha) functions in PPARgamma coactivator 1alpha (PGC-1alpha)-induced mitochondrial biogenesis. *Proc Natl Acad Sci U S A* 101(17):6472-6477.
22. Eisele PS, Salatino S, Sobek J, Hottiger MO, & Handschin C (2013) The peroxisome proliferator-activated receptor gamma coactivator 1alpha/beta (PGC-1) coactivators repress the transcriptional activity of NF-kappaB in skeletal muscle cells. *J Biol Chem* 288(4):2246-2260.

23. Siddharthan R, Siggia ED, & van Nimwegen E (2005) PhyloGibbs: a Gibbs sampling motif finder that incorporates phylogeny. *PLoS Comput Biol* 1(7):e67.
24. Mahony S & Benos PV (2007) STAMP: a web tool for exploring DNA-binding motif similarities. *Nucleic Acids Res* 35(Web Server issue):W253-258.
25. Mangelsdorf DJ & Evans RM (1995) The RXR heterodimers and orphan receptors. *Cell* 83(6):841-850.
26. Hai T & Curran T (1991) Cross-family dimerization of transcription factors Fos/Jun and ATF/CREB alters DNA binding specificity. *Proc Natl Acad Sci U S A* 88(9):3720-3724.
27. Qian J, Chen S, Huang Y, Shi X, & Liu C (2013) PGC-1alpha regulates hepatic hepcidin expression and iron homeostasis in response to inflammation. *Mol Endocrinol* 27(4):683-692.
28. Jang WG*, et al.* (2007) Glucocorticoid receptor mediated repression of human insulin gene expression is regulated by PGC-1alpha. *Biochem Biophys Res Commun* 352(3):716-721.
29. Sandri M*, et al.* (2006) PGC-1alpha protects skeletal muscle from atrophy by suppressing FoxO3 action and atrophy-specific gene transcription. *Proc Natl Acad Sci U S A* 103(44):16260-16265.
30. Shaulian E & Karin M (2002) AP-1 as a regulator of cell life and death. *Nat Cell Biol* 4(5):E131-136.
31. Curran T & Franza BR, Jr. (1988) Fos and Jun: the AP-1 connection. *Cell* 55(3):395-397.
32. Cam H, Easton JB, High A, & Houghton PJ (2010) mTORC1 signaling under hypoxic conditions is controlled by ATM-dependent phosphorylation of HIF-1alpha. *Mol Cell* 40(4):509-520.
33. Majmundar AJ, Wong WJ, & Simon MC (2010) Hypoxia-inducible factors and the response to hypoxic stress. *Mol Cell* 40(2):294-309.
34. Wagner PD (2001) Skeletal muscle angiogenesis. A possible role for hypoxia. *Adv Exp Med Biol* 502:21-38.
35. Arany Z*, et al.* (2008) HIF-independent regulation of VEGF and angiogenesis by the transcriptional coactivator PGC-1alpha. *Nature* 451(7181):1008-1012.
36. Pino E, Wang H, McDonald ME, Qiang L, & Farmer SR (2012) Roles for peroxisome proliferator-activated receptor gamma (PPARgamma) and PPARgamma coactivators 1alpha and 1beta in regulating response of white and brown adipocytes to hypoxia. *J Biol Chem* 287(22):18351-18358.
37. Zhao J*, et al.* (2012) Peroxisome proliferator activated receptor (PPAR)-gamma co-activator 1-alpha and hypoxia induced factor-1alpha mediate neuro- and vascular protection by hypoxic preconditioning in vitro. *Brain Res* 1447:1-8.
38. Charos AE*, et al.* (2012) A highly integrated and complex PPARGC1A transcription factor binding network in HepG2 cells. *Genome Res* 22(9):1668-1679.
39. Notredame C, Higgins DG, & Heringa J (2000) T-Coffee: A novel method for fast and accurate multiple sequence alignment. *J Mol Biol* 302(1):205-217.
40. Arnold P, Erb I, Pachkov M, Molina N, & van Nimwegen E (2012) MotEvo: integrated Bayesian probabilistic methods for inferring regulatory sites and motifs on multiple alignments of DNA sequences. *Bioinformatics* 28(4):487-494.
41. Gentleman RC*, et al.* (2004) Bioconductor: open software development for computational biology and bioinformatics. *Genome Biol* 5(10):R80.
42. R Development Core Team (2012) R: A language and environment for statistical computing. (R Foundation for Statistical Computing).
43. Al-Shahrour F, Diaz-Uriarte R, & Dopazo J (2004) FatiGO: a web tool for finding significant associations of Gene Ontology terms with groups of genes. *Bioinformatics* 20(4):578-580.
44. Siepel A*, et al.* (2005) Evolutionarily conserved elements in vertebrate, insect, worm, and yeast genomes. *Genome Res* 15(8):1034-1050.

2.7 Supplemental Methods

ChIP and ChIP Sequencing

For each immunoprecipitation, approximately $1x10^8$ C2C12 cells were differentiated into myotubes and infected with Ad-flag-PGC-1α. For cross-linking protein complexes to DNA binding elements, the cells were incubated in a 1% formaldehyde solution for 10 minutes, followed by the addition of glycine to a final concentration of 125mM to quench the effect of the formaldehyde. The cells were rinsed in 1xPBS, harvested in ice-cold 1xPBS using a silicone scraper and pelleted by centrifugation. The pelleted cells were either used immediately or flash frozen and stored for later. The cells were then lysed at 4°C using two lysis buffers containing 0.5% NP-40/0.25% Triton X-100 and 0.1% Na-deoxycholate/0.5% N-lauroylsarcosine, respectively. The chromatin was then sheared by sonication to obtain DNA fragments of about 100-600bp in length. 50µl of the sonicated lysate was saved as input DNA. The immunoprecipitation was performed overnight at 4°C using magnetic beads (Dynabeads® Protein G, Invitrogen), which were previously coated with monoclonal anti-flag antibodies (Monoclonal ANTI-FLAG® M2 Antibody, Sigma). The beads carrying the precipitate were washed six times with RIPA buffer and once with TE that contained 50mM NaCl to eliminate unspecific binding of DNA to the beads. For elution, the beads were resuspended in elution buffer containing 1% SDS, placed in 65°C water bath for 15 minutes and vortexed every 2 minutes. To reverse the cross-links, the samples were incubated at 65°C overnight. The following day, the RNA and the cellular proteins were digested using RNase A and proteinase K. The DNA was precipitated and used for sequencing after success of the chromatin immunoprecipitation was validated by semiquantitative real-time PCR.

The ChIP-Seq experiment of over-expressed PGC-1α in C2C12 cells was performed in biological duplicates. At the joint Quantitative Genomics core facility of the University of Basel and the Department of Biosystems Science and Engineering (D-BSSE) of the ETH Zurich in Basel, DNA libraries were prepared using the standard Illumina ChIP-Seq protocol, as described by the manufacturer, and the immunoprecipitated samples sequenced on the Genome Analyzer II.

In order to keep only high quality data, the sequenced reads were filtered based on the quality score of each read and its alignments. Read were retained when Phred score >= 20, read length >= 25 bps and number of wrongly called nucleotides (Ns) <= 2. Those reads that passed the filter, (6'711'717 for the first immunoprecipitated sample (IP), 36'580'431 for the second IP, 17'899'074 for the first Whole Cell Extract (WCE), and 35'525'221 for the second WCE), were aligned to the mouse genome, UCSC mm9 assembly, using Bowtie version 0.12.7 (1) using parameters --best --strata -a --m 100. The number of aligned reads equaled 5'699'648 for the first IP sample, 16'053'370 for the first WCE, 21'448'059 for the second IP, and 32'244'584 for the second WCE.

2.8 Supplemental Figures and Tables

Suppl. Fig. S1. Peak Z score distribution and KEGG functional analysis. Related to Figure 1.

(A) Distribution of the Z scores for all sliding windows considered by the peak-finding algorithm along the mouse genome. The chosen cutoff for peak calling is depicted by the dotted line.

(B) Subset of the top significantly enriched KEGG terms identified for direct and indirect up-regulated PGC-1α target genes.

(C) Subset of the top significantly enriched KEGG terms identified for direct and indirect down-regulated PGC-1α target genes.

(D) ChIP-Seq signal around the promoter region of the five directly down-regulated genes (*Cacna1s*, *Mybph*, *Myh1*, *Myh4*, *Pfkfb3*) involved in regulating the contractile properties of fast-twitch muscle fibers.

Suppl. Fig. S2. Motif activities clustered by Z score in direct/indirect activation/repression. Related to Figure 2.

(A) Motifs showing different types of regulation (1=yes, 0=not).

Suppl. Fig. S3. PC2 interpretation and enriched motifs in "non ESRRA-like" peaks. Related to Figure 3.

(A) Top scoring results of motif search performed on the 3656 "non ESRRA-like" peaks with MotEvo.

(B) Correlation between Principal Component 2 scores and binding site posterior sum for each peak relative to the top 10 PCA motifs. "r" refers to the Pearson correlation coefficient.

Suppl. Fig. S4. siRNA knock-down efficiency for the putative PGC-1α partner TFs. Related to Figure 4.

(A-F) siRNA knock-down efficiency for ATF3 (A), GTF2I (B), JUN (C), NFE2L2 (D), NFYC (E) and ZFP143 (F) knock-down. Bars represent fold change over GFP/siCtrl levels. Error bars represent SEM. *p < 0.05; **p < 0.01; ***p < 0.001.

Suppl. Table 1. Real-time primer sequences.

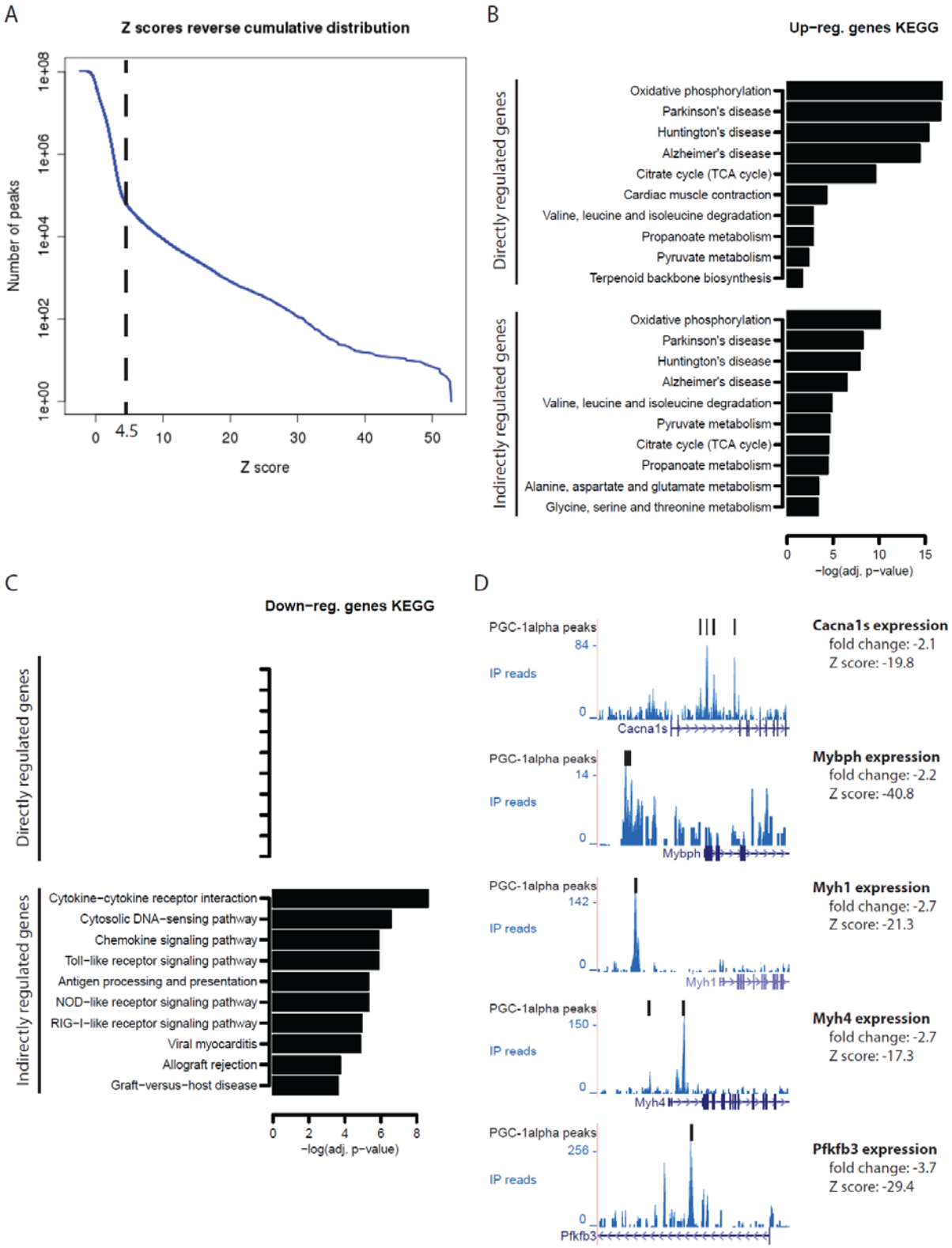
A
Z scores reverse cumulative distribution
Number of peaks
1e+00
1e+02
1e+04
1e+06
1e+08
0
4.5
10
20
30
40
50
Z score
B
Up−reg. genes KEGG
Directly regulated genes
Oxidative phosphorylation
Parkinson's disease
Huntington's disease
Alzheimer's disease
Citrate cycle (TCA cycle)
Cardiac muscle contraction
Valine, leucine and isoleucine degradation
Propanoate metabolism
Pyruvate metabolism
Terpenoid backbone biosynthesis
Indirectly regulated genes
Oxidative phosphorylation
Parkinson's disease
Huntington's disease
Alzheimer's disease
Valine, leucine and isoleucine degradation
Pyruvate metabolism
Citrate cycle (TCA cycle)
Propanoate metabolism
Alanine, aspartate and glutamate metabolism
Glycine, serine and threonine metabolism
0
5
10
15
−log(adj. p−value)
C
Down−reg. genes KEGG
Directly regulated genes
Indirectly regulated genes
Cytokine−cytokine receptor interaction
Cytosolic DNA−sensing pathway
Chemokine signaling pathway
Toll−like receptor signaling pathway
Antigen processing and presentation
NOD−like receptor signaling pathway
RIG−I−like receptor signaling pathway
Viral myocarditis
Allograft rejection
Graft−versus−host disease
0
2
4
6
8
−log(adj. p−value)
D
PGC-1alpha peaks
84
IP reads
0
Cacna1s
Cacna1s expression
fold change: -2.1
Z score: -19.8
PGC-1alpha peaks
14
IP reads
0
Mybph
Mybph expression
fold change: -2.2
Z score: -40.8
PGC-1alpha peaks
142
IP reads
0
Myh1
Myh1 expression
fold change: -2.7
Z score: -21.3
PGC-1alpha peaks
150
IP reads
0
Myh4
Myh4 expression
fold change: -2.7
Z score: -17.3
PGC-1alpha peaks
256
IP reads
0
Pfkfb3
Pfkfb3 expression
fold change: -3.7
Z score: -29.4

Suppl. Fig. S1.

A

Motif name	Z direct	Z indirect	Z avg. direct	Z avg. indirect	Directly activated	Indirectly activated	Directly repressed	Indirectly repressed
AIRE.p2	0.38	2.24	-0.91	5.40	0	1	0	0
ATF6.p2	0.24	2.97	-0.51	-7.25	0	0	0	1
BPTF.p2	1.38	2.56	3.37	-6.25	0	0	0	1
CEBPA,B_DDIT3.p2	1.03	2.13	2.51	-5.20	0	0	0	1
DMAP1_NCOR{1,2}_SMARC.p2	0.25	4.22	-0.60	-8.73	0	0	0	1
EHF.p2	0.73	2.77	1.77	6.35	0	1	0	0
ELF1,2,4.p2	3.11	1.32	7.59	3.13	1	0	0	0
ELK1,4_GABP{A,B1}.p3	1.18	2.46	2.89	5.95	0	1	0	0
ESR1.p2	2.33	4.53	5.69	11.04	1	1	0	0
ESRRA.p2	6.04	15.49	14.78	37.94	1	1	0	0
FOXO1,3,4.p2	0.46	2.51	1.13	6.12	0	1	0	0
GATA1..3.p2	1.21	3.39	-2.92	-8.04	0	0	0	1
GTF2I.p2	2.09	2.38	5.10	-5.80	1	0	0	1
HES1.p2	0.34	2.52	0.84	6.10	0	1	0	0
HNF4A_NR2F1,2.p2	2.26	1.54	5.52	3.64	1	0	0	0
IRF1,2,7.p3	1.77	24.23	4.34	-14.48	0	0	0	1
LEF1_TCF7_TCF7L1,2.p2	0.17	2.55	0.37	-6.11	0	0	0	1
LMO2.p2	2.36	1.65	5.78	3.98	1	0	0	0
MEF2{A,B,C,D}.p2	0.97	2.67	2.35	-6.51	0	0	0	1
MYFfamily.p2	0.36	2.38	0.79	-5.12	0	0	0	1
MYOD1.p2	1.49	2.05	3.65	-4.99	0	0	0	1
NFATC1..3.p2	0.16	3.46	-0.24	-8.42	0	0	0	1
NFE2L1.p2	1.79	2.32	4.36	5.23	0	1	0	0
NFKB1_REL_RELA.p2	0.50	6.54	1.19	-16.01	0	0	0	1
NFY{A,B,C}.p2	2.37	3.56	5.80	7.62	1	1	0	0
NKX3-1.p2	0.60	2.43	1.48	5.93	0	1	0	0
NR5A1,2.p2	3.53	7.73	8.66	17.00	1	1	0	0
NRF1.p2	1.60	4.61	3.91	6.21	0	1	0	0
PAX4.p2	2.50	1.53	6.11	-3.68	1	0	0	0
POU5F1_SOX2{dimer}.p2	0.24	2.32	0.57	5.65	0	1	0	0
REST.p3	0.48	2.41	1.15	5.70	0	1	0	0
RREB1.p2	1.56	2.39	3.82	-5.42	0	0	0	1
RUNX1..3.p2	0.09	3.94	0.11	-9.61	0	0	0	1
RXR{A,B,G}.p2	2.29	4.30	5.59	10.50	1	1	0	0
RXRA_VDR{dimer}.p2	0.71	2.54	1.71	6.20	0	1	0	0
RXRG_dimer.p3	1.67	2.01	4.09	4.89	0	1	0	0
SOX{8,9,10}.p2	0.16	2.17	0.30	-5.28	0	0	0	1
SP1.p2	3.99	0.61	9.76	0.33	1	0	0	0
SPI1.p2	1.69	2.70	4.14	-6.19	0	0	0	1
STAT1,3.p3	0.74	2.53	1.79	-6.17	0	0	0	1
STAT2,4,6.p2	0.35	4.81	0.52	-9.67	0	0	0	1
TBP.p2	1.11	3.20	2.71	-4.04	0	0	0	1
TEAD1.p2	0.99	2.23	-2.43	-5.43	0	0	0	1
TFAP2B.p2	1.75	2.72	4.26	-6.61	0	0	0	1
TFCP2.p2	1.07	2.62	2.57	-5.80	0	0	0	1
TGIF1.p2	0.57	2.34	1.34	-5.68	0	0	0	1
TLX1..3_NFIC{dimer}.p2	0.84	4.91	-2.05	-11.97	0	0	0	1
TLX2.p2	0.57	2.86	1.37	-6.76	0	0	0	1
YY1.p2	0.88	2.97	2.09	5.77	0	1	0	0
ZIC1..3.p2	0.20	2.99	-0.46	-7.24	0	0	0	1
ZNF143.p2	2.48	4.65	6.05	9.68	1	1	0	0
ZNF384.p2	0.64	2.34	-1.55	-5.27	0	0	0	1

Suppl. Fig. S2.

A

Motif name	Z score	TFBSs count	Peaks percentage
BACH2	59.05	712	16.96%
FOS_FOS{B,L1}_JUN{B,D}	51.92	1125	20.18%
FOSL2	49.84	724	16.55%
NFE2	46.72	548	12.76%
NFE2L2	39.79	372	8.84%
REST	35.42	71	0.93%
CTCF	33.65	97	2.46%
CDX1,2,4	27.37	218	4.59%
MZF1	23.94	228	4.95%
RREB1	22.80	108	2.02%
SPI1	21.90	218	5.50%
BPTF	21.88	278	4.80%
GTF2I	21.17	228	4.95%
PATZ1	20.97	162	3.92%
FOX{I1,J2}	20.47	211	4.33%

B

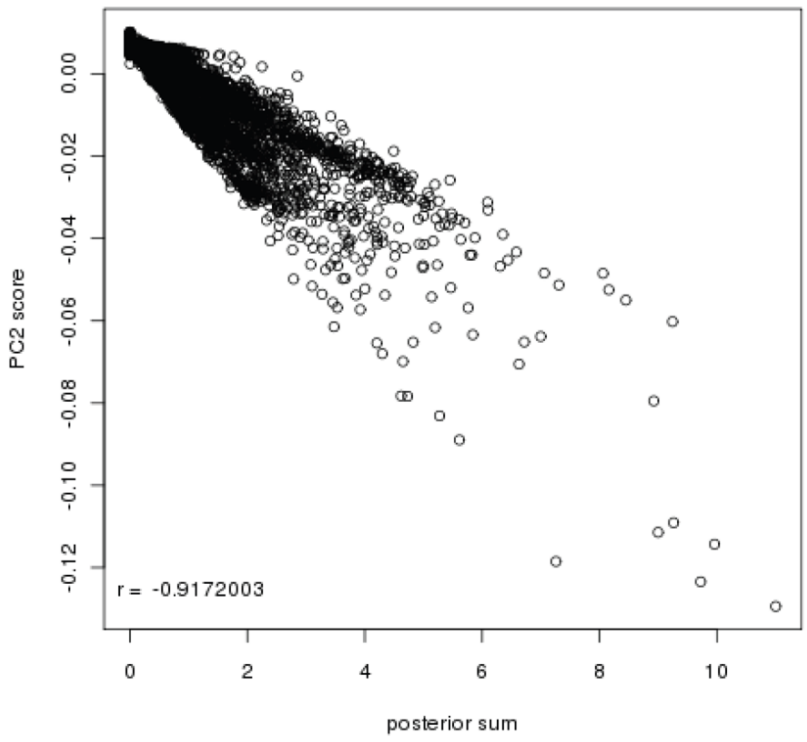

Suppl. Fig. S3.

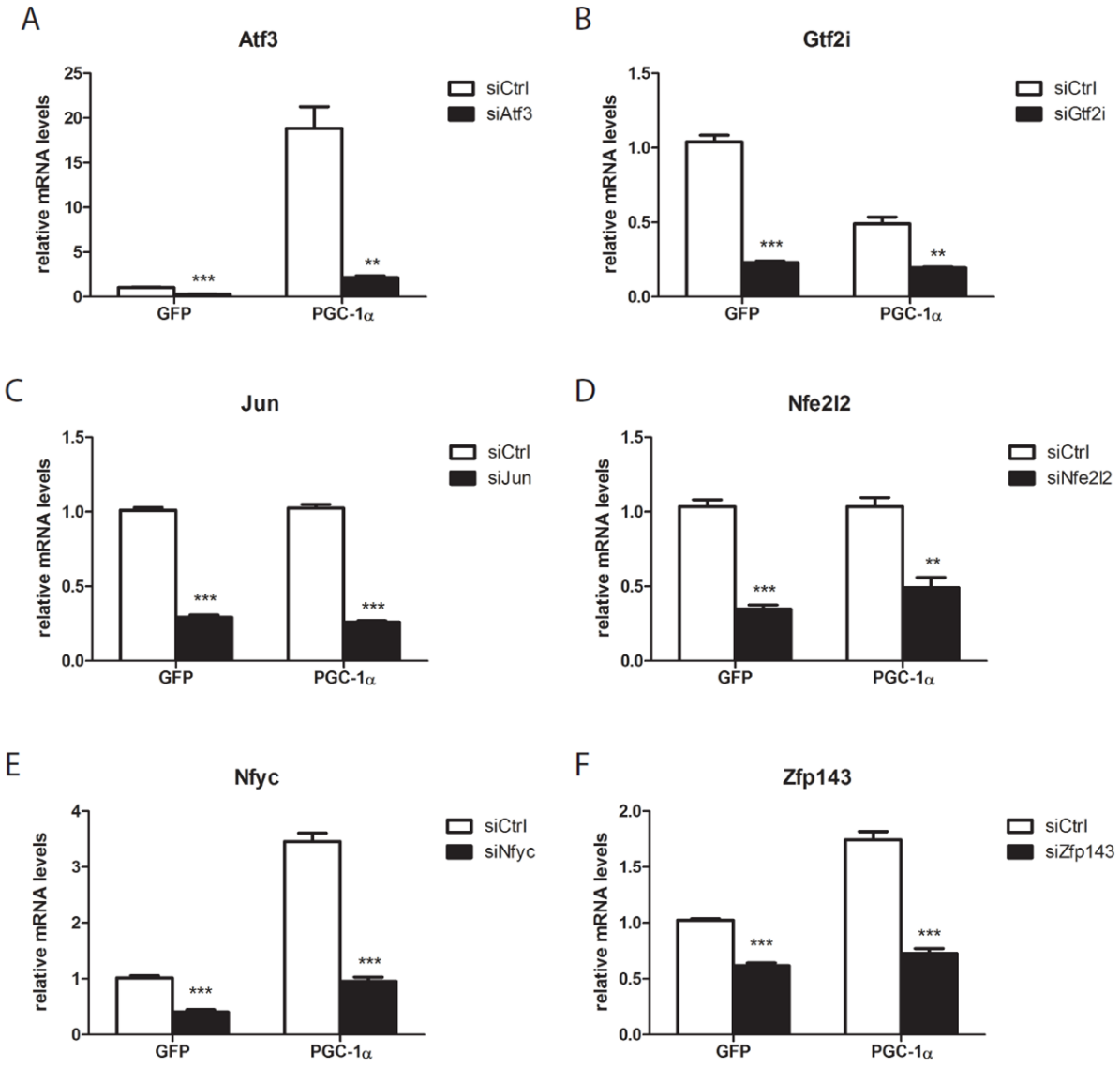
A
Atf3
relative mRNA levels
25
20
15
10
5
0
***
**
GFP
PGC-1α
siCtrl
siAtf3
B
Gtf2i
relative mRNA levels
1.5
1.0
0.5
0.0
***
**
GFP
PGC-1α
siCtrl
siGtf2i
C
Jun
relative mRNA levels
1.5
1.0
0.5
0.0
***
***
GFP
PGC-1α
siCtrl
siJun
D
Nfe2l2
relative mRNA levels
1.5
1.0
0.5
0.0
***
**
GFP
PGC-1α
siCtrl
siNfe2l2
E
Nfyc
relative mRNA levels
4
3
2
1
0
***
***
GFP
PGC-1α
siCtrl
siNfyc
F
Zfp143
relative mRNA levels
2.0
1.5
1.0
0.5
0.0
***
***
GFP
PGC-1α
siCtrl
siZfp143

Suppl. Fig. S4.

Real-time PCR primers used for testing the efficiency of the ChIP		
gene promoter or intron	forward primer	reverse primer
Tbp intron	TGTGAGCTCCTTGGCTTTTT	ATAGTTGCCCAGCAATCAGG
promoter of *Aco2*	CACCGATAGTTGCTTTCCAGATAC	AACCATCTGACAGGCATAGTCAAT
promoter of *Cycs*	AAGGGCGCCCTCTGGGCACATC	ATCCCCGTCGCGCGCTCACCG
promoter of *Acadm*	CCTTGCCCGAGCCTAAAC	GTCTGGCTGCGCCCTCT
promoter of *Atp5b*	CTGGAAACTTCCACCCTCACTA	GAGAGGTTTTTGGCGGAACTA
promoter of *Idh3a*	GGACGGCGTCAAGGTCAAG	GCCTAGGTGGCCTGTCTGTG

Real-time PCR primers used for testing the knock-down efficiency by siRNAs		
gene	forward primer	reverse primer
Rn18s	AGTCCCTGCCCTTTGTACACA	CGATCCGAGGGCCTCACTA
Fos	TACTACCATTCCCCAGCCGA	GCTGTCACCGTGGGGATAAA
Jun	TGGGCACATCACCACTACAC	TCTGGCTATGCAGTTCAGCC
Atf3	TCTGCGCTGGAGTCAGTTAC	CCGCCTCCTTTTCCTCTCAT
Gtf2i	TTCGAAGGCTTTGCAAGGAAG	TTCGGGGTCCTCACTGGTTT
Nfe2l2	AGTGGATCCGCCAGCTACTC	ATGGGAATGTCTCTGCCAAA
Nfyc	CCACCAGTTCTACGACCACC	GGCCTGTACAATCTGCACCT
Zfp143	GTGGTCGGTCCTTTACCACA	AAATGCCCTCCCACATCCAG

Real-time primers used for target gene validation		
gene	forward primer	reverse primer
Aim1l	CCTGTTGCGTCCATAAGGGT	GCTCTGAGTTCCACATCCCC
Atp1b1	GCTACGAGGCCTACGTGCTA	TGCCACAGTCCTCGAAAATC
Atp5g1	CAGAGGCCCCATCTAAGCAG	TGTCCCGGGAAATGACACTG
Cdk15	ATGCAGTTGCTACCACCGTT	CCGTGGAACTGGATGCTTCT
Cdr2l	GGAACAGGAAAACGAACGGC	ACCACCGTGTACTCACGTTC
Dot1l	TGACCTCAGATGAGGAGCCA	TGTCTTCGGGGGAGATTTGC
Eef1a2	CAAGATGGACTCCACGGAAC	CTGGGTTGTAGCCGATCTTC
Eif2b4	ACGGCAAGACCCAATCAGAG	AAGTTCTGCCTTACTCCGGC
Fa2h	GTGGACTGGCAGAAACCTCT	TCTGAGTGGAAGAGGCGAAT
Fabp3	CATGTGCAGAAGTGGAACGG	CTCACCACACTGCCATGAGT
Fam131c	CTGGCTACGTCATCCCTTGT	TCCAGCCTTTCCACTCGAT
Gabpa	GTCGAGGTGGTCATCGATCC	GTAATGTGCTTGGTGCCGTC
Gdf15	CACGCATGCGCAGATCAAAG	TGTGCATAAGAACCACCGGG
Gtpbp2	TGGAAACCTCAAAGCTCGGG	GTACGGAGGGTTGTTGGCTT
Il1a	TGCAAGCTATGGCTCACTTC	GATACTGTCACCCGGCTCTC
Inpp5j	ACAAGGGCGGAGTAAGTGTG	TGAAAGTTATCCTTGCGCTGT
Jam2	GTATTACTGCGAAGCCCGGA	CAACCGTTGCTATGATGCCG
Ldhb	GACTCCGAAAATTGTGGCCG	TTCTCTGCACCAGGTTGAGC
Lpin1	CGGCCCTCAACACCAAAAAG	AATTCACCCCACAGCCAGAG
Lrrc2	GTGGAAGGAGCTGCCTGATT	AACAGCTCGATGTACGTGGG
Met	GCTGAGAAACTCTTCCGGCT	AGCCGGCCCATGAATAAGTC
Ndufa9	TTCTGTGGCTCATCCCATCG	TGTAGCCCCAAACACAGTGG
Nmnat1	GGTCGGTGATGCGTACAAGA	CCACGTATCCACTTCCACCC
Nppb	GGCCTCACAAAAGAACACCC	TGCCCAAAGCAGCTTGAGAT

Nr0b2	CCTCTTCAACCCAGATGTGC	GGGCTCCAAGACTTCACACA
Osbpl1a	TCCCCCAATCAGTGCATTCC	GCTTCTACACTCTTGCCCCA
Qrsl1	GTTGGATCAGGGTGCCCTAC	GGGGTTTCTAACTGGCCCAA
Rasl10b	AGACCTGGAAGTGCGGCTAC	GGCAGCGTGCACGTGTTT
Rrm2	TTGCAGCGAGTGATGGCATA	CCATGGCAATTTGGAAGCCA
Samm50	TTTTGATGGACTTGGGCGGA	TGAGATCGCCGCATTACCTC
Slc25a4	GGTACTTCCCCACTCAAGCC	AGCAAAGTAGCGCCAGAACT
Slc25a35	TAGTCGTGGCAATGACACCC	TCCAAGATCCCCCGGTACAT
Slc6a19	TCCACTCAACCAGAACCAGAC	TGAGTCACTGATGGAAGTGGAG
Srxn1	CCAGGGTGGCGACTACTACT	AGGTCTGAAAGGGTGGACCTC
Stard7	CTCTACGGCCGCCTGTATTC	CGCCATCAAAACAGAGGCAT
Stk19	GTCCTCACTGTCCGAGATGC	CACCATGCTCAGTACAGCCT
Syt7	ACTGGGCAAACGCTACAAGA	TGCAGGCAACTTGATGGCTT
Tbrg4	AACGACAGCCGTACATTGGT	AGCTCCAGGCACTTGTCTTC
Tfam	GAGCGTGCTAAAAGCACTGG	GCTACCCATGCTGGAAAAACA
Tinagl1	TTCTTGTACCAGCGTGGCAT	CCCCACCCAGTGATCTTGAC
Tomm5	CGGAGGAGATGAAGCGGAAG	TATGGAGTGACTCGCAGCAG
Trak2	GCTGAAGAGACGTTCCGCTA	ATCTCGATCCCTCTCTGCCA
Trmt61a	GCTCCTTCTCTCCGTGCATT	TGCGCACATTGTAGACCTGT
Trp53inp2	TACCCCTCCCGCCTGTTTTA	CTGCCGGTGACATAAACGGA
Ttc7b	TGCTCCCCACGATCAAGAAC	ATCTCCCGACTCCTCTCGTC
Tusc2	GCAGTGCCTCCCTTCGTATT	CTGCCCATTCTTGGTGACGA
Twf2	TGCTACCTCCTCTTCCGACT	ATAGCATCTTCAGCCGCACC
Wnt7b	TTTCTCTGCTTTGGCGTCCT	GGCCAGGAATCTTGTTGCAG

Suppl. Table 1. Real-time primer sequences. Semiquantitative real-time PCR primers used for validation experiments.

2.9 Supplemental References

1. Langmead B, Trapnell C, Pop M, & Salzberg SL (2009) Ultrafast and memory-efficient alignment of short DNA sequences to the human genome. *Genome Biol* 10(3):R25.

3 MANUSCRIPT-2: ERRα as the major effector of gene program regulation by PGC-1α operates in presence and absence of PGC-1α to induce gene expression

(Manuscript in preparation)

Silvia Salatino[1,*], Mario Baresic[1,2,3,*], Erik van Nimwegen[2,3,#], and Christoph Handschin[1,#]

[1]Focal Area Growth & Development and [2]Focal Area Computational & Systems Biology, Biozentrum, University of Basel, Basel, Switzerland

[3]Swiss Institute of Bioinformatics, Basel, Switzerland

[*]These authors contributed equally to this manuscript

[#]Correspondence to: erik.vannimwegen@unibas.ch or christoph.handschin@unibas.ch

Running title: PGC-1α and ERRα together and independently regulate gene transcription in skeletal muscle cells

In this study I:

- contributed to the planning and design of this project.
- performed all the wet-lab experiments: cell culture, chromatin immunoprecipitation, expression arrays (until the generation of data, but not the implementation of the data into our results), knockdown of ERRa by adenoviral vectors and the validation of the knockdown by real-time PCR.
- contributed to the analysis and the interpretation of the results.
- contributed to the writing of the manuscript.

3.1 Abstract

Skeletal muscle tissue reacts to exercise training by inducing changes, which allow the muscle to adapt to increased physical activity. The transcriptional coactivator PGC-1α is induced by exercise and subsequently mediates all exercise-induced adaptations of skeletal muscle by coordinating the activity of key transcription factors like the ERRα. Although ERRα is established as an effector of PGC-1α transcriptional activity, it is not clear to which extent PGC-1α requires ERRα to induce its target genes and how precisely this transcriptional network regulates gene expression. By performing genome-wide chromatin occupation studies we mapped the recruitment of PGC-1α and ERRα to DNA and thereby identified which subset of PGC-1α target genes is regulated by direct binding of PGC-1α, ERRα or both factors together. Surprisingly, we revealed that ERRα can occupy promoters of PGC-1α target genes and regulate their expression without being coactivated by PGC-1α. These ERRα binding sites are enriched for the Sp1 motif and therefore we suggest that these two transcription factors might interact to regulate gene expression. This study provides a global analysis of the gene transcription regulation by ERRα and PGC-1α in skeletal muscle cells and predicts additional transcription factors which mediate the PGC-1α-induced gene expression.

3.2 Introduction

The expression and activity of the transcriptional coactivator peroxisome proliferator-activated receptor γ coactivator 1α (PGC-1α) can be induced and modulated by physiological stimuli, which require metabolic changes like cold exposure, fasting or exercise (Handschin and Spiegelman, 2006). PGC-1α integrates these signals and subsequently enhances the activity of transcription factors that are key regulators of metabolic processes. These transcription factors include most members of the nuclear receptor superfamily but also other transcription factors (Puigserver and Spiegelman, 2003). Therefore, PGC-1α has emerged as a major controller of mitochondrial biogenesis and oxidative phosphorylation (OXPHOS) across different tissues (Puigserver and Spiegelman, 2003). The potency of PGC-1α as a coactivator can in part be explained by its capability to bind to proteins with histone acetylase activity or to the mediator and SWI/SNF complexes and to bring them in the proximity of transcription factors (Liu and Lin, 2011; Puigserver and Spiegelman, 2003). In skeletal muscle, most signaling pathways typically induced by exercise at some point converge on PGC-1α and modify its expression or activity (Handschin, 2010). PGC-1α in turn then participates in the regulation of the expression of genes, which are induced in skeletal muscle in response to exercise (Handschin, 2010). In addition to inducing the entire genetic program for oxidative phosphorylation and mitochondrial biogenesis in skeletal muscle, PGC-1α also regulates the expression of genes which are important for angiogenesis, neuromuscular junction, glucose uptake and fiber type switch (Handschin, 2010).

The orphan nuclear receptor ERRα, NRF-1 and NRF-2 are induced and subsequently coactivated by PGC-1α in order to drive the expression of some PGC-1α target genes in skeletal muscle cells (Mootha et al., 2004; Wu et al., 1999). Recently, we have identified ERRα as the major mediator of PGC-1α induced gene expression in cultured skeletal muscle cells (Baresic et al., 2013). However, to which extent the induction of PGC-1α target genes requires ERRα is not known. In other words, it is not fully clear which genes are induced by PGC-1α and ERRα cooperatively and which in absence of PGC-1α or which transcription factors cooperate with PGC-1α to regulate the expression of these ERRα independent PGC-1α target genes. Besides, most work investigating how PGC-1α regulates gene expression focuses on direct coactivation of transcription factors by PGC-1α in the promoters of target genes (Michael et al., 2001; Mootha et al., 2004; Schreiber et al., 2004; Wu et al., 1999). However, it is as well possible that many PGC-1α target genes are regulated by transcription factors which are induced but not coactivated by PGC-1α.

By comparing genomic locations occupied by ERRα with those occupied by PGC-1α on a genome-wide scale, we show that ERRα and PGC-1α co-localize in promoter regions of their target genes and identify which genes are cooperatively transcribed by these two factors. Surprisingly, we find that even though PGC-1α induces ERRα, it does not coactivate ERRα on all of its target genes. Thus, ERRα binds to promoters of some of its target genes and transcribes them without being coactivated by PGC-1α. Furthermore, the motif for specificity protein 1 (Sp1) is enriched in ERRα binding sites

that do not overlap with PGC-1α binding sites, suggesting that ERRα and Sp1 might cooperatively regulate transcription.

3.3 Results

3.3.1 ERRα is able to regulate transcription independently from PGC-1α

The capability of ERRα to control the transcription of its downstream target genes has been postulated to be strictly dependent on the coactivation of PGC-1α, to the extent that this co-regulator – more precisely its homolog PGC-1β – has been proposed to act as a "protein ligand" for ERRα (Kamei et al., 2003). To verify this assumption and to identify all regions genome-wide that are bound by this transcription factor in skeletal muscle, we performed a chromatin immunoprecipitation experiment followed by high-throughput sequencing (ChIP-Seq) of ERRα in differentiated C2C12 murine myotubes. These ERRα binding sites were then compared to a previously sequenced set of PGC-1α recruitment regions (Baresic et al., 2013) obtained within the same context of adenovirus-induced PGC-1α over-expression.

In order to identify all genomic locations significantly enriched in ERRα binding, we passed a sliding window along the genome and compared, for each consecutive window, the local IP read density with the whole cell extract (WCE) background read amount. All regions with a Z score bigger than 3.5 were merged in a final total of 3225 peaks, which included binding regions in the vicinity of known ERRα target genes (Fig. S1A), like the pyruvate dehydrogenase lipoamide kinase isozyme 4 (Pdk4) and the isocitrate dehydrogenase 3 [NAD+] alpha (Idh3a) (Tiraby et al., 2011; Zhang et al., 2006). The enrichment of IP fragments from the ChIP-Seq experiment was validated for some of these ERRα target genes by semiquantitative real-time PCR (Fig. S1B).

Most surprisingly, when we compared ERRα and PGC-1α occurrences genome-wide (Fig. 1A), we noticed that the majority of ERRα (~60%) peaks are actually not overlapping any PGC-1α peak, suggesting that the so-far believed concept of symbiotic cooperation between these two proteins is in fact only restricted to a small percentage of their targets (~40% for ERRα and ~18%). Some examples of this differential regulation are depicted in Fig. 1B. Moreover, of the 1321 ERRα peaks overlapping a PGC-1α site (that is, their centers are at most 200 bps apart), the vast majority are well centered on the closest PGC-1α peak at a distance of a couple of dozen base pairs (Fig. 1C). Noticeably, a big fraction of ERRα resides within 1kb from the closest RefSeq transcription start site (Fig. 1D), which differs from the PGC-1α peaks that were located mostly distally from TSSs.

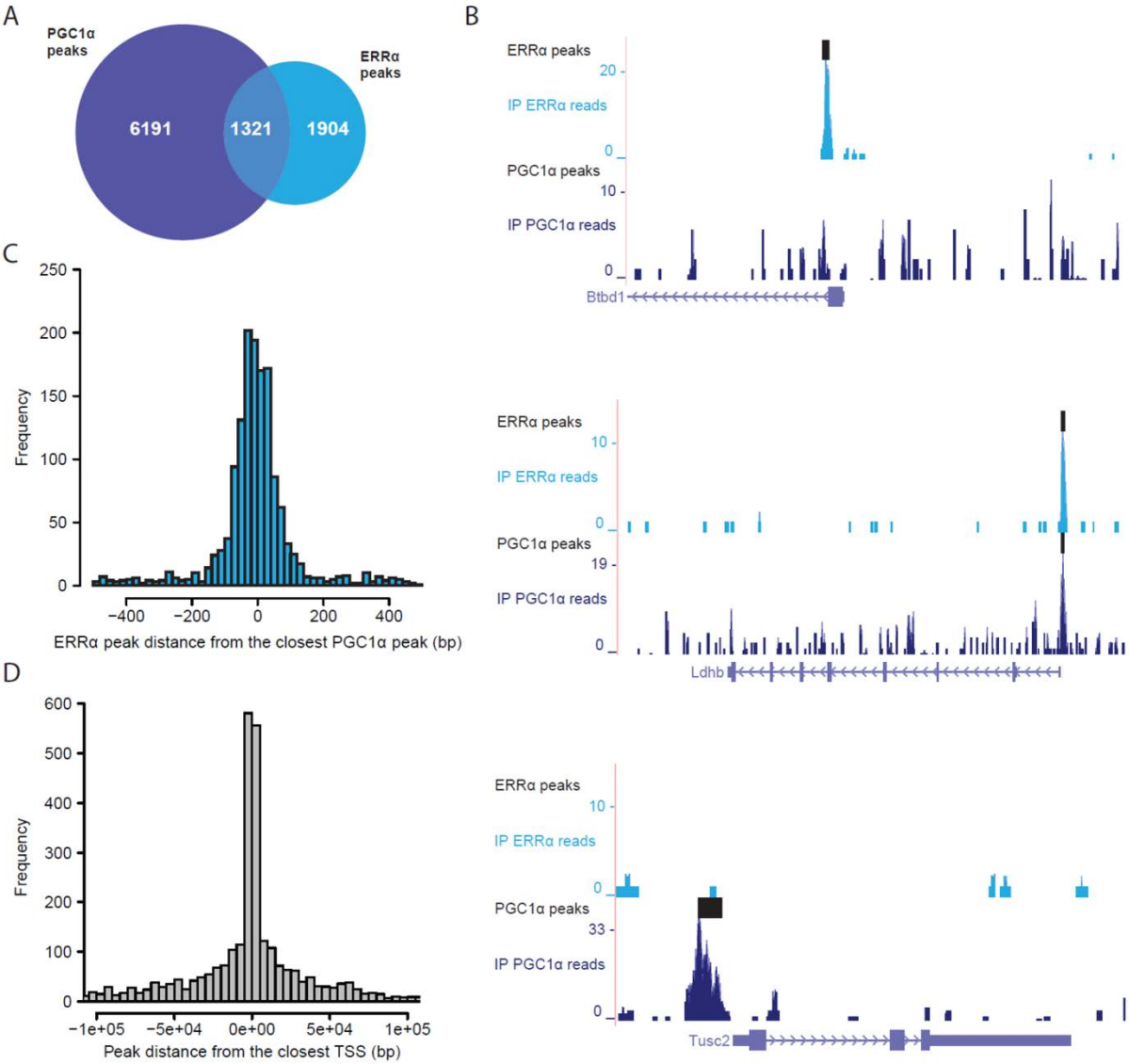

Figure 1. ERRα and PGC-1α control the expression of distinct sets of target genes.

(A) Venn diagram depicting the number of ChIP-Seq binding peaks for PGC-1α (blue) and for ERRα (cyan).

(B) PGC-1α and ERRα read densities around the TSS of the genes Btbd1, Ldhb and Tusc2 obtained from the UCSC Genome Browser. The first plot is an example of a gene directly regulated by ERRα, but not by PGC-1α; the second is directly regulated by both ERRα and PGC-1α; the third is directly regulated by PGC-1α, but not by ERRα.

(C) Distribution of ERRα peaks from their closest PGC-1α peaks.

(D) Distribution of ERRα peaks from the nearest RefSeq transcription start site (TSS).

3.3.2 ERRα targets up-regulation is enhanced when also PGC-1α is present

To integrate the results obtained from the ChIP-Seq experiment with functional data, we further analyzed the impact of ERRα on its downstream targets in terms of their gene expression patterns in differentiated muscle cells under the following conditions: (i) shGFP-transfected cells over-expressing GFP; (ii) shGFP-transfected cells over-expressing PGC-1α; (iii) shERRα-transfected cells over-expressing PGC-1α and supplemented with the ERRα inverse agonist XCT-790. By comparing the second with the first and the third with the second condition, we sought to assess both the effect of PGC-1α over-expression and the response to ERRα knockdown (Fig. 2A).

After mapping the microarray probes to known transcripts and, through these, to a reference set of mouse promoters (Pachkov et al., 2013), we noticed that more promoters were significantly up-regulated (1863, corresponding to 1165 genes) than down-regulated (658, corresponding to 470 genes) following PGC-1α over-expression. In contrast, following ERRα knock-down, we observed the opposite effect: 910 promoters (corresponding to 597 genes) were significantly induced whereas 1952 promoters (corresponding to 1205 genes) were repressed (Fig. 2B).

By combining the expression array with ERRα and PGC-1α genomic occupancy data, we wanted to check whether the binding of PGC-1α to the same sites where ERRα is recruited has any remarkable effect on the expression of the ERRα target genes. Therefore, we used only those peaks that were associated to a promoter located within 1 kb from the peak center. Most interestingly, we found that the presence of PGC-1α at regulatory regions of ERRα targets' determines a clear shift in the distribution of gene expression towards up-regulation and that the top induced genes are those hosting in their neighborhood both a peak for ERRα and for PGC-1α (Fig. 2C).

As these findings suggested that, at least for some targets, PGC-1α is required to boost the expression level of the gene, we verified whether such a dependency can be also observed with regards to ERRα. Thus, based on the expression levels in the ERRα knock-down condition, we distinguished between ERRα-dependent (871 genes) and ERRα-independent (763 genes) PGC-1α targets. We furthermore used these differentially regulated genes as input for the functional annotation tool FatiGO (Al-Shahrour et al., 2004) to stratify these in terms of the regulatory pathways involved (Fig. 2D-F). Surprisingly, most of the top enriched terms for induced genes were common to ERRα-dependent and ERRα-independent PGC-1α targets (761 and 404 genes, respectively) However, although all pathways had smaller (thus, more significant) p-values in ERRα-dependent targets, certain ontology terms were only found in the ERRα-dependent targets, in particular those related to ubiquinone metabolism and to tRNA processing.

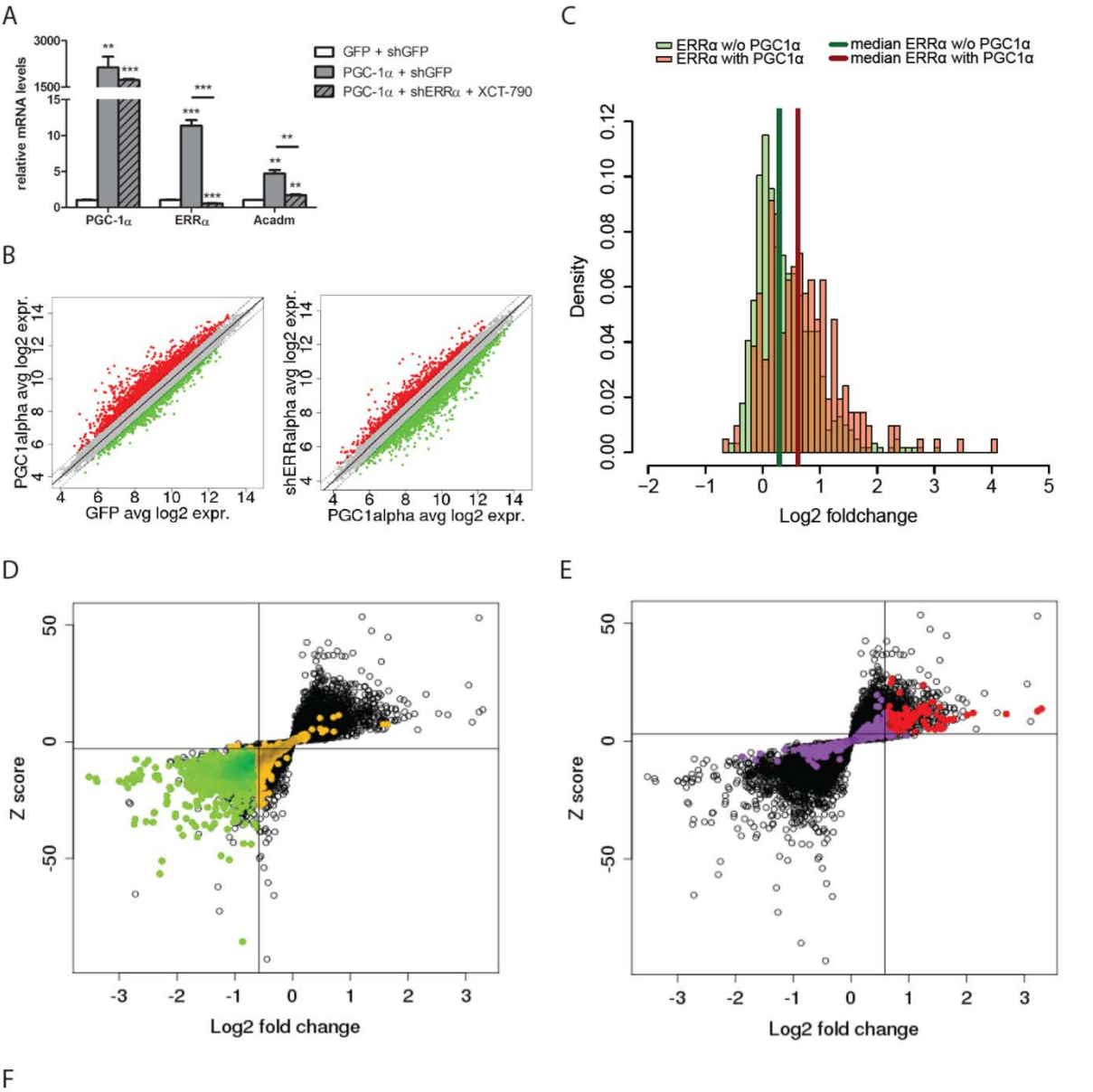

F

ERRα-dep. PGC1α induced genes (761)	ERRα-indep. PGC1α induced genes (404)	ERRα-dep. PGC1α repressed genes (110)	ERRα-indep. PGC1α repressed genes (359)
3.66E-127 mitochondrion	3.77E-29 mitochondrial part	1.97E-03 myofibril	6.30E-07 contractile fiber
8.69E-97 mitochondrial part	3.72E-14 organelle inner membrane	1.97E-03 contractile fiber	1.09E-04 myofibril
1.33E-65 organelle inner membrane	1.36E-06 gen. of prec. metab. and energy	8.36E-03 muscle organ development	1.27E-04 cytoskeletal protein binding
2.22E-41 Oxidative phosphorylation	1.23E-04 mitochondrion organization	2.18E-02 skeletal muscle tissue development	5.22E-04 muscle contraction
1.56E-40 Parkinson's disease	3.95E-04 tRNA processing	2.18E-02 tissue development	6.90E-04 muscle organ development
7.55E-40 gen. of prec. metab. and energy	2.57E-03 organelle outer membrane		7.91E-03 GTPase activity
7.85E-37 Huntington's disease	2.70E-03 outer membrane		1.08E-02 sarcoplasmic reticulum
4.11E-34 electron transport chain	7.02E-03 protein targeting to mitochondrion		1.08E-02 sarcolemma
1.83E-32 Alzheimer's disease	7.02E-03 ubiquinone biosynthetic process		1.13E-02 sarcoplasm
2.22E-31 oxidation-reduction process	7.02E-03 electron transport chain		1.36E-02 calcium ion binding
1.22E-30 respiratory chain	1.73E-02 quinone cofactor metabolic process		1.45E-02 striated muscle contraction
5.66E-25 oxidoreductase activity	1.81E-02 soluble fraction		1.45E-02 skeletal muscle tissue development
1.38E-19 Citrate cycle (TCA cycle)	2.08E-02 cellular respiration		1.88E-02 cell-cell junction
6.08E-19 cellular respiration	2.69E-02 nucleotide metabolic process		1.96E-02 cellular component movement
1.88E-15 acetyl-CoA metabolic process	3.34E-02 mitochondrial DNA replication		2.72E-02 actin binding
4.17E-14 aerobic respiration	3.34E-02 mitochondrial DNA metabolic process		2.72E-02 calmodulin binding
1.18E-13 cofactor binding	3.41E-02 tRNA binding		2.72E-02 GTP binding
1.72E-13 organic acid metabolic process	3.41E-02 NADH dehydr. activity		3.20E-02 guanyl nucleotide binding
1.72E-13 carboxylic acid metabolic process	3.41E-02 NADH dehydr. (ubiquinone) activity		3.61E-02 endoplasmic reticulum
2.73E-13 tricarboxylic acid cycle	3.41E-02 methyltransferase activity		3.63E-02 hydrolase activity, acting on acid anhydrides

Figure 2. ERRα targets transcription levels increase upon PGC-1α recruitment.

(A) qRT-PCR analysis of PGC-1α, ERRα and Acadm mRNA levels in response to PGC-1α over-expression (OV) and shERRα knock-down (KD) + XCT-790. Data are normalized to mRNA levels in GFP infected cells. Error bars represent ± SEM. *p < 0.05; **p < 0.01; ***p < 0.001.

(B) Log2 expression levels of all mouse promoters in the PGC-1α OV condition versus GFP control (left panel) and in the PGC-1α OV + shERRα KD + XCT-790 versus PGC-1α OV (right panel). Promoters are colored in red (up-regulation) when their fold change is bigger than 1.5 and in green (down-regulation) when their fold change is smaller than -1.5 (obtained by taking the inverse of the linear binding ratio).

(C) Distribution of the log2 fold change for the promoters associated to an "only ERRα peak" (green) compared to the distribution of the log2 fold change for the promoters associated to an "overlapping ERRα and PGC-1α peak" (red); the overlay of the two distributions is indicated in orange. Each distribution is normalized to the total number of promoters within the corresponding set.

(D-E) Distributions of all mouse promoters log2 fold change and Z score for the comparison shERRα versus PGC-1α over-expression. The black lines indicate the cutoffs used to define ERRα-dependent and ERRα-independent promoters. Highlighted are the promoters significantly: (i) induced by PGC-1α OV (panel D) and either repressed by the ERRα KD (green) or not repressed (yellow); (ii) repressed by PGC-1α OV (panel E) and either induced by the ERRα KD (red) or not induced (purple).

(F) Subset of the top significantly enriched GO and KEGG terms identified for ERRα-dependent and ERRα-independent PGC-1α target genes, either induced or repressed (for the color code, see Fig. 2D-E).

Symmetrically, also repressed PGC-1α targets show minor differences in terms of ontologies enriched among ERRα-dependent and ERRα-independent genes. Both groups show over-representation of terms related to myofibril contraction and muscle tissue development, although the ERRα-independent targets are also enriched in actin, calmodulin and GTP binding (Fig. 2F).

After defining the four categories of genes depicted in Fig. 2F, we furthermore checked whether these targets were associated to any of the following peak groups: (i) a PGC-1α peak, (ii) an ERRα peak, (iii) peaks belonging to each of the two chipped proteins or (iv) no peaks. To our surprise, although there were more ERRα binding events in the vicinity of ERRα-dependent PGC-1α targets (99 cases), we observed no difference in their percentages compared to the ERRα-independent PGC-1α targets (13.01% and 13.12%, respectively). However, it is conceivable that some genes might be regulated by more distally located peaks, which cannot be identified by the limitation of our assignment of ChIP-Seq peaks to the closest promoter within a maximum distance of 10 kb. Moreover, we noticed that > 90% of the down-regulated targets are not associated to any peak and that the percentage of PGC-1α indirect targets within each one of the above mentioned four groups is always much bigger than the fraction of PGC-1α direct targets, supporting the hypothesis that PGC-1α-dependent gene repression is mainly an indirect event (Baresic et al., 2013; Eisele et al., 2013).

3.3.3 Sp1 contributes to the up-regulation of ERRα targets in muscle cells

As a following step, we analyzed the occurrence of transcription factor DNA-binding motifs within the ERRα peaks. We used the software MotEvo (Arnold et al., 2012) to check which of the 190 known mammalian regulatory motifs downloaded from SwissRegulon (Pachkov et al., 2013) were significantly over-represented in our peaks compared to a set of shuffled background regions. As we expected, the most enriched motif, with a Z score of 123.15, was ESRRA (the motif corresponding to the Estrogen-related receptor alpha), even though transcription factor binding sites (TFBSs) for this motif were found in only ~48% of the peaks. Given the high promiscuity that exists between nuclear receptors consisting of different configurations of hexameric repeats (Mangelsdorf and Evans, 1995), it might happen that the precise identity of the nuclear receptor bound at each peak is difficult to deduce from DNA-binding motifs and that, like in our case, a site for ERRα could be better matched by the position weight matrix (PWM) of another nuclear receptor. For this reason, we clustered all motifs based on the similarity of their sequence logo to that of ESRRA and we could identify sites for these grouped motifs in ~82% of the ERRα peaks.

In addition, to explain most of the binding site variation observed across the ERRα peaks, we applied the principal component analysis (PCA) to a site-count matrix N, whose elements N_{pm} represent the number of predicted TFBSs for each motif m in each ERRα peak region p. Out of a total of 190, the first component was the most informative one, accounting for ~10% of the total variation in the dataset (Fig. S2A). As shown in Figure 3A, the distribution of motif projections on the first two principal components clearly indicate two distinct clusters of motifs that stick out from the cloud of those having projections close to zero. The first group, characterized by motifs with negative eigenvalues along the first component, includes ESRRA and other nuclear receptors which have very similar logos to that of the ERRα motif. This cluster reflects the most abundant sites which can be found within the ERRα binding regions. The second group, instead, is characterized by a set of GC-rich motifs which are usually found in the proximity of transcription start sites.

The motif with the highest score along the first principal component, SP1, corresponds to the Specificity protein 1 (Sp1), a protein known to be often present at the promoter region of many genes and to be involved in several cellular processes, including cell growth, cell differentiation, chromatin remodeling and apoptosis. The activity of this protein can be significantly affected by post-translational modifications, leading Sp1 to act either as an activator or as a repressor (Song et al., 2002). We thus asked whether Sp1, in the context of ERRα binding, functions more as activator or as repressor on the common downstream target genes. To this purpose, we sought to combine the different classes of peaks (“only ERRα”, “only PGC-1α”, “overlapping ERRα and PGC-1α”) with the regulation of their assigned promoters (“up”, “down”, “non-changing”, “no promoter assigned”) in the plot shown in Figure S2B. Strikingly, whenever a site for Sp1 is present within the peak, it is more likely for the assigned promoter to be up-regulated, strongly suggesting that in the context of PGC-1α

over-expression, Sp1 plays a role as an activator. This effect is enhanced when Sp1 is found in an ERRα peak rather than with in a PGC-1α peak.

An additional confirmation of the fact that the SP1 motif is particularly enriched in ERRα peaks is shown by Figure 3B, which displays SP1 as the top scoring motif when the TFBS occurrences in ERRα peaks are compared to those predicted within PGC-1α peaks. This observation is further supported by Figure 3C, showing the decrease in terms of ranking position of SP1 when passing from "only ERRα peaks" (rank 2, right after ESRRA), to "overlapping peaks" (rank 14) and finally to "only PGC-1α peaks" (rank 33). Taken together, these results suggest not only a prevalent role of Sp1 in the context of ERRα binding, but also that this co-occurrence at ERRα peaks is restricted to the presence of ERRα itself, as Sp1 occurs less often in the "only PGC-1α peaks". Lastly, we noticed that the ERRα motif ESRRA is firmly in position 1 in each of the three lists. This might suggest that other transcription factors with very similar binding affinity to that of ERRα could be accommodated by the ESRRA motif. For example, this possibility might concern the ERRα homologous proteins ERRβ – which is induced by PGC-1α over-expression (1.9 fold change) and repressed by the ERRα knock-down (-2 fold change) – and ERRγ, for both of which we do not currently have a distinct motif.

A

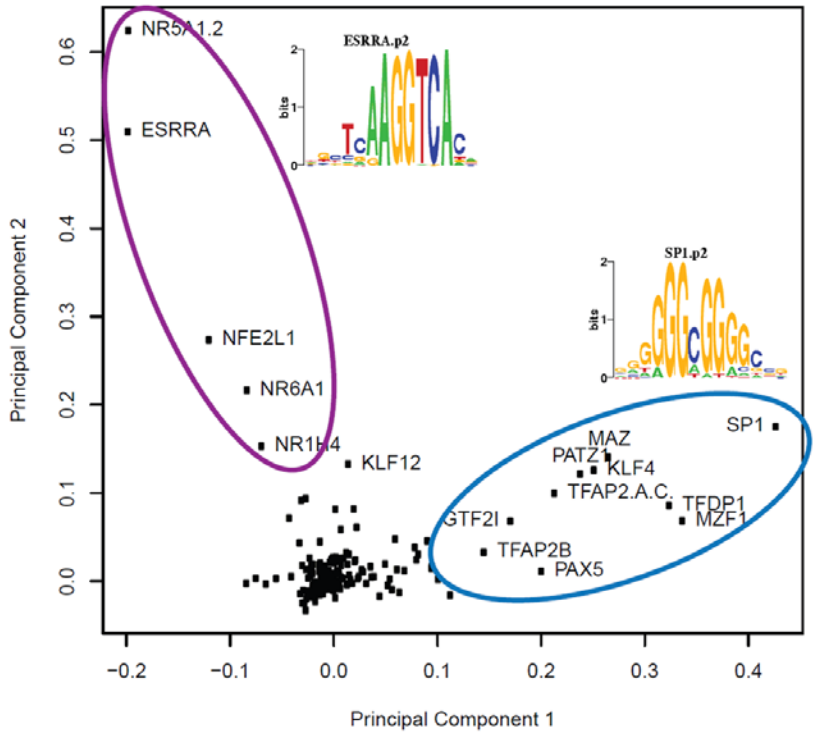

B

Only ERRα vs. Only PGC1α peaks	
Motif name	**Z score**
SP1	75.743
PAX5	70.135
TFAP2B	65.739
HIC1	58.572
TFDP1	56.139
PATZ1	50.776
MZF1	50.112
KLF4	47.719
RREB1	46.779
TFAP2{A,C}	46.252
.	.
.	.
.	.
MEF2{A,B,C,D}	-30.566
JUN	-31.842
HOX{A6,A7,B6,B7}	-33.038
PAX8	-34.177
NR3C1	-34.908
AR	-36.214
NFE2	-37.495
NFE2L2	-40.473
FOSL2	-43.223
FOS_FOS{B,L1}_JUN{B,D}	-45.066
BACH2	-54.446

C

Only ERRα peaks vs. Shuffled	
Motif name	**Z score**
ESRRA	76.085
SP1	54.775
NR5A1,2	54.674
RREB1	53.052
CTCF	51.883
NR6A1	50.912
MZF1	50.250
PAX5	50.125
HNF4A_NR2F1,2	39.765
ETS1,2	39.464
MYFfamily	36.078
SPI1	36.008
GTF2I	34.412
FOSL2	33.086
ELK1,4_GABP{A,B1}	33.048
KLF4	32.886
ZBTB16	32.345
PATZ1	31.260
NR1H4	31.122
BACH2	30.794
FOXD3	28.979
HMGA1,2	27.773
NFE2L1	27.125
TFAP2B	26.503
MAZ	26.168
FEV	25.964
ZNF148	25.551
CDX1,2,4	25.513
ELF1,2,4	25.296
FOS_FOS{B,L1}_JUN{B,D}	24.801
NFE2	24.730
PPARG	24.432
FOXO1,3,4	24.348

Overlapping peaks vs. Shuffled	
Motif name	**Z score**
ESRRA	103.058
NR5A1,2	72.343
NR6A1	69.900
HNF4A_NR2F1,2	60.241
FOSL2	56.376
BACH2	54.874
NR1H4	52.205
NFE2	45.014
FOS_FOS{B,L1}_JUN{B,D}	43.344
NFE2L2	42.853
CTCF	41.121
PPARG	39.875
RXRA_VDR{dimer}	37.259
SP1	34.383
RREB1	33.933
ESR1	30.776
NFE2L1	30.491
TFAP4	29.439
SPI1	28.132
ETS1,2	28.069
MZF1	27.477
GTF2I	27.202
SPZ1	26.858
RXR{A,B,G}	26.450
RORA	25.866
SMAD1..7,9	24.727
MYFfamily	24.597
FOXP3	24.315
PAX5	24.147
MAZ	23.869
KLF4	23.829
JUN	22.957
MYOD1	22.101

Only PGC1α peaks vs. Shuffled	
Motif name	**Z score**
ESRRA	142.906
BACH2	115.287
FOSL2	105.275
NR5A1,2	103.750
NR6A1	94.376
HNF4A_NR2F1,2	91.164
NFE2	90.741
FOS_FOS{B,L1}_JUN{B,D}	90.179
NFE2L2	83.923
PPARG	78.079
NR1H4	74.863
ESR1	62.744
TFAP4	60.011
RXRA_VDR{dimer}	59.015
MZF1	54.833
NFE2L1	54.808
SMAD1..7,9	51.946
SPI1	51.388
RREB1	50.391
RORA	50.150
JUN	48.977
NFIX	48.632
TLX1..3_NFIC{dimer}	47.702
EBF1	45.972
RXR{A,B,G}	45.403
TGIF1	44.700
NR3C1	43.371
AR	43.218
ZNF148	43.100
BPTF	42.689
GTF2I	42.608
CTCF	42.509
SP1	42.435

Figure 3. Sp1 is the top transcription factor partner for ERRα in skeletal muscle.

(A) PCA analysis of the 3225 ERRα peaks. The names of the motifs with the largest projections on the first two principal components are indicated. Purple and light blue ellipses highlight motif clusters, as identified by PC1, of nuclear hormone receptor-like motifs and SP1-like motifs, respectively.

(B) Top and bottom scoring results of motif search obtained by comparing the TFBSs predictions within the "only ERRα peaks" with those in the "only PGC-1α peaks".

(C) Top scoring motifs resulted from motif search performed on the "only ERRα peaks" (left panel), on the "overlapping ERRα and PGC-1α peaks" (central panel) and on the "only PGC-1α peaks" (right panel). For each dataset, the TFBSs occurrences were compared against binding site predictions performed on a background set of shuffled peaks. The motifs corresponding to ERRα and SP1 are depicted in purple and light blue.

3.3.4 Modeling and validating the indirect gene regulatory effects of PGC-1α in absence of ERRα binding

Provided that ERRα is the main functional partner of PGC-1α, we further investigated which other transcription factors might be mediating the indirect regulatory effects of PGC-1α in skeletal muscle. For this reason, we extended a previously introduced framework, called Motif Activity Response Analysis (MARA) (Suzuki et al., 2009), to incorporate the ChIP-Seq data with the gene expression profiles (see Methods for more details) and to model these observations in terms of the TFBSs occurring within promoters and of the unknown regulatory "activities" of each input motif.

In particular, we classified promoters into four groups: (i) associated to an ERRα peak, (ii) associated to a PGC-1α peak, (iii) associated to both an ERRα and a PGC-1α peak (either overlapping or not), (iv) not associated to any peak. For the first three groups, all "direct targets" of either one or both of the proteins, we modeled the promoter expression using the TFBSs predicted within the binding peak, while for the last group of "indirect targets", binding site predictions were made in the proximal promoter region, according to the usual MARA approach. For the purpose of this study, we focused on the indirect targets group, whose top 30 motifs are listed in Figure 4A.

The first consideration is that ESRRA is still the top motif of the list. This might be due to the above mentioned possibility of having homologous proteins recognized by the same PWM or to the fact that some real ERRα binding sites were just below the detection threshold of our peak caller. Secondly, we realized that the most active motifs host several known partners of either PGC-1α or ERRα: NR5A1 (also known as SF1), NR5A2 (also known as LHR1), NRF1, GABPA, MEF2C, RXRs and ESR1. Finally, since this analysis identified also several TFs as potential downstream effectors of PGC-1α, we decided to experimentally validate a couple of the so-far unknown ones: ZNF143 and NFYC. The former was chosen because, apart from the repressed IRF1,2,7 motif, it was the best scoring and uncharacterized motif from the list in Figure 4A. The latter was selected because it was the most induced (1.89 fold change) member among the NFY proteins composing the well-scoring motif NFY(A,B,C).

For both these transcription factors, whose activity was predicted to increase significantly upon PGC-1α over-expression and to decrease following ERRα knock-down (Fig. 4B), we performed an shRNA-based knock-down in C2C12 myotubes and analyzed, through a microarray, the expression levels of these two candidate transcription factors and of their target genes. This experiment resulted in a strong reduction of the expression of the TFs (Fig. 4C), as well as the expression levels of a total of 128 genes for ZNF143 and 73 for NFYC, which were all significantly induced by PGC-1α and repressed by the knock-down of the factor (for some examples, see Fig. 4C).

A

MARA results in the context of neither ERRα nor PGC1α peaks

Motif name	Z score
ESRRA.p2	9.792401
NR5A1,2.p2	6.865654
IRF1,2,7.p3	6.706547
NRF1.p2	4.718852
ZNF143.p2	**4.311363**
ELK1,4_GABP{A,B1}.p3	3.988591
MEF2{A,B,C,D}.p2	3.938221
RXR{A,B,G}.p2	3.714927
TBP.p2	3.483611
TCF4_dimer.p2	2.923206
ESR1.p2	2.89541
TFAP2B.p2	2.827928
GTF2I.p2	2.761647
NFY{A,B,C}.p2	**2.668979**
POU5F1.p2	2.493307
RREB1.p2	2.488123
TFDP1.p2	2.458457
TLX1..3_NFIC{dimer}.p2	2.432518
GATA1..3.p2	2.396587
CTCF.p2	2.347933
E2F1..5.p2	2.326616
HNF4A_NR2F1,2.p2	2.306275
NFATC1..3.p2	2.290732
ZNF384.p2	2.269327
SRF.p3	2.255106
TFCP2.p2	2.230955
STAT2,4,6.p2	2.201463
SOX2.p2	2.176791
RUNX1..3.p2	2.16979
SMAD1..7,9.p2	2.158032

B

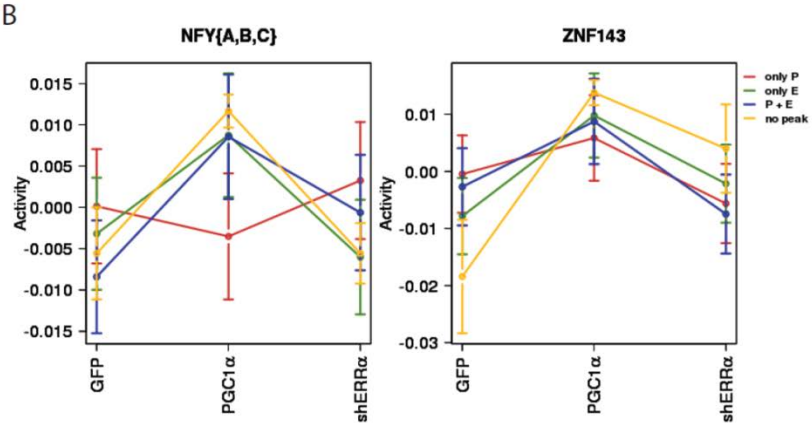

C

	PGC1α OV	siNFYC KD		PGC1α OV	siZNF143 KD
Nfyc	1.89	-2.60	Znf143	1.28	-1.73
Strbp	4.06	-2.04	Slc25a19	5.09	-1.17
Slc25a42	3.26	-1.30	Pptc7	3.90	-1.21
Atf3	5.58	-1.52	Pkn1	1.63	-1.18
Myo5b	2.95	-2.15	Gsto1	4.16	-1.90
Sdhaf1	1.77	-1.40	Lonp1	2.67	-1.63

Figure 4. Prediction and validation of the indirect gene regulatory effects of PGC-1α mediated by Nfyc and Znf143.

(A) Top 30 active motifs in the promoters not associated to any peak, as predicted by MARA. The motifs chosen for validation are highlighted in bold.

(B) Activity plots of the motifs NFY(A,B,C) and ZNF143, as predicted by MARA.

(C) Expression levels, as measured by a microarray experiment, of Nfyc, Znf143 and 10 other genes significantly up-regulated by PGC-1α over-expression and significantly down-regulated by either siNfyc or siZnf143 knock-down.

3.4 Discussion

ERRα has been described as an effector of PGC-1α induced regulation of gene expression in organs like skeletal muscle, adipose tissue or heart(Akter et al., 2008; Cho et al., 2013; Huss et al., 2002; Mootha et al., 2004; Schreiber et al., 2004). In skeletal muscle, PGC-1α appears to regulate all adaptations of this tissue to exercise (Handschin, 2010). To introduce some of these adaptations PGC-1α coactivates ERRα to increase its transcriptional activity. When expressed in skeletal muscle cells, PGC-1α induces the expression of ERRα and coactivates it to regulate the expression of genes involved in mitochondrial biogenesis, oxidative phosphorylation and fatty acid oxidation (Huss et al., 2004; Mootha et al., 2004; Schreiber et al., 2004). Similarly, by coactivating ERRα at the promoter of the PDK4 gene PGC-1α controls muscle glucose metabolism (Wende et al., 2005). The induction of VEGF and angiogenesis in skeletal muscle by PGC-1α involves transcriptional activity of ERRα (Arany et al., 2008). PGC-1α induces SIRT3 through ERRα to regulate the suppression of reactive oxygen species in skeletal muscle cells (Kong et al., 2010).

However, all these studies focused on the transcription of individual genes or a set of genes. It was not precisely known to which extent ERRα is required for the regulation of these gene programs by PGC-1α in skeletal muscle. The results of this study provide a global picture of the gene expression regulation by PGC-1α and ERRα. The co-occurrence of PGC-1α and ERRα in the promoters of genes which are induced by PGC-1α confirms that PGC-1α coactivates ERRα to drive the expression of these genes. Moreover, we have determined which subset of PGC-1α target genes is regulated by such direct mode of gene expression regulation by the PGC-1α/ERRα transcriptional duo. Intriguingly, ERRα seems to be able to bind to gene promoters and induce gene expression without being coactivated by PGC-1α. This is surprising, because ERRα is thought to be a rather silent and inactive transcription factor, which becomes active when bound and coactivated by PGC-1α (Schreiber et al., 2003). When the crystal structure of ERRα in complex with PGC-1α was analyzed, it was shown that the nuclear receptor ERRα is in a transcriptionally active conformation in the absence of ligands if complexed by PGC-1α (Kallen et al., 2004). Instead of binding small ligands, the ligand binding domain of ERRα interacted with a PGC-1α peptide (Kallen et al., 2004). This and other studies led to the perception of ERRα as an orphan nuclear receptor which can be activated by coactivators instead of small molecule ligands (Gaillard et al., 2006). We show here that ERRα can bind to promoters of genes and regulate their expression even if not directly bound to PGC-1α. However, why ERRα is coactivated by PGC-1α at some gene promoters, but not at others is not clear. Because adenoviral vectors have been used to overexpress of PGC-1α in our experiments, we can assume that PGC-1α molecules are highly abundant in C2C12 cells and thus are available for ERRα binding. The high abundance of Sp1 motifs in ERRα peaks which do not co-occur with PGC-1α peaks offers the possibility that Sp1 could regulate gene expression together with ERRα. In vascular smooth muscle cells, Sp1 was found to bind to the promoter of Mfn2, which is a known PGC-1α target gene in skeletal muscle, and regulate its expression (Sorianello et al., 2012; Zorzano, 2009). Additionally,

ERRα can bind to the human Sp1 promoter and regulate its expression (Sumi and Ignarro, 2005). However, further experiments are required to show that these two transcription factors together regulate gene expression in skeletal muscle cells. Nevertheless, even if the interaction of ERRα would bind to Sp1 to regulate gene expression, it is still not clear why ERRα complexes with Sp1 at some promoters and with PGC-1α at other promoters. However, this might be caused by minor aberrations of the ERRα response elements (ERREs) between the two promoter sets. Barry and colleagues have found that such minor changes in the ERRα binding site can influence the conformation of ERRα at the binding site and therefore affect its interaction with PGC-1α (Barry et al., 2006).

It was not surprising to find that PGC-1α can be recruited to the promoters of its target genes without being bound to ERRα. It was already previously shown that PGC-1α is capable of binding and coactivating numerous transcription factors in skeletal muscle. PGC-1α coactivates the nuclear respiratory factor 1 (NRF-1) in muscle cells to induce the expression of the mitochondrial transcription factor A (mtTFA) and thus regulate the transcription and replication of mitochondrial DNA (Wu et al., 1999). Another nuclear respiratory factor, NRF-2, is coactivated by PGC-1α to induce the expression of genes involved in oxidative phosphorylation and neuromuscular junction formation (Handschin et al., 2007; Mootha et al., 2004). Similarly, PGC-1α regulates the activity of the myocyte enhancer factor 2C (MEF2C) to induce the expression of GLUT4 and thus to control the glucose uptake in muscle (Michael et al., 2001). Nevertheless, it was surprising to find that the motif for ERRα scored high when motif search was performed in PGC-1α peaks which did not co-occur with ERRα. However, it needs to be considered that the motif of ERRα possibly scored high only because of its similarity to other nuclear receptor motifs. Alternatively, PGC-1α might have been recruited to these promoters by ERRβ or ERRγ. In hepatic and skeletal muscle cells, it was already shown that several members of the ERR family of transcription factors can regulate the expression of the same PGC-1α target gene (Cho et al., 2013; Zhang et al., 2006). Accordingly, genome-wide studies in the heart found that ERRα and ERRγ share many of their target genes and thus often bind to the promoters of a common set of genes (Dufour et al., 2007). Moreover, the expression of two of the three members of the ERR family of transcription factors was induced by PGC-1α in our experiments. Therefore, in addition to ERRα, PGC-1α might coactivate ERRβ or ERRγ.

The induction of some PGC-1α target genes does not require the recruitment of ERRα or of PGC-1α to their promoters. These indirect PGC-1α target genes might be regulated by transcription factors or coactivators which are themselves induced, but not coactivated by PGC-1α. One such downstream effector of the PGC-1α/ERRα signaling axis is Perm1, which is induced by PGC-1α and subsequently regulates the expression of some PGC-1α target genes (Cho et al., 2013). Our results indicate that transcription factors like Znf143, Nfyc or Gtf2i might be other downstream effectors of PGC-1α. Experiments performed in our laboratory, which involve knockdown of Znf143, Nfyc and Gtf2i revealed that Znf143, Gtf2i and to a lesser extent Nfyc regulated a subset of directly regulated PGC-1α target genes (Baresic et al., 2013). Whether these transcription factors also regulated the expression of

PGC-1α target genes without being coactivated by PGC-1α still remains unclear. However, considering that ERRα regulates gene expression in presence and absence of PGC-1α at the target gene promoter, such a mode of gene expression regulation could be expected as well with Znf143, Gtf2i or Nfyc.

In conclusion, this study represents a genome-wide map of the target gene occupation by the transcriptional network of PGC-1α and ERRα. We have identified which PGC-1α target genes in skeletal muscle cells are directly regulated by either ERRα or PGC-1α, by the two factors together or without the recruitment of any of the two factors to the target gene promoter. We predict which transcription factors besides ERRα might regulate the expression of PGC-1α target genes by acting either alone or by being coactivated by PGC-1α. In addition, we suggest Sp1 as a transcription factor, which possibly interacts with ERRα to regulate gene expression at promoters which are not occupied by PGC-1α.

3.5 Methods

Cell culture and knockdown of ERRα

The C2C12 myoblasts were cultured in Dulbecco's modified Eagle's medium (DMEM) supplemented with 10% fetal bovine serum (FBS), 100 Units/ml penicillin and 100ug/ml streptomycin. After the cells had reached approximately 90% confluence, the differentiation of myoblasts to myotubes was introduced by switching the growth medium to differentiation medium (DMEM supplemented with 2% horse serum) for 72 hours.

For the knockdown and inactivation of ERRα, differentiated C2C12 cells were infected with either the shERRα or shGFP (control) adenovirus (AV) and kept in culture for 4 days. These adenoviruses were a generous gift from Prof. A. Kralli from the Scripps Research Institute in La Jolla, California, USA. Subsequently, these cells were infected with either the flag-PGC-1α or GFP adenovirus and kept in culture for additional two days. The differentiation medium, which was used to infect cells, was supplemented with either 2μM of the ERRα inverse agonist XCT-790 (for cells previously infected with the shERRα AV) or with the vehicle (0.02% DMSO, for the remaining cells). The experiments have been performed in biological triplicates. The RNA was isolated using TRIzol® and was performed according to the TRIzol® reagent RNA isolation protocol (Invitrogen).

For the gene expression arrays, the RNAs from the following three conditions were used: shGFP AV + GFP AV + vehicle (0.02% DMSO); shGFP AV + flag-PGC-1α AV + vehicle (0.02% DMSO); shERRα AV + flag-PGC-1α AV + 2μM XCT-790.

ChIP and ChIP-Seq

The chromatin immunoprecipitation was performed according to the Agilent Mammalian ChIP-on-chip Protocol version 10.0. For every immunoprecipitation, we used approximately $1x10^8$ C2C12 cells, which were differentiated to myotubes and infected with flag-PGC-1α adenovirus. For the cross-linking, the cells were incubated in a 1% formaldehyde solution for 10 minutes. After the lysis and sonication but before the immunoprecipitation, 50μl of the lysate was saved for the extraction of input DNA. For the immunoprecipitation of ERRα, the magnetic beads (Dynabeads® Protein G, Invitrogen) were coated with the monoclonal anti-ERRα antibody (ERRα Rabbit Monoclonal Antibody, Clone ID: EPR46Y, Epitomics). The chromatin immunoprecipitation was performed overnight on a rotating platform at 4°C. The PGC-1α ChIP-Seq data was obtained from previous experiments and was performed using the monoclonal anti-flag antibodies (Monoclonal ANTI-FLAG® M2 Antibody, Sigma) for the immunoprecipitation (submitted but yet not published data).

High-throughput sequencing

The ERRα ChIP-Seq experiment in C2C12 cells undergoing PGC-1α over-expression was performed at the joint Quantitative Genomics core facility of the University of Basel and the Department of Biosystems Science and Engineering (D-BSSE) of the ETH Zurich in Basel. The DNA libraries for

ERRα and the whole cell extract (WCE) were prepared using the standard Illumina ChIP-Seq protocol, as described by the manufacturer. The immunoprecipitated samples were sequenced on the Illumina® HiSeq2000 sequencer.

The sequenced reads underwent a quality filter which discarded all reads having Phred score >= 20, read length >= 25 bps and wrongly called nucleotides (Ns) per read <= 2. The reads that passed the filter were used as input for Bowtie version 0.12.7 (Langmead et al., 2009) and aligned to the UCSC mm9 mouse genome assembly. Moreover, to avoid any PCR amplification error which might have arisen during sample preparation, we removed redundant reads mapping to the same location with the same orientation and we kept only one read per position. Consequently, we obtained 2'155'507 reads for the IP and 84'175'472 reads for the WCE.

Peak calling

To detect regions that were significantly enriched in ERRα binding, we estimated the fraction of all ChIP reads f_{IP} that fell within consecutive 200 bps sliding windows genome-wide and, in parallel, the fraction f_{WCE} of reads from the whole cell extract that fell in a 2000 bps long window centered on the ChIP one. Using these two sets of values, we quantified the ChIP enrichment of each window as:

$$Z = \frac{f_{IP} - f_{WCE}}{\sqrt{\sigma^2{}_{IP} + \sigma^2{}_{WCE}}}$$

where $\sigma^2{}_{IP}$ and $\sigma^2{}_{WCE}$ are the IP and WCE read frequency variances, given by:

$$\sigma^2{}_{IP} = \frac{f_{IP} * (1 - f_{IP})}{N_{IP}} \text{ and } \sigma^2{}_{WCE} = \frac{f_{WCE} * (1 - f_{WCE})}{N_{WCE}}$$

respectively. All consecutive windows having a Z-score greater than 3.5 were merged and the top scoring one from each window cluster was considered as the peak summit and used for further analyses.

ERRα peaks were annotated to the closest *Mus musculus* RefSeq transcripts and defined as "Intergenic", "Intronic", "Exonic", "Upstream of TSS" or "Downstream of TSS" in case they were located, respectively, farer than 10 kb from the closest transcript, within an intron, within an exon, between -10 and 0 kb from the nearest TSS, or between 0 and 10 kb from the closest TES.

Transcription factor binding sites over-representation

In order to account for the conservation of TFBSs across related species, we aligned the ERRα binding peaks to their orthologous regions from 6 mammalian species – human (hg18), opossum (monDom4), dog (canFam2), rhesus macaque (rheMac2), horse (equCab1) and cow (bosTau3) – using the software T-Coffee (Notredame et al., 2000). Using the MotEvo algorithm (Arnold et al., 2012) on these alignments, we predicted binding sites within our peaks for a collection of 190 mammalian regulatory motifs (also called WMs) that was downloaded from the SwissRegulon database (Pachkov et al., 2013).

To assess the over-representation of the predicted binding sites (i.e. those with a posterior probability greater than 0.1) within the ERRα peaks, we created a set of background regions by shuffling the columns of the multiple alignments and maintaining, at the same time, both the phylogeny and the gap patterns of the original aligned sequences. MotEvo was run on the shuffled alignments using the same settings as for the original sequences. Significant enrichment of binding sites for each motif *x* in the ERRα peaks was computed by collecting the sum n_x of the posterior probabilities for its predicted TFBSs along ERRα peak alignments and the corresponding sum n'_x in the shuffled alignments; we quantified the motif over-representation as:

$$Z = \frac{f_x - f'_x}{\sqrt{\frac{f_x * (1 - f_x)}{L_x} + \frac{f'_x * (1 - f'_x)}{L'_x}}}$$

where L_x and L'_x are the total lengths of the original and shuffled alignments, respectively, while f_x and f'_x are given by the equations:

$$n_x * l_x = f_x * L_x \text{ and } n'_x * l_x = f'_x * L'_x$$

with l_x the length of motif *x*.

Principal Component Analysis of TFBSs occurrence within peaks

A Principal Component Analysis (PCA) was performed using the "svd" package of R programming language. The input data for the PCA was a $p \times m$ matrix *N*, composed by the total number of binding sites N_{pm} predicted for each of the 3225 binding peaks *p* (rows) using our collection of 190 mammalian regulatory motifs *m* (columns). Singular Value Decomposition (SVD) was applied to the mean centered matrix $\widetilde{N}_{pm} = N_{pm} - \langle N_m \rangle$ using the 'svd' package of the statistical software 'R'.

Gene expression array analysis

The .CEL files containing the raw probe intensities were processed using the Bioconductor package 'affy' (Gentleman et al., 2004), which corrects for background and unspecific binding. After using the 'Mclust' R package(R Development Core Team, 2012) to distinguish expressed from non-expressed probes, the intensity values were quantile normalized across all samples and mapped to the mouse transcripts UCSC collection. These were further associated to a comprehensive collection of mouse promoters that was downloaded from the SwissRegulon database (Pachkov et al., 2013). For each promoter, the change in log2 expression levels (log2FC) was compared between the following conditions: over-expressed PGC-1α (treatment) and GFP (control); ERRα knock-down with the addition of XCT790 (treatment) and over-expressed PGC-1α (control).

The significance of the expression change was assessed by a Z score, which was computed as:

$$Z = \frac{\bar{\bar{E}}_{treatment} - \bar{\bar{E}}_{control}}{\sqrt{\frac{\sigma^2{}_{treatment}}{n} + \frac{\sigma^2{}_{control}}{n}}}$$

where $n = 3$ was the number of replicate samples, $\bar{E}_{treatment}$ is the mean log2 expression across the treatment samples, $\bar{E}_{control}$ is the mean log2 expression across the control samples, and ${\sigma^2}_{treatment}$ and ${\sigma^2}_{control}$ are the variances of log2 expression levels across the replicates for the treatment and control samples, respectively. A log2FC threshold of ±0.5849625 (corresponding, in a more used notation, to 1.5 fold change, when taking the inverse of the linear binding ratio) and a Z score cutoff of ±3 were used to identify significantly up-/down-regulated promoters.

The criterion adopted to assign peaks to promoters was proximity. Each peak was assigned to its closest promoter (and, thus, to its associated gene symbol) whenever the distance between their central positions was smaller than 10 kb; otherwise, the peak was not assigned to any promoter.

Ontology terms over-representation analysis

KEGG pathways and Gene Ontology terms over-representation analysis was performed using the functional analysis software FatiGO (Al-Shahrour et al., 2004). As input, we used all gene IDs associated to the promoters that were assigned to the ERRα and PGC-1α peaks. Only ontology terms having an FDR-adjusted p-value <= 0.05 were considered significant.

Motif activity response analysis

The information obtained from the sequencing data and from the microarrays were integrated by extending MARA (Suzuki et al., 2009) in order to model the direct and indirect regulatory effects that ERRα and PGC-1α exert on their downstream targets.

Using the input expression data and the computationally predicted transcription factor binding sites, MARA infers, for each of 190 regulatory motifs *m* (associated with roughly 350 mouse TFs), the activity A_{ms} of the motif in each sample *s* when the motif occurs *outside* of a binding peak, and the activity A^*_{ms} of the motif when it occurs *within* a binding peak. A significant change in the motif activity A_{ms} upon knock-down of ERRα and/or over-expression of PGC-1α indicates an indirect regulatory effect of either ERRα, PGC-1α or both of them on the motif *m*, whereas a change in the motif activity A^*_{ms} reflects a direct regulatory effect as mediated by the motif *m*. For each promoter *p* that was not associated with any binding peak (which we denote as "indirect target"), we modeled its log-expression in sample *s,* e_{ps}, in terms of the predicted number of TFBSs N_{pm} that occur in the proximal promoter region (running from -500 to +500 relative to TSS) for each regulatory motif *m.* That is, MARA assumes the linear model:

$$e_{ps} = c_p + \tilde{c}_s + \sum_m N_{pm} A_{ms}$$

where c_p is the basal expression of promoter *p*, $\tilde{c}_s$ is a sample-dependent normalization constant, and A_{ms} is the regulatory activity of motif *m* in sample *s*, which is inferred by the model. Formally, A_{ms} quantifies the amount by which the expression of promoter *p* in sample *s* would be reduced if a binding site for motif *m* were to be deleted from the promoter.

For each "direct target" promoter *p* that has an associated binding peak (which could be an ERRα, a PGC-1α or an overlapping ERRα/PGC-1α peak) within 10 kb, we modeled its expression in terms of the predicted TFBSs in the binding peak, i.e.:

$$e_{ps} = c_p + \tilde{c}_s + \sum_m N^*_{pm} A^*_{ms}$$

where N^*_{pm} is the number of predicted TFBSs for motif *m* in the peak associated with promoter *p*, and A^*_{ms} is the motif activity of regulator *m* in sample *s* when this motif occurs in the context of either ERRα binding, PGC-1α recruitment or both.

Besides motif activities MARA also calculates error-bars δ_{ms} for each motif *m* in each sample *s*. Using these, MARA calculates, for each motif *m*, an overall significance measure for the variation in motif activities across the samples analogous to a z-statistic:

$$Z_m = \sqrt{\frac{1}{S}\sum_m (A_{ms})^2}$$

For each motif we calculate a z-score Z_m associated with its indirect activity changes, a z-score $Z^*_{m,ERR\alpha}$ associated with its direct activity changes in the context of ERRα binding, a z-score $Z^*_{m,PGC1\alpha}$ associated with its direct activity changes in the context of PGC-1α recruitment and a z-score $Z^*_{m,BOTH}$ associated with its direct activity changes in the context of both ERRα binding and PGC-1α recruitment.

Real-time PCR

Real-time PCR was used to validate the efficiency of the ERRα knockdown and to verify that the ChIP of ERRα was successful. The sequences of all primers, which were used in real-time PCRs, are depicted in Suppl. Table 1.

Statistical analysis of Real-time PCR data sets. The values are presented as the mean +- SEM. A Student's t test was performed and a p-value < 0.05 was considered as significant. *<0.05, **<0.01, ***<0.001

3.6 References

Akter, M.H., Yamaguchi, T., Hirose, F., and Osumi, T. (2008). Perilipin, a critical regulator of fat storage and breakdown, is a target gene of estrogen receptor-related receptor alpha. Biochem Biophys Res Commun *368*, 563-568.

Al-Shahrour, F., Diaz-Uriarte, R., and Dopazo, J. (2004). FatiGO: a web tool for finding significant associations of Gene Ontology terms with groups of genes. Bioinformatics *20*, 578-580.

Arany, Z., Foo, S.Y., Ma, Y., Ruas, J.L., Bommi-Reddy, A., Girnun, G., Cooper, M., Laznik, D., Chinsomboon, J., Rangwala, S.M.*, et al.* (2008). HIF-independent regulation of VEGF and angiogenesis by the transcriptional coactivator PGC-1alpha. Nature *451*, 1008-1012.

Arnold, P., Erb, I., Pachkov, M., Molina, N., and van Nimwegen, E. (2012). MotEvo: integrated Bayesian probabilistic methods for inferring regulatory sites and motifs on multiple alignments of DNA sequences. Bioinformatics *28*, 487-494.

Baresic, M., Salatino, S., van Nimwegen, E., and Handschin, C. (2013). Transcriptional network analysis in muscle reveals AP-1 as a partner of PGC-1α in the hypoxic gene program (*manuscript submitted for publication*).

Barry, J.B., Laganiere, J., and Giguere, V. (2006). A single nucleotide in an estrogen-related receptor alpha site can dictate mode of binding and peroxisome proliferator-activated receptor gamma coactivator 1alpha activation of target promoters. Mol Endocrinol *20*, 302-310.

Cho, Y., Hazen, B.C., Russell, A.P., and Kralli, A. (2013). Peroxisome Proliferator-activated Receptor gamma Coactivator 1 (PGC-1)- and Estrogen-related Receptor (ERR)-induced Regulator in Muscle 1 (PERM1) Is a Tissue-specific Regulator of Oxidative Capacity in Skeletal Muscle Cells. J Biol Chem *288*, 25207-25218.

Dufour, C.R., Wilson, B.J., Huss, J.M., Kelly, D.P., Alaynick, W.A., Downes, M., Evans, R.M., Blanchette, M., and Giguere, V. (2007). Genome-wide orchestration of cardiac functions by the orphan nuclear receptors ERRalpha and gamma. Cell Metab *5*, 345-356.

Eisele, P.S., Salatino, S., Sobek, J., Hottiger, M.O., and Handschin, C. (2013). The peroxisome proliferator-activated receptor gamma coactivator 1alpha/beta (PGC-1) coactivators repress the transcriptional activity of NF-kappaB in skeletal muscle cells. J Biol Chem *288*, 2246-2260.

Gaillard, S., Grasfeder, L.L., Haeffele, C.L., Lobenhofer, E.K., Chu, T.M., Wolfinger, R., Kazmin, D., Koves, T.R., Muoio, D.M., Chang, C.Y.*, et al.* (2006). Receptor-selective coactivators as tools to define the biology of specific receptor-coactivator pairs. Mol Cell *24*, 797-803.

Gentleman, R.C., Carey, V.J., Bates, D.M., Bolstad, B., Dettling, M., Dudoit, S., Ellis, B., Gautier, L., Ge, Y., Gentry, J.*, et al.* (2004). Bioconductor: open software development for computational biology and bioinformatics. Genome Biol *5*, R80.

Handschin, C. (2010). Regulation of skeletal muscle cell plasticity by the peroxisome proliferator-activated receptor gamma coactivator 1alpha. J Recept Signal Transduct Res *30*, 376-384.

Handschin, C., Kobayashi, Y.M., Chin, S., Seale, P., Campbell, K.P., and Spiegelman, B.M. (2007). PGC-1alpha regulates the neuromuscular junction program and ameliorates Duchenne muscular dystrophy. Genes Dev *21*, 770-783.

Handschin, C., and Spiegelman, B.M. (2006). Peroxisome proliferator-activated receptor gamma coactivator 1 coactivators, energy homeostasis, and metabolism. Endocr Rev *27*, 728-735.

Huss, J.M., Kopp, R.P., and Kelly, D.P. (2002). Peroxisome proliferator-activated receptor coactivator-1alpha (PGC-1alpha) coactivates the cardiac-enriched nuclear receptors estrogen-related receptor-alpha and -gamma. Identification of novel leucine-rich interaction motif within PGC-1alpha. J Biol Chem *277*, 40265-40274.

Huss, J.M., Torra, I.P., Staels, B., Giguere, V., and Kelly, D.P. (2004). Estrogen-related receptor alpha directs peroxisome proliferator-activated receptor alpha signaling in the transcriptional control of energy metabolism in cardiac and skeletal muscle. Mol Cell Biol *24*, 9079-9091.

Kallen, J., Schlaeppi, J.M., Bitsch, F., Filipuzzi, I., Schilb, A., Riou, V., Graham, A., Strauss, A., Geiser, M., and Fournier, B. (2004). Evidence for ligand-independent transcriptional activation of the human estrogen-related receptor alpha (ERRalpha): crystal structure of ERRalpha ligand binding

domain in complex with peroxisome proliferator-activated receptor coactivator-1alpha. J Biol Chem *279*, 49330-49337.

Kamei, Y., Ohizumi, H., Fujitani, Y., Nemoto, T., Tanaka, T., Takahashi, N., Kawada, T., Miyoshi, M., Ezaki, O., and Kakizuka, A. (2003). PPARgamma coactivator 1beta/ERR ligand 1 is an ERR protein ligand, whose expression induces a high-energy expenditure and antagonizes obesity. Proc Natl Acad Sci U S A *100*, 12378-12383.

Kong, X., Wang, R., Xue, Y., Liu, X., Zhang, H., Chen, Y., Fang, F., and Chang, Y. (2010). Sirtuin 3, a new target of PGC-1alpha, plays an important role in the suppression of ROS and mitochondrial biogenesis. PLoS One *5*, e11707.

Langmead, B., Trapnell, C., Pop, M., and Salzberg, S.L. (2009). Ultrafast and memory-efficient alignment of short DNA sequences to the human genome. Genome Biol *10*, R25.

Liu, C., and Lin, J.D. (2011). PGC-1 coactivators in the control of energy metabolism. Acta Biochim Biophys Sin (Shanghai) *43*, 248-257.

Mangelsdorf, D.J., and Evans, R.M. (1995). The RXR heterodimers and orphan receptors. Cell *83*, 841-850.

Michael, L.F., Wu, Z., Cheatham, R.B., Puigserver, P., Adelmant, G., Lehman, J.J., Kelly, D.P., and Spiegelman, B.M. (2001). Restoration of insulin-sensitive glucose transporter (GLUT4) gene expression in muscle cells by the transcriptional coactivator PGC-1. Proc Natl Acad Sci U S A *98*, 3820-3825.

Mootha, V.K., Handschin, C., Arlow, D., Xie, X., St Pierre, J., Sihag, S., Yang, W., Altshuler, D., Puigserver, P., Patterson, N.*, et al.* (2004). Erralpha and Gabpa/b specify PGC-1alpha-dependent oxidative phosphorylation gene expression that is altered in diabetic muscle. Proc Natl Acad Sci U S A *101*, 6570-6575.

Notredame, C., Higgins, D.G., and Heringa, J. (2000). T-Coffee: A novel method for fast and accurate multiple sequence alignment. J Mol Biol *302*, 205-217.

Pachkov, M., Balwierz, P.J., Arnold, P., Ozonov, E., and van Nimwegen, E. (2013). SwissRegulon, a database of genome-wide annotations of regulatory sites: recent updates. Nucleic Acids Res *41*, D214-220.

Puigserver, P., and Spiegelman, B.M. (2003). Peroxisome proliferator-activated receptor-gamma coactivator 1 alpha (PGC-1 alpha): transcriptional coactivator and metabolic regulator. Endocr Rev *24*, 78-90.

R Development Core Team (2012). R: A language and environment for statistical computing. (Vienna, Austria, R Foundation for Statistical Computing).

Schreiber, S.N., Emter, R., Hock, M.B., Knutti, D., Cardenas, J., Podvinec, M., Oakeley, E.J., and Kralli, A. (2004). The estrogen-related receptor alpha (ERRalpha) functions in PPARgamma coactivator 1alpha (PGC-1alpha)-induced mitochondrial biogenesis. Proc Natl Acad Sci U S A *101*, 6472-6477.

Schreiber, S.N., Knutti, D., Brogli, K., Uhlmann, T., and Kralli, A. (2003). The transcriptional coactivator PGC-1 regulates the expression and activity of the orphan nuclear receptor estrogen-related receptor alpha (ERRalpha). J Biol Chem *278*, 9013-9018.

Song, C.Z., Keller, K., Murata, K., Asano, H., and Stamatoyannopoulos, G. (2002). Functional interaction between coactivators CBP/p300, PCAF, and transcription factor FKLF2. J Biol Chem *277*, 7029-7036.

Sorianello, E., Soriano, F.X., Fernandez-Pascual, S., Sancho, A., Naon, D., Vila-Caballer, M., Gonzalez-Navarro, H., Portugal, J., Andres, V., Palacin, M.*, et al.* (2012). The promoter activity of human Mfn2 depends on Sp1 in vascular smooth muscle cells. Cardiovasc Res *94*, 38-47.

Sumi, D., and Ignarro, L.J. (2005). Sp1 transcription factor expression is regulated by estrogen-related receptor alpha1. Biochem Biophys Res Commun *328*, 165-172.

Suzuki, H., Forrest, A.R., van Nimwegen, E., Daub, C.O., Balwierz, P.J., Irvine, K.M., Lassmann, T., Ravasi, T., Hasegawa, Y., de Hoon, M.J.*, et al.* (2009). The transcriptional network that controls growth arrest and differentiation in a human myeloid leukemia cell line. Nat Genet *41*, 553-562.

Tiraby, C., Hazen, B.C., Gantner, M.L., and Kralli, A. (2011). Estrogen-related receptor gamma promotes mesenchymal-to-epithelial transition and suppresses breast tumor growth. Cancer Res *71*, 2518-2528.

Wende, A.R., Huss, J.M., Schaeffer, P.J., Giguere, V., and Kelly, D.P. (2005). PGC-1alpha coactivates PDK4 gene expression via the orphan nuclear receptor ERRalpha: a mechanism for transcriptional control of muscle glucose metabolism. Mol Cell Biol *25*, 10684-10694.

Wu, Z., Puigserver, P., Andersson, U., Zhang, C., Adelmant, G., Mootha, V., Troy, A., Cinti, S., Lowell, B., Scarpulla, R.C*., et al.* (1999). Mechanisms controlling mitochondrial biogenesis and respiration through the thermogenic coactivator PGC-1. Cell *98*, 115-124.

Zhang, Y., Ma, K., Sadana, P., Chowdhury, F., Gaillard, S., Wang, F., McDonnell, D.P., Unterman, T.G., Elam, M.B., and Park, E.A. (2006). Estrogen-related receptors stimulate pyruvate dehydrogenase kinase isoform 4 gene expression. J Biol Chem *281*, 39897-39906.

Zorzano, A. (2009). Regulation of mitofusin-2 expression in skeletal muscle. Appl Physiol Nutr Metab *34*, 433-439.

3.7 Supplemental Figures and Tables

Suppl. Figure S1. Related to Figure 1.

(A) ERRα read densities around the TSS of the known target genes Pdk4 and Idh3a, as displayed by the UCSC Genome Browser.

(B) Real-time PCR validation of the ChIP enrichment measured at the promoter of a set of ERRα target genes. Bars represent fold enrichment over that of the TBP intron.

Suppl. Figure S2. Related to Figure 2.

(A) Fraction of explained variance of the top 10 PCA components.

(B) Barchart representing the different classes of peaks ("only ERRα", "only PGC1α", "overlapping ERRα and PGC1α") together with the regulation of their associated promoters ("up", "down", "non-changing", "no promoter assigned"). Numbers shown on top of each box represent the absolute peak counts.

Suppl. Table 1. Real-time primer sequences.

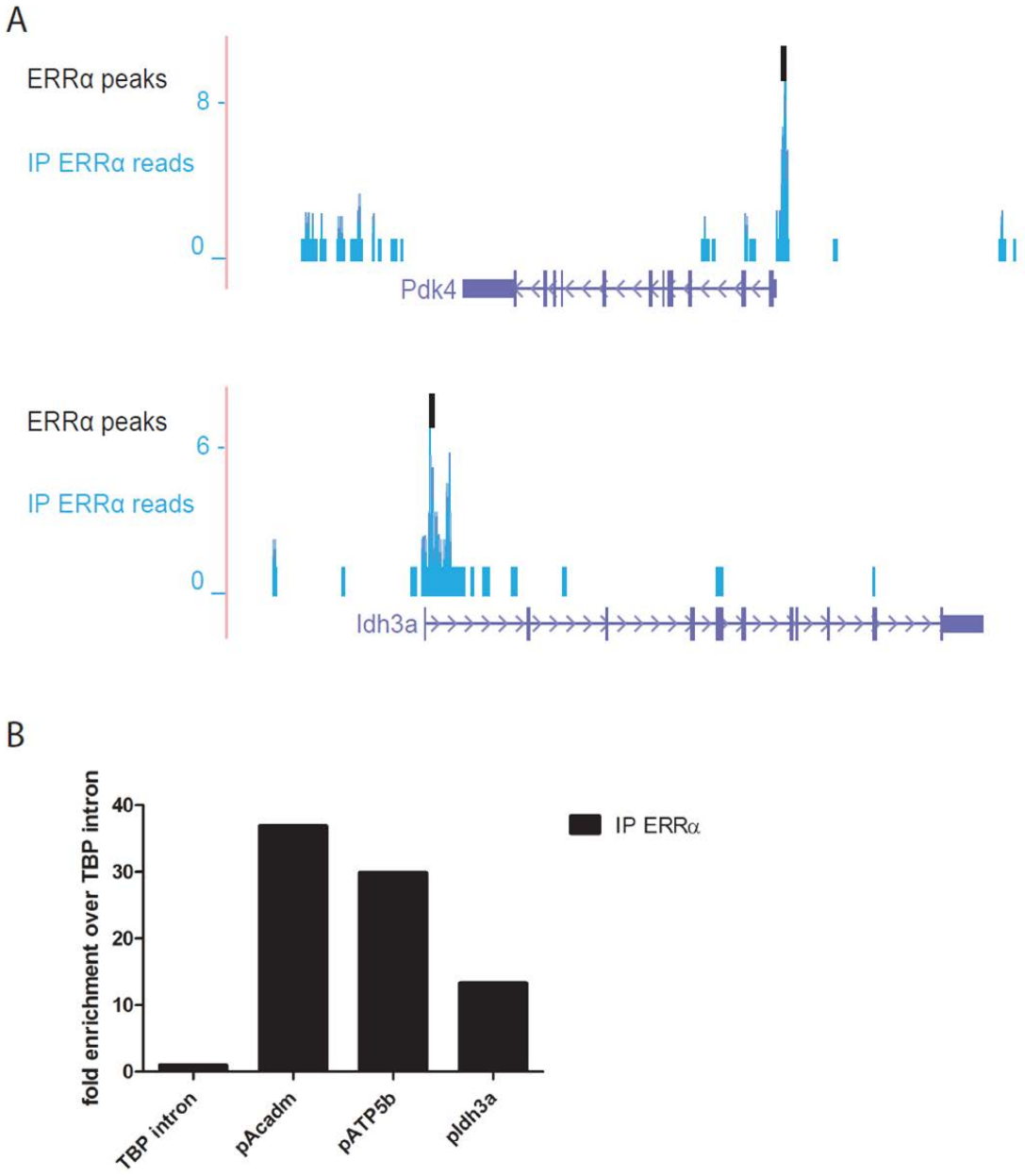

Suppl. Figure S1.

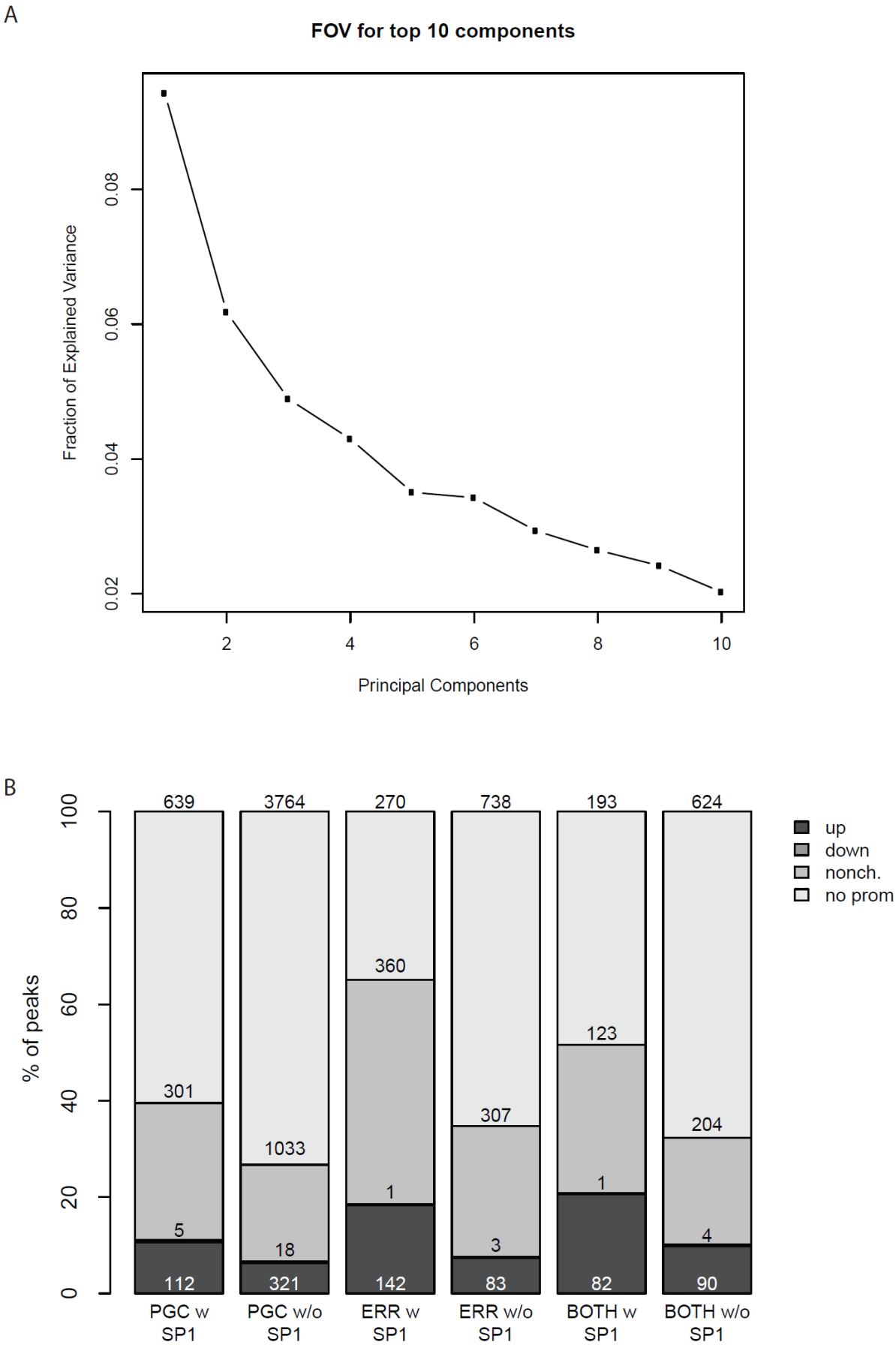

Suppl. Figure S2.

Real-time primers

Real-time PCR primers used for ChIP validation		
gene promoter or intron	forward primer	reverse primer
Tbp intron	TGTGAGCTCCTTGGCTTTTT	ATAGTTGCCCAGCAATCAGG
promoter of *Acadm*	CCTTGCCCGAGCCTAAAC	GTCTGGCTGCGCCCTCT
promoter of *Atp5b*	CTGGAAACTTCCACCCTCACTA	GAGAGGTTTTTGGCGGAACTA
promoter of *Idh3a*	GGACGGCGTCAAGGTCAAG	GCCTAGGTGGCCTGTCTGTG

Real-time PCR primers used for testing the knockdown of *Esrra*		
gene	forward primer	reverse primer
Rn18s	AGTCCCTGCCCTTTGTACACA	CGATCCGAGGGCCTCACTA
Ppargc1a	TGATGTGAATGACTTGGATACAGACA	GCTCATTGTTGTACTGGTTGGATATG
Esrra	ACTGCAGAGTGTGTGGATGG	GCCCCCTCTTCATCTAGGAC
Acadm	AACACTTACTATGCCTCGATTGCA	CCATAGCCTCCGAAAATCTGAA

Suppl. Table 1.

4 MANUSCRIPT-3: Inhibition of cyclic nucleotide phosphodiesterase families does not enhance PGC-1α expression in mouse skeletal muscle

(Manuscript in preparation)

Mario Baresic[1], Martine Christe[1], Markus Beer[1], and Christoph Handschin[1,#]

[1]Focal Area Growth & Development, Biozentrum, University of Basel, Basel, Switzerland
#Correspondence to: christoph.handschin@unibas.ch

Running title: Controlling PGC-1α-through PDE inhibition

4.1 Abstract

Increased expression of the peroxisome proliferator-activated receptor γ coactivator 1 α (PGC-1α) in skeletal muscle has been associated with health benefits and was shown to ameliorate Duchenne muscular dystrophy, protect from sarcopenia and reduce the denervation induced atrophy of the skeletal muscle. Therefore, inducing a long-lasting PGC-1α mRNA expression might represent a therapeutic approach to treat these diseases. cAMP regulates PGC-1α expression in brown fat and the liver. In skeletal muscle, CREB binds to the PGC-1α promoter and the activation of β2-adrenergic receptor (β2-AR) signalling or protein kinase A (PKA) strongly boosts PGC-1α expression. While pathways which induce intracellular cAMP production induce PGC-1α expression, it is not known if preventing cAMP degradation has a similar effect. Cyclic nucleotide phosphodiesterases (PDEs) hydrolyse cAMP to AMP and therefore we hypothesised that elevating cAMP levels through PDE inhibition would induce PGC-1α mRNA expression. We show here that β2-AR signalling activation through clenbuterol leads to a transient PGC-1α mRNA and protein induction. Inhibition of PDE1 and PDE4 by vinpocetine and rolipram, respectively, increases the expression of the alternative exon 1 of PGC-1α in skeletal muscle cells but not in muscles *in vivo*. Surprisingly, PDE4 inhibition by rolipram led to higher PGC-1α protein levels suggesting that this regulation is not achieved through mRNA induction and thus raises the question if the PDE4 regulates PGC-1α protein stability.

4.2 Introduction

Skeletal muscle quickly adapts to exercise. Some of these changes can be beneficial for health and help to prevent the development of medical conditions connected to the modern lifestyle, like obesity, diabetes or hypertension. Thus, regular physical activity represents an effective way to reduce the risk of developing metabolic disorders and other medical conditions (Booth et al., 2002; Dyson, 2010; Henriksen, 2002). The adaptation of skeletal muscle tissue to regular endurance exercise includes mitochondrial biogenesis, higher capillarisation of the skeletal muscle and an increased expression of enzymes which are important for the anti-oxidant defence (Lira et al., 2010; Olesen et al., 2010).

The transcriptional coactivator peroxisome proliferator-activated receptor-γ coactivator 1α (PGC-1α) appears to be the main mediator of these exercise induced changes in skeletal muscle. PGC-1α expression in skeletal muscle is induced by exercise training and its expression and activity are regulated by signalling pathways which are typically activated by contracting muscles (Akimoto et al., 2005; Baar et al., 2002; Handschin et al., 2003; Jager et al., 2007; Pilegaard et al., 2003). When expressed in muscle, PGC-1α induces mitochondrial biogenesis, leads to a fibre type switch towards more oxidative fibres and induces angiogenesis by regulating the expression of VEGF and other angiogenic factors (Arany et al., 2008; Lin et al., 2002; Wu et al., 1999). The induced expression of PGC-1α has even been discussed in the context of mimicking exercise (Matsakas and Narkar, 2010).

More importantly, muscle PGC-1α levels directly affect the degree of damage in different muscle related diseases. Transgenic overexpression of PGC-1α in skeletal muscle has been shown to ameliorate Duchenne muscular dystrophy, protect from sarcopenia and reduce denervation-induced atrophy of the skeletal muscle (Handschin et al., 2007; Sandri et al., 2006; Wenz et al., 2009). Thus, pharmacologically controlling muscle PGC-1α might represent an effective strategy to treat muscle dystrophies, sarcopenia or atrophy in bed-ridden patients.

Because PGC-1α expression in skeletal muscle is induced by the protein kinase A activator forskolin and considering that the binding of the cAMP response element-binding protein (CREB) to the promoter of PGC-1α is required for PGC-1α induction through CamKIV in skeletal muscle (Handschin et al., 2003), we hypothesised that elevating cAMP levels would induce PGC-1α expression. This is supported by the finding that β-adrenergic receptor activation by clenbuterol strongly induces PGC-1α expression (Miura et al., 2007). Similarly, the induction of PGC-1α expression by cAMP was shown in other tissues like liver and brown fat (Herzig et al., 2001; Puigserver et al., 1998).

The cyclic nucleotide phosphodiesterases (PDEs) hydrolyse cAMP to AMP and thus play an important role by degrading this second messenger (Omori and Kotera, 2007). By inhibiting PDEs expressed in skeletal muscle cells, we expect cAMP levels to increase and lead to induced PGC-1α expression. Mammalian PDEs are encoded by 21 genes, many of which can be alternatively spliced, are subdivided into 11 families and show a tissue specific distribution (Bingham et al., 2006; Omori and Kotera, 2007). Members of the PDE1, PDE4, PDE7 and PDE11 family are known to be expressed in

skeletal muscle and the inhibition of PDE4 and PDE5 in skeletal muscle was found to reduce atrophy or ameliorate Duchenne muscular dystrophy (Adamo et al., 2010; Bingham et al., 2006; Hinkle et al., 2005; Omori and Kotera, 2007). There are however differences in the distribution pattern between species and the expression profile of some PDEs is still unknown (Omori and Kotera, 2007). This tissue specific distribution and the fact that dysfunctions of PDE activity have been associated to several diseases have led to the development of specific PDE inhibitors (Francis et al., 2011). Therefore, a PDE inhibitor which induces PGC-1α expression in one tissue might have no or little inhibitory activity in other tissues. Inhibitors of the PDE4 and PDE5 family have been suggested as drugs to reduce skeletal muscle atrophy or to treat Duchenne muscular dystrophy (Francis et al., 2011; Hinkle et al., 2005; Malik et al., 2012).

By using unspecific PDE inhibitors like 3-isobutyl-1-methylxanthine (IBMX) we sought to determine the role of phosphodiesterases in the regulation of PGC-1α expression. Next we tried to identify the PDE family involved in this regulation and elucidate if the inhibition of that particular PDE eventually leads to long-lasting PGC-1α induction. The PGC-1α mRNA can also be transcribed from an alternative promoter and thus give rise to alternative splice variants (Miura et al., 2008). Furthermore, these alternative splice variants of PGC-1α appear to be preferentially induced by exercise and adrenergic receptor signalling (Miura et al., 2008). Therefore we measured the expression of the transcription of the PGC-1α which is derived from the alternative promoter (alternative exon 1) as well as total PGC-1α levels by measuring the expression of exon 2 of PGC-1α, as this exon is supposed to be present in the alternative and regular transcript variants.

4.3 Results

4.3.1 The inhibition of PDE1 and PDE4 in skeletal muscle cells increases the expression of the alternative exon 1 of PGC-1α in skeletal muscle cells

To examine if cAMP signalling is involved in regulation of PGC-1α expression, C2C12 myotubes were treated with the protein kinase A activator forskolin or with the unspecific phosphodiesterase inhibitor IBMX and compared to vehicle treated cells. Both treatments lead to higher PGC-1α mRNA levels, however this induction was not significant (Fig. 1A). Nevertheless, there was a clear tendency to higher PGC-1α levels, especially when the mRNA levels of the alternative exon 1 of PGC-1α were compared (Fig. 1A). Considering that IBMX is a general, but not very potent inhibitor of all phosphodiesterase families, and in order to determine which PDE family might be involved in the regulation of PGC-1α expression, the myotubes were treated with specific phosphodiesterase inhibitors and the expression levels of PGC-1α and PGC-1β were compared. To rule out the possibility that intracellular cAMP is pumped out of the skeletal muscle cell instead of being degraded as reported by other Godinho et al, the experiment was performed in the absence and presence of the organic anion transport inhibitor probenecid (Godinho and Costa, 2003) (Fig. 1B, 1C). The inhibition of PDE1 by the specific inhibitor vinpocetine led to an increased expression of the alternative exon 1 of PGC-1α (Fig. 1B). When the cells were treated with probenecid, the PDE4 inhibitor rolipram induced the expression of the alternative exon 1 of PGC-1α (Fig 1C). To find out if the cAMP effector protein Epacs (exchange proteins directly activated by cAMP) play a role in cAMP mediated regulation of PGC-1α expression, we included in this study the selective Epac activator 8CPT-2Me-cAMP. The treatment with 8CPT-2Me-cAMP did not produce any significant change neither in the expression of PGC-1α nor PGC-1β. Last, there was no significant change in PGC-1β mRNA levels observed neither with the specific PDE inhibitors nor with IBMX treatment (Fig. 1A-1C).

4.3.2 The PDE4 inhibitor rolipram moderately increases PGC-1α protein but not mRNA levels in skeletal muscles *in vivo*.

Based on the observation from our *in vitro* experiments and considering that rolipram has been reported to reduce skeletal muscle atrophy, we decided to assess the effect of the PDE4 inhibitor rolipram on the expression of PGC-1α in skeletal muscle *in vivo* (Hinkle et al., 2005). Rolipram was administered by intraperitoneal injections to 10 weeks old male mice either alone or in the presence of the specific β2-adrenergic receptor agonist clenbuterol. β2-AR activation by clenbuterol has been reported to transiently induce PGC-1α expression in skeletal muscle (Miura et al., 2007). We predicted that the inhibition PDE4 inhibition following clenbuterol treatment might delay the cAMP hydrolysis and thus lead to a prolonged and eventually higher PGC-1α induction. PGC-1α, PGC-1β and Acadm mRNA and PGC-1α protein levels were measured 6 hours after drug administration. The PGC-1α mRNA levels in the *tibialis anterior* and *gastrocnemius* muscle were strongly augmented by clenbuterol alone or when administered together with rolipram (Fig 2 A,B,E and F).

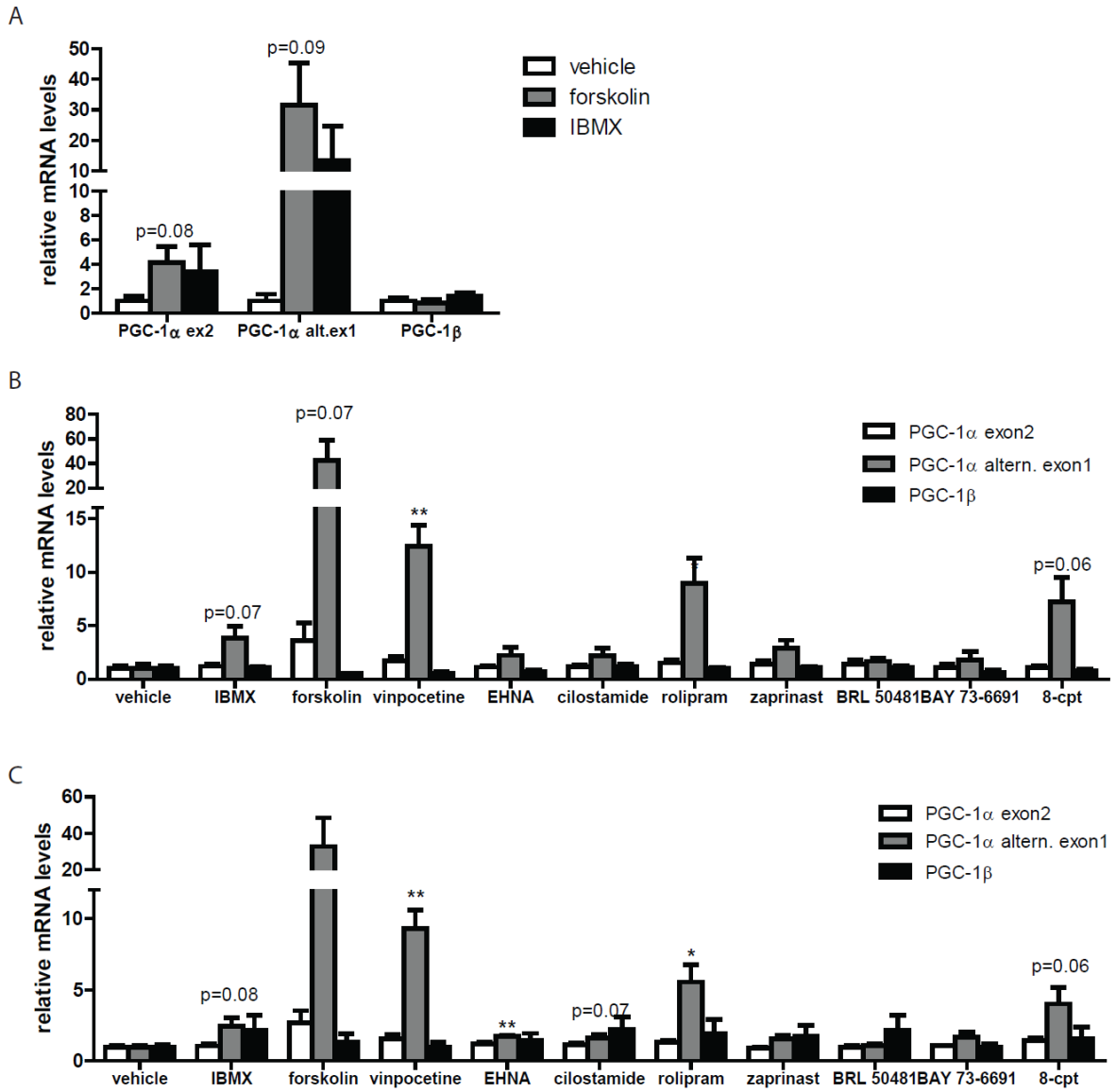

Figure 1. PGC-1α but not PGC-1β expression is induced following PKA activation or PDE inhibition *in vitro*.

(A) Differentiated primary myotubes from wild-type mice were treated with either DMSO, forskolin or IBMX for 3 hours. Expression of PGC-1α exon 2, PGC-1α alternative exon 1 and PGC-1β was determined by real-time PCR.

(B) Differentiated C2C12 myotubes were treated with either DMSO, IBMX, forskolin, vinpocetine, EHNA, cilostamide, rolipram zaprinast BRL 50481, BAY 73-6691 or 8cpt-2Me-cAMP for 3 hours. Expression of PGC-1α exon 2, PGC-1α alternative exon 1 and PGC-1β was determined by real-time PCR.

(C) Same like (B) but the cells were treated in the presence of 100µM probenecid.

Figure 2

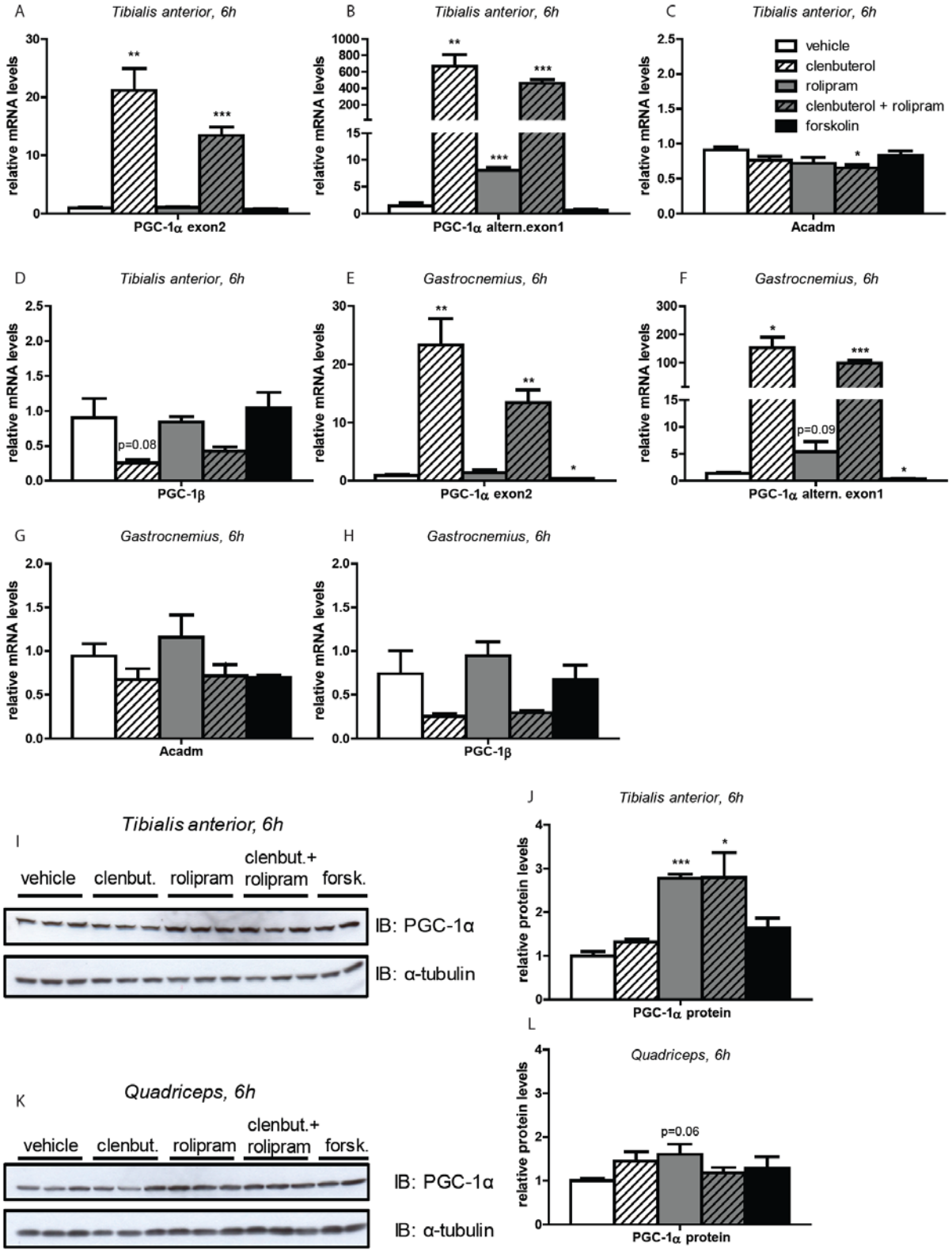
A
Tibialis anterior, 6h
relative mRNA levels
PGC-1α exon2
B
Tibialis anterior, 6h
relative mRNA levels
PGC-1α altern.exon1
C
Tibialis anterior, 6h
vehicle
clenbuterol
rolipram
clenbuterol + rolipram
forskolin
relative mRNA levels
Acadm
D
Tibialis anterior, 6h
relative mRNA levels
p=0.08
PGC-1β
E
Gastrocnemius, 6h
relative mRNA levels
PGC-1α exon2
F
Gastrocnemius, 6h
relative mRNA levels
p=0.09
PGC-1α altern. exon1
G
Gastrocnemius, 6h
relative mRNA levels
Acadm
H
Gastrocnemius, 6h
relative mRNA levels
PGC-1β
I
Tibialis anterior, 6h
vehicle
clenbut.
rolipram
clenbut.+ rolipram
forsk.
IB: PGC-1α
IB: α-tubulin
J
Tibialis anterior, 6h
relative protein levels
PGC-1α protein
K
Quadriceps, 6h
vehicle
clenbut.
rolipram
clenbut.+ rolipram
forsk.
IB: PGC-1α
IB: α-tubulin
L
Quadriceps, 6h
relative protein levels
p=0.06
PGC-1α protein

Figure 2. Rolipram moderately increases PGC-1α protein levels without inducing the mRNA expression.

(A-D) Expression of PGC-1α exon 2, PGC-1α alternative exon 1, Acadm and PGC-1β in mouse *tibialis anterior* muscle 6 hours after administration of either PBS, clenbuterol, rolipram, clenbuterol together with rolipram or forskolin by intraperitoneal injections. mRNA levels were determined by real-time PCR.

(E-H) Expression of PGC-1α exon 2, PGC-1α alternative exon 1, Acadm and PGC-1β in mouse *gastrocnemius* muscle 6 hours after administration of either PBS, clenbuterol, rolipram, clenbuterol together with rolipram or forskolin by intraperitoneal injections. mRNA levels were determined by real-time PCR.

(I) PGC-1α protein levels in mouse *tibialis anterior* muscle determined by immunoblotting 6 hours after administration of either PBS, clenbuterol, rolipram, clenbuterol together with rolipram or forskolin by intraperitoneal injections.

(J) Quantification of protein levels from (I) normalized to α-tubulin.

(K) PGC-1α protein levels in mouse *quadriceps* muscle determined by immunoblotting 6 hours after administration of either PBS, clenbuterol, rolipram, clenbuterol together with rolipram or forskolin by intraperitoneal injections.

(L) Quantification of protein levels from (K) normalized to α-tubulin.

Rolipram treatment led only to a weak induction of PGC-1α alternative exon 1 expression in *tibialis anterior*, leaving the normal PGC-1α exon 1 levels unchanged (Fig. 2 A,B,E and F). The observed strong induction of PGC-1α observed with clenbuterol was not accompanied by an induction of the typical PGC-1α target gene Acadm (Fig 2C and G). PGC-1β expression tended to be reduced upon clenbuterol treatment (Fig 2 D and H). However, this suppression was not significant. Surprisingly, unlike the mRNA levels, the PGC-1α protein levels in *tibialis anterior* muscle were slightly increased following rolipram treatment alone or when administered together with clenbuterol (Fig. 2I and J). This induction could not be observed in the *quadriceps* muscle (Fig. 2K and L). Unexpectedly, forskolin did not induce PGC-1α mRNA and protein in skeletal muscle (Fig. 2). Instead, in *gastrocnemius* muscle forskolin treatment slightly suppressed PGC-1α mRNA (Fig 2E and F).

4.3.3 Clenbuterol boosts both PGC-1α mRNA and protein, while PDE1 inhibition by vinpocetine does not alter skeletal muscle PGC-1α levels *in vivo*.

Next we sought to look into the regulation of PGC-1α expression following PDE1 inhibition by vinpocetine. Like in the previous experiment, vinpocetine was administered by intraperitoneal injections into 11 weeks old male mice either alone or in the presence of clenbuterol. Similarly, we expected a prolonged PGC-1α induction by clenbuterol when the hydrolysis of cAMP is inhibited by vinpocetine. To examine this, PGC-1α mRNA and protein levels were measured 6 hours and 24 hours after the drug administration. Aminophylline, a nonselective PDE inhibitor, was included in this experiment because it was shown to restore muscle structure in a zebrafish model of Duchenne muscular dystrophy (Kawahara et al., 2011). In *tibialis anterior* muscle, clenbuterol strongly induced

PGC-1α mRNA expression, while it suppressed PGC-1β expression 6 hours after drug administration (Fig. 3A, B and C). This suppression was probably a compensation for the induction of PGC-1α. The induction of PGC-1α was transient, because 24 hours after drug administration all induction was gone (Fig. 3D, E and F).

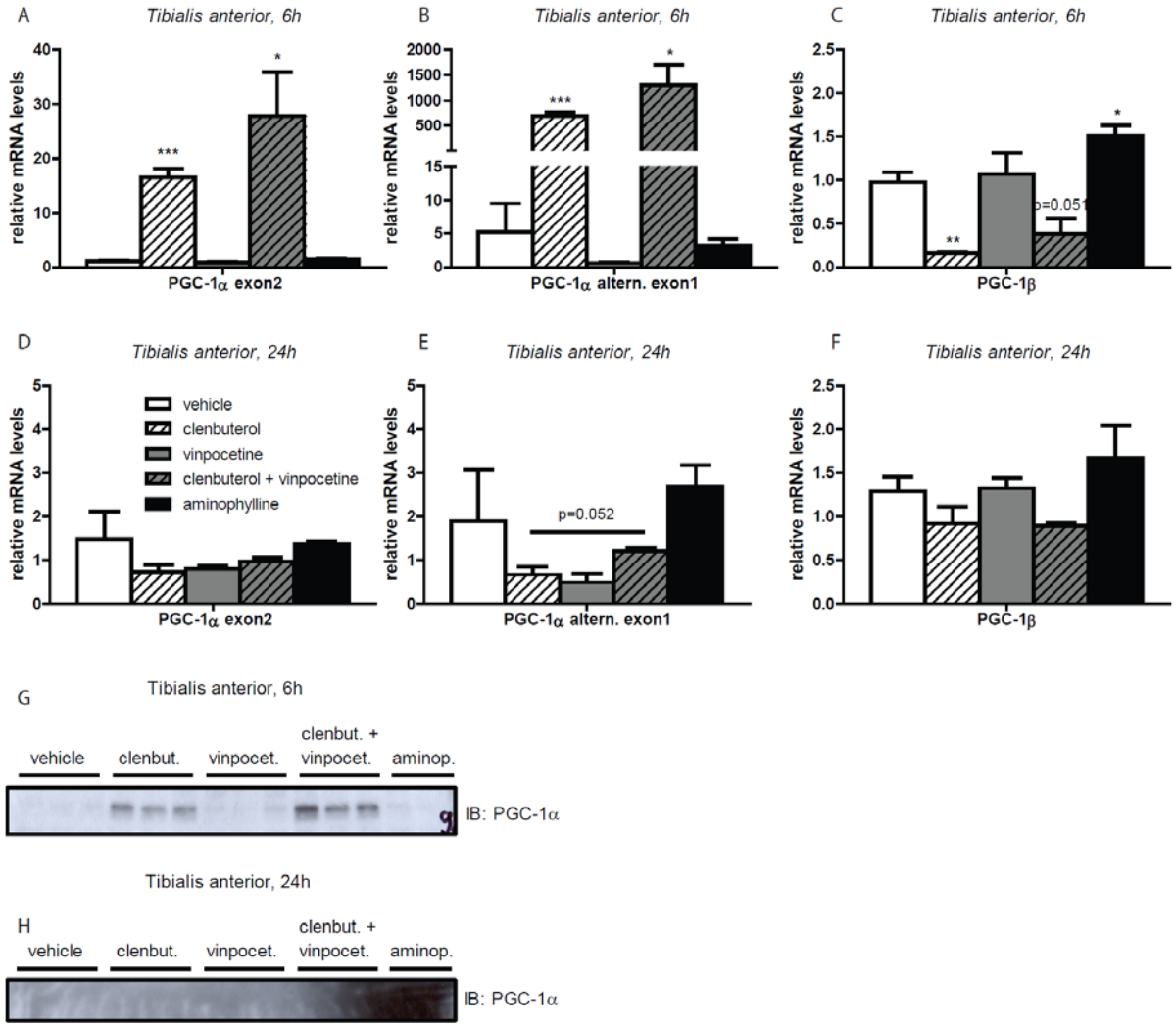

Figure 3. Clenbuterol boosts both PGC-1α mRNA and protein, while PDE1 inhibition by vinpocetine does not alter skeletal muscle PGC-1α levels *in vivo*.

(A-C) Expression of PGC-1α exon 2, PGC-1α alternative exon 1 and PGC-1β in mouse *tibialis anterior* muscle 6 hours after administration of either DMSO, clenbuterol, vinpocetine, clenbuterol together with vinpocetine or aminophylline by intraperitoneal injections. mRNA levels were determined by real-time PCR.

(D-F) Same like (A-C) but 24 hours after drug administration.

(G-H) PGC-1α protein levels in mouse *tibialis anterior* muscle determined by immunoblotting 6 hours (G) or 24 hours (H) after administration of either DMSO, clenbuterol, vinpocetine, clenbuterol together with vinpocetine or aminophylline by intraperitoneal injections.

Vinpocetine treatment alone did not have any effect on PGC-1α or PGC-1β expression neither after 6 hours, nor after 24 hours. When administered together with clenbuterol, vinpocetine seemed to further increase the clenbuterol induced PGC-1α expression and diminish the clenbuterol induced suppression of PGC-1β 6 hours after drug administration, suggesting that it might enhance the beneficial effects of clenbuterol treatment (Fig. 3A, B and C). Unfortunately, this difference was not significant and similarly to the clenbuterol treatment, 24 hours after administration all PGC-1α mRNA induction was lost (Fig. 3A, B, C, D, E and F). The nonselective PDE inhibitor aminophylline did not alter PGC-1α expression in the *tibialis anterior* muscle 6 hours after drug administration, but unexpectedly, it moderately raised the expression of PGC-1β at this time point (Fig. 3A, B and C). Like with other treatments, this effect was lost 24 hours after drug administration (Fig. 3D, E and F). When it comes to PGC-1α protein levels, only clenbuterol treatment provoked a strong induction, but like the PGC-1α mRNA the PGC-1α protein levels returned to normal levels 24 hours after drug administration (Fig. 3G and H).

4.3.4 Clenbuterol and aminophylline treatments provoked moderate and transient changes in liver and kidney and caused no changes in the white adipose tissue.

Next we examined if the β-adrenergic receptor stimulation by clenbuterol or the inhibition of PDEs by vinpocetine and aminophylline caused any changes in PGC-1α and PGC-1β expression in organs other than skeletal muscle like liver, kidney and fat. In liver, PGC-1α is known to be regulated by cAMP and to induce gluconeogenesis while exercise and adrenaline induce PGC-1α expression in white adipose tissue (Sutherland et al., 2009; Yoon et al., 2001). The regulation of PGC-1α and its role in kidney are not known. Thus we measured the levels of PGC-1α and PGC-1β in these tissues 6 and 24 hours following clenbuterol, vinpocetine and aminophylline treatment. First, vinpocetine treatment alone did not cause any changes in the expression of these genes. Only when combined with clenbuterol, vinpocetine led to a weak but significant induction of PGC-1α expression in the liver, six hours after administration (Fig. 4). In liver, clenbuterol induced PGC-1α expression 6 hours after administration while not changing PGC-1β. This induction was significantly lower when clenbuterol was administered together with vinopocetine (Fig. 4A). Interestingly, while aminophylline moderately raised PGC-1β mRNA levels in muscle, it lowered PGC-1β levels in the liver (Fig. 4A). However 24 h after drug administration the effects of all treatments were lost, confirming the transient nature of these changes (Fig. 4B). In kidney clenbuterol treatment alone or in combination reduced both PGC-1α and PGC-1β gene expression. This suppression was equal when clenbuterol was administered alone or in combination with vinpocetine and was lost after 24 hours (Fig. 4C and D). In the white adipose tissue neither of the drugs showed any effect at the time points we measured the gene expression (Fig. 4E and F).

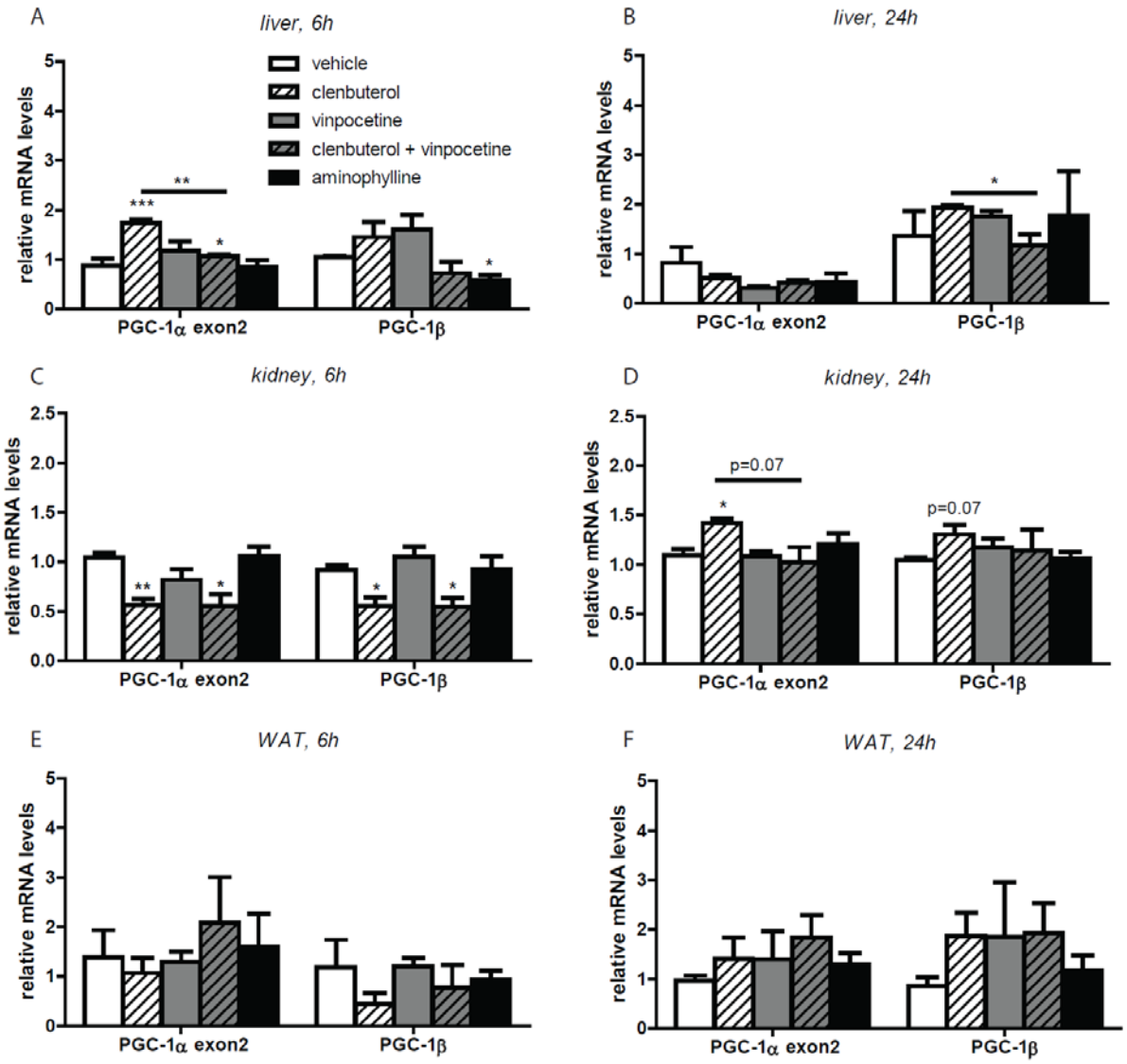

Figure 4. Clenbuterol and aminophylline treatments provoked moderate and transient changes in liver and kidney and caused no changes in the white adipose tissue.

(A-B) Expression of PGC-1α exon 2, PGC-1α alternative exon 1, and PGC-1β in liver 6 hours (A) or 24 hours (B) after administration of either DMSO, clenbuterol, vinpocetine, clenbuterol together with vinpocetine or aminophylline by intraperitoneal injections. mRNA levels were determined by real-time PCR.

(C-D) Expression of PGC-1α exon 2, PGC-1α alternative exon 1, and PGC-1β in kidney 6 hours (C) or 24 hours (D) after administration of either DMSO, clenbuterol, vinpocetine, clenbuterol together with vinpocetine or aminophylline by intraperitoneal injections. mRNA levels were determined by real-time PCR.

(E-F) Expression of PGC-1α exon 2, PGC-1α alternative exon 1, and PGC-1β in visceral white adipose tissue 6 hours (E) or 24 hours (F) after administration of either DMSO, clenbuterol, vinpocetine, clenbuterol together with vinpocetine or aminophylline by intraperitoneal injections. mRNA levels were determined by real-time PCR.

4.4 Discussion

The main goal of this study was to test if by intervening in cAMP signalling through inhibition of PDEs we can induce the expression of PGC-1α or PGC-1β in skeletal muscle and if so to determine which PDE family is involved in this regulation. In this study we show that the activation of β2-adrenergic receptor signalling transiently induces PGC-1α expression in skeletal muscle (Fig. 2 and 3). Furthermore, using forskolin in skeletal muscle cells to activate the protein kinase A, an effector protein of cAMP which is downstream of β2-adrenergic receptor activation, we observed a strong tendency towards increased PGC-1α levels (Fig. 1). Forskolin administration *in vivo* did not change PGC-1α or PGC-1β levels (Fig. 2). This might be due to different regulation in skeletal muscle tissue compared to isolated skeletal muscle cells, however it is also possible that forskolin administered by intraperitoneal injection was insufficiently concentrated, did not reach skeletal muscle tissue or simply that we measured at a wrong time point. Nevertheless, these observations strongly suggest that elevated cAMP levels indeed regulate PGC-1α expression. Similar results have already been shown by other groups, thus confirming the role of cAMP in PGC-1α regulation (Miura et al., 2008; Miura et al., 2007; Pearen et al., 2008). PDE inhibition by the nonselective PDE inhibitor IBMX in skeletal muscle cells led to a tendency towards increased PGC-1α, which is comparable to forskolin treatment (Fig. 1A). However, when selective PDE inhibitors were used, only a weak induction of PGC-1α with vinpocetine and rolipram was observed (Fig 1B). This cannot be explained by export of cAMP out of the cells as suggested by Godinho & Costa because when the same experiment was performed in cells treated with probenecid, PGC-1α induction by PDE inhibition was still very modest (Fig 1C)(Godinho and Costa, 2003).

When applied *in vivo*, rolipram lead to a very modest induction of the alternative exon 1 of PGC-1α, but did not further increase the PGC-1α expression when administered together with clenbuterol (Fig. 2). The PGC-1α protein levels were significantly higher following rolipram treatment in the *tibialis anterior* muscle but not in the *quadriceps* muscle, meaning that this induction is probably regulated through another pathway than direct induction of PGC-1α mRNA expression, supposedly by PGC-1α protein stabilization (Fig. 2I, J, K and L). This regulation might explain the already published inhibition of skeletal muscle atrophy by rolipram (Hinkle et al., 2005). Vinpocetine administration alone had no influence on PGC-1α expression in skeletal muscle but tends to further increase the clenbuterol-induced PGC-1α expression (Fig. 3A and B). It also led to a weaker compensatory PGC-1β suppression compared to clenbuterol treatment alone (Fig. 3C). Last, liver PGC-1α levels were significantly less induced following clenbuterol and vinpocetine treatment compared to clenbuterol treatment alone (Fig. 4A). Thus the role of vinpocetine in PGC-1α regulation should be further studied.

Once generated in the cell, cAMP can only be eliminated by hydrolysis or eventually by export out of the cell (Godinho and Costa, 2003). Thus, we expected that PDE inhibition should prolong the transient PGC-1α induction by clenbuterol. This was not the case in our study, because all effects of

clenbuterol were gone after 24 hours despite the PDE inhibition. Possible explanations are that cAMP is hydrolysed by PDE families which are insensitive to IBMX or rolipram like PDE8 or PDE7. Moreover, the binding affinity of the catalytic site of PDE4 for rolipram depends on conformational changes of the enzyme (Omori and Kotera, 2007). Another explanation is that *in vivo,* cAMP is indeed exported to the extracellular space. Additionally, compartmentalised cAMP signalling might play a role for the regulation of PGC-1α expression and thus global intracellular changes of cAMP concentration would not affect the regulation of PGC-1α expression or the activation of other cAMP effector proteins like Epacs (Houslay, 2010). Last, the expression profiles of PDEs are not identical in mice and humans, thus it is worth studying the effect of PDE inhibition in human skeletal muscle cells (Bingham et al., 2006; Omori and Kotera, 2007).

An identification of a PDE which regulates PGC-1α expression might represent a first step towards the development of a drug for the treatment of many medical conditions for which PGC-1α expression shows therapeutic effects. PDEs are important drug targets for the treatment of numerous diseases like asthma, depression or erectile dysfunction, thus many specific PDE inhibitors have already been developed (Omori and Kotera, 2007). Interestingly, in our study clenbuterol treatment suppressed PGC-1α and PGC-1β expression in kidney (Fig. 4C). The role of these coactivators in this tissue is not yet known but PDE inhibitors or agonists might be used to study it. PGC-1α is expressed in kidney and if PGC-1α and PGC-1β turn out to regulate important processes in this organ, PDEs might also become important drug targets in this context (Puigserver et al., 1998).

4.5 Methods

Cell culture and treatments

C2C12 cells were grown in Dulbecco's modified Eagle's medium (DMEM) supplemented with 10% fetal bovine serum (FBS), 100 Units/ml penicillin and 100ug/ml streptomycin. To obtain myotubes, the C2C12 myoblasts were allowed to reach 90% confluence and the medium was changed to DMEM supplemented with 2% horse serum (differentiation medium) for 72 hours. 8cpt-2Me-cAMP was purchased from Tocris bioscience. All drugs other drugs were purchased from Sigma Aldrich. The drugs were dissolved in DMSO and used in following concentrations: IBMX (3-Isobutyl-1-methylxanthin) 100µM, forskolin 100µM, vinpocetine 140µM, EHNA hydrochloride 20µM, cilostamide 5µM, rolipram 20µM, zaprinast 10µM, BRL 50481 5µM, BAY 73-6691 5µM, 8CPT-2Me-cAMP 22µM, probenecid 100µM. These concentrations correspond to approximately 10-20 fold IC50 (EC50 for 8CPT-2Me-cAMP and forskolin) concentrations.

Primary skeletal muscle cells were isolated from 6 weeks old wild-type C57BL/6J mice as described previously (Megeney et al., 1996). The myoblasts were grown in Ham's/F-10 medium supplemented with 20% FBS (Hyclone, heat inactivated at 56 degrees for 30 min), 1x Pen/Strep, 2.5 ng/mL bFGF (Invitrogen). For differentiation the cells were shifted to DMEM with 5% horse serum for 72 hours.

Real-time PCR and target gene validation

The sequences of the primers used in real-time PCR experiments are depicted Table 1 below. The values are presented as the mean +/- SEM. Student's t test was performed and a p-value < 0.05 was considered as significant. (*$p<0.05$, **$p<0.01$, ***$p<0.001$).

Real-time PCR primers used		
gene	forward primer	reverse primer
Rn18s	AGTCCCTGCCCTTTGTACACA	CGATCCGAGGGCCTCACTA
Tbp	GGCCTCTCAGAAGCATCACTA	GCCAAGCCCTGAGCATAA
Ppargc1a exon2	TGGGCACATCACCACTACAC	TCTGGCTATGCAGTTCAGCC
Ppargc1a altern. exon1	TCTGCGCTGGAGTCAGTTAC	CCGCCTCCTTTTCCTCTCAT
Ppargc1b	TTCGAAGGCTTTGCAAGGAAG	TTCGGGGTCCTCACTGGTTT
Acadm	AGTGGATCCGCCAGCTACTC	ATGGGAATGTCTCTGCCAAA

Table 1. Real-time primer sequences.

Experimental animals and drug administration

Clenbuterol, rolipram and forskolin treatment:

Following drugs were dissolved in PBS and administered by intraperitoneal injections to 10 weeks old wild-type C57BL/6J mice: PBS as vehicle, clenbuterol 1mg/kg b.w., rolipram 5mg/kg b.w., a combination of clenbuterol and rolipram 1mg/kg and 5mg/kg b.w. respectively and forskolin 0.7mg/kg b.w. All mice were sacrificed 6h after drug administration. *Gastrocnemius*, *tibialis anterior* and

quadriceps muscles were collected and RNA and protein were isolated. RNA was reverse transcribed and transcript levels were measured by real-time PCR. Protein levels of PGC-1α and α-tubulin were measured by immunoblotting using following antibodies: anti-PGC-1 from Millipore (Chemicon) and anti-α-tubulin (11H10) from Cell Signaling.

Clenbuterol, vinpocetine and aminophylline treatment:

Following drugs were dissolved in DMSO and administered by intraperitoneal injections to 11 weeks old wild-type C57BL/6J mice: DMSO as vehicle, clenbuterol 1mg/kg b.w., vinpocetine 10mg/kg b.w., a combination of clenbuterol and vinpocetine 1mg/kg and 10mg/kg b.w. respectively and aminophylline hydrate 20mg/kg. First group of mice was sacrificed 6h and a second group 24hafter drug administration. *Tibialis anterior* muscle, liver, kidney and visceral fat were collected and frozen. RNA and protein were isolated and the RNA was reversed transcribed and used for quantification by real-time PCR. Protein levels of PGC-1α and α-tubulin were measured by immunoblotting using following antibodies: anti-PGC-1α mouse (4C1.3) from Millipore (Calbiochem) and anti-α-tubulin (11H10) from Cell Signaling.

4.6 References

Adamo, C.M., Dai, D.F., Percival, J.M., Minami, E., Willis, M.S., Patrucco, E., Froehner, S.C., and Beavo, J.A. (2010). Sildenafil reverses cardiac dysfunction in the mdx mouse model of Duchenne muscular dystrophy. Proc Natl Acad Sci U S A *107*, 19079-19083.

Akimoto, T., Pohnert, S.C., Li, P., Zhang, M., Gumbs, C., Rosenberg, P.B., Williams, R.S., and Yan, Z. (2005). Exercise stimulates Pgc-1alpha transcription in skeletal muscle through activation of the p38 MAPK pathway. J Biol Chem *280*, 19587-19593.

Arany, Z., Foo, S.Y., Ma, Y., Ruas, J.L., Bommi-Reddy, A., Girnun, G., Cooper, M., Laznik, D., Chinsomboon, J., Rangwala, S.M*., et al.* (2008). HIF-independent regulation of VEGF and angiogenesis by the transcriptional coactivator PGC-1alpha. Nature *451*, 1008-1012.

Baar, K., Wende, A.R., Jones, T.E., Marison, M., Nolte, L.A., Chen, M., Kelly, D.P., and Holloszy, J.O. (2002). Adaptations of skeletal muscle to exercise: rapid increase in the transcriptional coactivator PGC-1. Faseb J *16*, 1879-1886.

Bingham, J., Sudarsanam, S., and Srinivasan, S. (2006). Profiling human phosphodiesterase genes and splice isoforms. Biochem Biophys Res Commun *350*, 25-32.

Booth, F.W., Chakravarthy, M.V., Gordon, S.E., and Spangenburg, E.E. (2002). Waging war on physical inactivity: using modern molecular ammunition against an ancient enemy. J Appl Physiol *93*, 3-30.

Dyson, P.A. (2010). The therapeutics of lifestyle management on obesity. Diabetes Obes Metab *12*, 941-946.

Francis, S.H., Blount, M.A., and Corbin, J.D. (2011). Mammalian cyclic nucleotide phosphodiesterases: molecular mechanisms and physiological functions. Physiol Rev *91*, 651-690.

Godinho, R.O., and Costa, V.L., Jr. (2003). Regulation of intracellular cyclic AMP in skeletal muscle cells involves the efflux of cyclic nucleotide to the extracellular compartment. Br J Pharmacol *138*, 995-1003.

Handschin, C., Kobayashi, Y.M., Chin, S., Seale, P., Campbell, K.P., and Spiegelman, B.M. (2007). PGC-1alpha regulates the neuromuscular junction program and ameliorates Duchenne muscular dystrophy. Genes Dev *21*, 770-783.

Handschin, C., Rhee, J., Lin, J., Tarr, P.T., and Spiegelman, B.M. (2003). An autoregulatory loop controls peroxisome proliferator-activated receptor gamma coactivator 1alpha expression in muscle. Proc Natl Acad Sci U S A *100*, 7111-7116.

Henriksen, E.J. (2002). Invited review: Effects of acute exercise and exercise training on insulin resistance. J Appl Physiol *93*, 788-796.

Herzig, S., Long, F., Jhala, U.S., Hedrick, S., Quinn, R., Bauer, A., Rudolph, D., Schutz, G., Yoon, C., Puigserver, P*., et al.* (2001). CREB regulates hepatic gluconeogenesis through the coactivator PGC-1. Nature *413*, 179-183.

Hinkle, R.T., Dolan, E., Cody, D.B., Bauer, M.B., and Isfort, R.J. (2005). Phosphodiesterase 4 inhibition reduces skeletal muscle atrophy. Muscle Nerve *32*, 775-781.

Houslay, M.D. (2010). Underpinning compartmentalised cAMP signalling through targeted cAMP breakdown. Trends Biochem Sci *35*, 91-100.

Jager, S., Handschin, C., St-Pierre, J., and Spiegelman, B.M. (2007). AMP-activated protein kinase (AMPK) action in skeletal muscle via direct phosphorylation of PGC-1alpha. Proc Natl Acad Sci U S A *104*, 12017-12022.

Kawahara, G., Karpf, J.A., Myers, J.A., Alexander, M.S., Guyon, J.R., and Kunkel, L.M. (2011). Drug screening in a zebrafish model of Duchenne muscular dystrophy. Proc Natl Acad Sci U S A *108*, 5331-5336.

Lin, J., Wu, H., Tarr, P.T., Zhang, C.Y., Wu, Z., Boss, O., Michael, L.F., Puigserver, P., Isotani, E., Olson, E.N*., et al.* (2002). Transcriptional co-activator PGC-1 alpha drives the formation of slow-twitch muscle fibres. Nature *418*, 797-801.

Lira, V.A., Benton, C.R., Yan, Z., and Bonen, A. (2010). PGC-1alpha regulation by exercise training and its influences on muscle function and insulin sensitivity. Am J Physiol Endocrinol Metab *299*, E145-161.

Malik, V., Rodino-Klapac, L.R., and Mendell, J.R. (2012). Emerging drugs for Duchenne muscular dystrophy. Expert Opin Emerg Drugs *17*, 261-277.

Matsakas, A., and Narkar, V.A. (2010). Endurance exercise mimetics in skeletal muscle. Curr Sports Med Rep *9*, 227-232.

Megeney, L.A., Kablar, B., Garrett, K., Anderson, J.E., and Rudnicki, M.A. (1996). MyoD is required for myogenic stem cell function in adult skeletal muscle. Genes Dev *10*, 1173-1183.

Miura, S., Kai, Y., Kamei, Y., and Ezaki, O. (2008). Isoform-specific increases in murine skeletal muscle peroxisome proliferator-activated receptor-gamma coactivator-1alpha (PGC-1alpha) mRNA in response to beta2-adrenergic receptor activation and exercise. Endocrinology *149*, 4527-4533.

Miura, S., Kawanaka, K., Kai, Y., Tamura, M., Goto, M., Shiuchi, T., Minokoshi, Y., and Ezaki, O. (2007). An increase in murine skeletal muscle peroxisome proliferator-activated receptor-gamma coactivator-1alpha (PGC-1alpha) mRNA in response to exercise is mediated by beta-adrenergic receptor activation. Endocrinology *148*, 3441-3448.

Olesen, J., Kiilerich, K., and Pilegaard, H. (2010). PGC-1alpha-mediated adaptations in skeletal muscle. Pflugers Arch *460*, 153-162.

Omori, K., and Kotera, J. (2007). Overview of PDEs and their regulation. Circ Res *100*, 309-327.

Pearen, M.A., Myers, S.A., Raichur, S., Ryall, J.G., Lynch, G.S., and Muscat, G.E. (2008). The orphan nuclear receptor, NOR-1, a target of beta-adrenergic signaling, regulates gene expression that controls oxidative metabolism in skeletal muscle. Endocrinology *149*, 2853-2865.

Pilegaard, H., Saltin, B., and Neufer, P.D. (2003). Exercise induces transient transcriptional activation of the PGC-1alpha gene in human skeletal muscle. J Physiol *546*, 851-858.

Puigserver, P., Wu, Z., Park, C.W., Graves, R., Wright, M., and Spiegelman, B.M. (1998). A cold-inducible coactivator of nuclear receptors linked to adaptive thermogenesis. Cell *92*, 829-839.

Sandri, M., Lin, J., Handschin, C., Yang, W., Arany, Z.P., Lecker, S.H., Goldberg, A.L., and Spiegelman, B.M. (2006). PGC-1alpha protects skeletal muscle from atrophy by suppressing FoxO3 action and atrophy-specific gene transcription. Proc Natl Acad Sci U S A *103*, 16260-16265.

Sutherland, L.N., Bomhof, M.R., Capozzi, L.C., Basaraba, S.A., and Wright, D.C. (2009). Exercise and adrenaline increase PGC-1{alpha} mRNA expression in rat adipose tissue. J Physiol *587*, 1607-1617.

Wenz, T., Rossi, S.G., Rotundo, R.L., Spiegelman, B.M., and Moraes, C.T. (2009). Increased muscle PGC-1alpha expression protects from sarcopenia and metabolic disease during aging. Proc Natl Acad Sci U S A *106*, 20405-20410.

Wu, Z., Puigserver, P., Andersson, U., Zhang, C., Adelmant, G., Mootha, V., Troy, A., Cinti, S., Lowell, B., Scarpulla, R.C.*, et al.* (1999). Mechanisms controlling mitochondrial biogenesis and respiration through the thermogenic coactivator PGC-1. Cell *98*, 115-124.

Yoon, J.C., Puigserver, P., Chen, G., Donovan, J., Wu, Z., Rhee, J., Adelmant, G., Stafford, J., Kahn, C.R., Granner, D.K.*, et al.* (2001). Control of hepatic gluconeogenesis through the transcriptional coactivator PGC-1. Nature *413*, 131-138.

5 FINAL DISCUSSION

5.1 Summary of major findings

-Identification of all interactions of PGC-1α with the genome and how it regulates gene expression:

The data sets, which are generated in this thesis, represent a collection of all interactions of PGC-1α or ERRα with the genome in cultured skeletal muscle cells. The peaks were assigned to adjacent genes to understand why PGC-1α is recruited to these locations in the genome and how it regulates gene expression. The data from expression arrays was included in the analysis and revealed that the genes involved in cellular respiration, electron transport chain or metabolic pathways in general were up-regulated, which was also expected (Manuscript 1, Figure 1) (Handschin and Spiegelman, 2006; Mootha et al., 2004). While it was known that PGC-1α regulates metabolic gene expression, the precise mechanism underlying this regulation was not known. Published papers on PGC-1α induction of gene expression mostly focused on direct regulation of gene expression, where PGC-1α binds a transcription factor in the promoter of the induced gene (Michael et al., 2001; Mootha et al., 2004; Puigserver et al., 2003; Puigserver et al., 1998). Surprisingly, the induction of gene expression by PGC-1α was not only directly by binding to transcription factors in promoters, but also indirectly, without the need for PGC-1α to be present at the promoters of some induced genes. (Manuscript 1, Figure 1). Actually, almost two thirds of all up-regulated genes were indirectly induced by PGC-1α. Therefore PGC-1α induces gene expression by both direct and indirect regulation of gene expression. The expression of inflammatory genes was repressed by PGC-1α (Manuscript 1, Figure 1). This was to some extent expected because previous work suggested a role for PGC-1α in regulating inflammatory genes. This is also confirmed by work of colleagues from our lab (Eisele et al., 2013; Handschin and Spiegelman, 2008). This suppression was almost exclusively indirectly because it did not require the recruitment of PGC-1α to the promoters of suppressed genes. This indicates that PGC-1α does not act as a corepressor in skeletal muscle cells. How this suppression is accomplished is not clear yet, but it might be by inducing transcription factors involved in immunosuppression. Alternatively, it might by attenuating the activity of pro-inflammatory transcription factors like NF-κB as suggested by our MARA results.

-ERRα, as the major transcriptional binding partner for PGC-1α, can regulate gene expression in presence or absence of PGC-1α

De novo motif search and the comparison of DNA sequences in peaks to known transcription factor motifs identified ERRα as the major transcriptional partner and mediator of PGC-1α induced regulation of gene expression (Manuscript 1, Figure 3). Unexpectedly, the evaluation of the ERRα ChIP-Sequencing data demonstrated that ERRα can be transcriptionally active and regulate gene expression with and without PGC-1α. Why PGC-1α coactivates ERRα at some targets, but not at others is not clear. However, it might explain how PGC-1α indirectly regulates gene expression, because PGC-1α also induces the expression of ERRα (Mootha et al., 2004). Moreover, the abundance

of the motif for the transcription factor specificity protein 1 (Sp1) is very high in ERRα peaks, especially in a subset of ERRα peaks. This subset is represented by peaks which are adjacent to ERRα target genes, which do not require direct coactivation by PGC-1α for the induction of their expression. This raises the possibility that SP-1 and ERRα might cooperatively regulate the expression of some ERRα target genes.

Several other transcription factors cooperate with PGC-1α in skeletal muscle cells:

In addition to ERRα, PGC-1α seems to regulate many other transcription factors, as revealed by the principal component analysis (PCA) and motif search in DNA fragments, which are derived from peak sequences (Manuscript 1, Figure 3). By combining motifs, which are found in peak sequences, with expression array data, we predicted which subset of PGC-1α target genes is regulated by a particular transcription factor. The knockdown of the predicted transcription factors Fos, Jun, Atf3, Gtf2i, Zfp143 and Nfe2l2 but not Nfyc led to a diminished or absent induction of many of their predicted target genes (Manuscript 1, Figure 4). This strongly indicates that these predicted transcription factors indeed cooperate with PGC-1α in skeletal muscle cells and regulate gene expression. It is likely that other transcription factors, which were predicted by the motif search, also are transcriptional partners for PGC-1α.

PGC-1α regulates the response to hypoxia possibly by coactivating the AP-1 transcription factor complex:

The transcription factors Fos, Jun and Atf3, which in our experiments have been found to be involved in the expression of a subset of PGC-1α target genes, are all subunits of the activator protein 1 (AP-1) transcription factor complex (Shaulian, 2010; Shaulian and Karin, 2002; Vesely et al., 2009). The gene ontology analysis of directly regulated PGC-1α target genes with AP-1 motif in the peak revealed that these genes are involved in the regulation of the cellular response to hypoxia and the mTOR signaling pathway (Manuscript1, Figure 5). PGC-1α was previously found to be inducible by hypoxia and subsequently coactivate ERRα to regulate the expression of VEGF and angiogenesis (Arany et al., 2008). Our results propose a possible coactivation of the AP-1 complex by PGC-1α to control the expression of other hypoxia induced genes.

PDE1 and PDE4 inhibition does not lead to increased PGC-1α mRNA levels in skeletal muscle:

Because the activation of PKA by forskolin or inhibition of PDE1 or PDE4 by specific PDE inhibitors increased PGC-1α mRNA levels in cultured skeletal muscle cells, we assumed that modulating cAMP levels by PDE inhibition might have a similar effect *in vivo* (Manuscript 3). The activation of β2-AR signaling transiently increased the PGC-1α mRNA levels in murine skeletal muscles. However, neither the inhibition of PDE1 by vinpocetine nor PDE4 by rolipram had any effect on PGC-1α expression. These PDE inhibitors neither induced the expression of PGC-1α when administered alone, nor did they prolong the transient induction of PGC-1α when administered together with the β2-AR signaling activator clenbuterol. These findings can be interpreted as evidence that PDE1 and PDE4 are not regulating PGC-1α expression in muscle in vivo, but cannot exclude the involvement of cAMP and

other PDEs in the regulation of PDE expression. Members of the PDE7 or PDE11 family are highly expressed in skeletal muscle and hydrolyze cAMP (Bender and Beavo, 2006; Omori and Kotera, 2007). Similarly, members of cAMP hydrolyzing PDE families PDE2, PDE3, PDE8 and PDE10 do not show high expression in skeletal muscle but might still be involved in regulation of PGC-1α expression due to the possibility of compartmentalized signaling (Francis et al., 2011). Therefore, because cAMP signaling induces PGC-1α expression in different tissues including skeletal muscle, we can assume that PDE inhibition would delay the degradation of the second messenger and thus shape PGC-1α expression (General Introduction, Chapters 1.3 and 1.4). However, whether this is true and which PDE family would be in this case responsible for the hydrolysis of cAMP to lower its levels subsequent to an induction, still needs to be identified. Last, a difference in the species specific PDE expression pattern between human and mouse muscle cells cannot be excluded.

5.2 Discussion

The data obtained from our ChIP-Seq experiments can be considered as a snapshot of all interactions of PGC-1α with the genome in a typical skeletal muscle cell. The peaks represent the localization of all PGC-1α recruitments to chromatin across the entire genome. In general, the binding of a transcription factor to DNA should not be considered as a binary event, where only the state „bound" and „not bound" can occur. The nature of transcription factor binding is rather equilibrium of binding and dissociation from DNA and the signal strength represents the strength of interaction with the genome at a particular location (Furey, 2012). In theory, a strong signal can arise from a strong interaction in a small number of cells or a weaker interaction but in a larger share of cells. The chromatin from many millions of cells, typically $1x10^8$ cells for each immunoprecipitation, is used as starting material. Therefore, ChIP-Seq data does not only consist of sharp peaks and background noise, but also of binding events, which are more of continuous nature. This poses a difficulty at setting a cut-off for the peak-calling. Also, the number of peaks increases with the sequencing depth, meaning that the more reads we obtain from sequencing experiments, the more peaks will be identified in the data set (Park, 2009). This should be considered when interpreting the number of peaks in our data sets.

There is no standard procedure to study such big data sets. Once the reads are mapped and the peak calling is done, there are different ways to continue with the downstream analysis. Researchers can focus on individual genes in these data sets and study the role of PGC-1α in the regulation of these particular genes. Alternatively, they can use different informatics tools to analyze all binding events together. Because the aim of this thesis was to study the regulation of gene expression by PGC-1α globally, we applied the latter approach to be able to draw general conclusions on PGC-1α transcriptional activity. This is now the first time that the recruitment of PGC-1α to DNA was studied in skeletal muscle cells on a genome-wide scale.

The genomic location of PGC-1α peaks alone does not tell much about how PGC-1α acts to control transcription. The PGC-1α peaks were assigned to genes in their proximity and the expression of these genes was measured by expression arrays. This allowed us to investigate to which genes or gene regulatory sequences PGC-1α tends to be recruited to and if this recruitment is functional, in terms of gene expression changes. The finding that 14% of all peaks are upstream of promoters combined with the fact that the peaks are symmetrically distributed around the promoter leads to the conclusion that around 28% of all peaks are around the transcription start site (TSS) (Manuscript 1, Figure 1). This clearly reflects the direct participation of PGC-1α in gene transcription. This is in agreement with the finding from Charos and colleagues, who reported that around 38% of PGC-1α peaks are found around the TSS in HepG2 cells (Charos et al., 2012). This value is higher than the one which is observed in our experiments. However, this higher value is observed when 1886 PGC-1α peaks (FDR=1%) were considered for the analysis. It can be expected that this value would drop if the 9366 PGC-1α peaks

(FDR=5%) were taken into calculation. Also, the mode of action of PGC-1α in hepatic cells might be different than the one observed in skeletal muscle cells.

Intriguingly, almost half of the PGC-1α peaks in our experiment are located in intergenic regions, which is unexpected, considering that PGC-1α is a transcriptional coactivator (Manuscript 1, Figure 1). It is very well possible that PGC-1α interacts with enhancers or other remote regulatory sequences which can be located 50kb or more away from the TSS. However, this probably is not the only reason and does not account for all intergenic peaks. Some peaks might be located on genes but still considered as peaks in intergenic regions due to the assignment of peaks to genes. Peaks which are more than 10 kilobases (kb) away from a TSS are considered as peaks in intergenic regions. This cut-off was set to avoid a false assignment of a peak to distant genes. However, eukaryotic genes harbor introns and a typical gene like Ppargc1a itself spans over 100kb. The mouse dystrophin gene Dmd covers more than 2'200 kb (2,2 megabases)! Therefore, it is very likely that many peaks in our experiments are located on genes but are considered as lying in intergenic regions. However, this is inevitable in our gene assignment. There are no 100% error-free methods to assign genes to peaks, and every method is a trade-off between reducing the assignment to false genes and introducing such artifacts. Nevertheless, it is possible that PGC-1α actually binds to distant genomic locations. In this case, the purpose of these interaction events cannot be explained yet.

While it was expected to find that PGC-1α induces the expression of genes which are involved in metabolism, it was not known how the expression of these genes is precisely regulated (Manuscript 1, Figure 1) (Mootha et al., 2004). So far, published work on PGC-1α induced gene expression mostly describes a direct mode of regulation, where PGC-1α binds a transcription factor in the promoter of the induced gene (Michael et al., 2001; Mootha et al., 2004; Puigserver et al., 2003; Puigserver et al., 1998). It was not known if this is the major way how PGC-1α induces gene expression. We were surprised to find that in addition to directly inducing gene expression, PGC-1α induced two thirds of its target genes indirectly, without being present at the promoters of these target genes. Therefore, we can assume that PGC-1α does not coactivate the transcription factors which transcribe these indirectly regulated PGC-1α target genes. However, it is possible that PGC-1α induces the expression of transcription factors, which than in turn transcribe genes in absence of PGC-1α.

In contrast, almost all down-regulated genes are suppressed in an indirect manner, without the need for PGC-1α to be present at the transcription site. The promoters of only 36 out of 727 suppressed genes are occupied by PGC-1α. This is less than 5% of all down-regulated genes. This strongly indicates that PGC-1α primarily acts as a coactivator and does not directly corepress transcription in skeletal muscle cells. Consequently, the suppression of inflammatory genes by PGC-1α appears to be indirect (Manuscript 1, Figure 1). Therefore, it is likely that PGC-1α induces the expression of a transcription regulator which suppresses the expression of inflammatory or immune response genes. Alternatively, it is possible that the direct suppression of target genes by PGC-1α occurs immediately after PGC-1α itself is induced. In that case, PGC-1α would be recruited to DNA to suppress gene expression and

then quickly dissociate from the DNA. Because our ChIP experiment is performed 48h after C2C12 cells were treated with PGC-1α coding adenovirus, this early association of PGC-1α with DNA cannot be detected. With the present data, we cannot provide an answer if the latter mode of gene suppression by PGC-1α is true or not, but it is not very likely.

Together these findings identify PGC-1α as a coregulator, which operates in a direct and indirect way to induce the expression of mainly metabolic genes. The suppression of genes involved in immune response and apoptosis by PGC-1α appears to be almost exclusively indirect. In contrast to our mode of PGC-1α mediated regulation of gene expression, Charos and colleagues observed that PGC-1α and its transcriptional partners associated with both up-regulated and down-regulated genes in hepatic cells (Charos et al., 2012). Moreover, they report that the association of PGC-1α and ERRα is even higher with down-regulated genes (Figure 6).

This would suggest that PGC-1α and the transcription factors which are bound to it directly repress gene expression. It cannot be excluded that the mode of action of PGC-1α differs between skeletal muscle and liver cells, but it still would be surprising to identify ERRα and HNF4α as a strong repressors of gene expression.

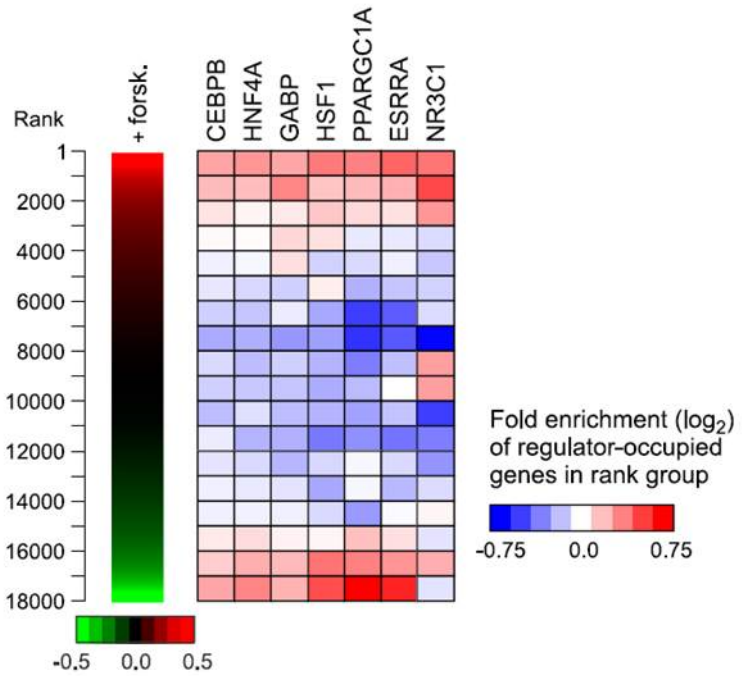

Figure 1. Correlation of transcription regulator binding and gene expression in HepG2 cells following forskolin treatment. Figure taken from (Charos et al., 2012).

As described in the introduction to this thesis, PGC-1α does not directly bind DNA but rather acts as a master regulator by coordinating the activity of numerous transcription factors. Therefore, we expected to find more than one transcription factor to interact with PGC-1α. Nevertheless, it was still surprising to find that more than 139 transcription factor motifs were overrepresented in PGC-1α

peaks (139 Motifs with a Z-score≥2.0). It is not very likely that all these transcription factors really are coactivated by PGC-1α. Some of the transcription factors from these motifs are not even expressed in our skeletal muscle cells. Therefore, several constraints have been used to exclude such transcription factors and obtain a list of likely transcriptional partners for PGC-1α (Manuscript 1, Figure 3). The resulting list contained 15 motifs and some of the transcription factors from these motifs were knocked down to validate their involvement in the regulation of PGC-1α target genes (Manuscript 1, Figures 4 and 5). This predicts that in skeletal muscle cells, PGC-1α might be regulating the activity of many transcription factors. Moreover, considering that the performed motif search did not contain motifs for all transcription factors which can be found in the mouse genome, this list might even be longer. The human genome encodes around 2000 transcription factors and a similar number of transcription factors can be expected in the mouse genome (Lodish et al., 2012; Vaquerizas et al., 2009). Therefore, such a prediction, based on motif search also has its limitations, especially if we consider that some transcription factors bind to similar consensus motifs. This can theoretically lead to detection of false negatives and false positives. Motifs for transcription factors which are not coactivated by PGC-1α but recognize a similar motif like one of true PGC-1α partners might be overrepresented in the motif search. These motifs would score high only because their similarity to a real binding partner for PGC-1α. This might be the case for the many members of the nuclear receptors superfamily, which due to their evolutionary conserved structure often bind to similar consensus sites (Mangelsdorf et al., 1995). On the other hand, the fact that some transcription factors recognize similar DNA sequences also could lead to detection of false negatives. The orphan nuclear receptors estrogen-related receptor β and γ (ERRβ and ERRγ) both recognize similar DNA elements like ERRα and eventually might regulate gene transcription together with PGC-1α in our experiments (Tremblay and Giguere, 2007). However, these transcription factors cannot be identified as binding partners for PGC-1α by the motif search alone, because they recognize same DNA elements.

Because of these limitations of the motif search, there were uncertainties whether our predictions for putative transcription partners for PGC-1α are reliable or not. ERRα was already previously described as an important binding partner for PGC-1α and all our results indicated that ERRα is the major effector of PGC-1α mediated regulation of gene expression (Mootha et al., 2004; Schreiber et al., 2004). The results from motif activity response analysis (MARA), principal component analysis (PCA) and MotEvo all identified ERRα as the top scoring transcription factor motif. Many of the remaining predicted transcription factors have never been shown to cooperatively regulate gene expression with PGC-1α. In order to have a biological validation of our predictions, we knocked down seven of the predicted transcription factors while overexpressing PGC-1α, namely Fos, Jun, Atf3, Gtf2i, Nfe2l2, Nfyc and Zfp143. If these transcription factors really regulate the expression of PGC-1α target genes, we should observe a decreased induction of the PGC-1α target genes, which have a PGC-1α peak with the motif for the corresponding transcription factor in their promoter. The finding that the knockdown of all these transcription factors, except for Nfyc, reduced the induction of these

predicted target genes, confirmed that our predictions indeed seem to be true (Manuscript 1, Figure 4). However, to prove that these transcription factors really are coactivated by PGC-1α, we would need to show their physical interaction with PGC-1α, possibly by performing co-immunoprecipitation experiments.

Similarly, the knockdown of ERRα in the presence of the inverse agonist XCT790 confirmed that ERRα is a transcription factor which mediates induction of gene expression by PGC-1α. Similarly, the ChIP-Sequencing of ERRα showed that ERRα and PGC-1α often colocalized in the promoters of their common target genes. The surprising observation that PGC-1α does not coactivate ERRα on all of its target genes provides an explanation how PGC-1α might indirectly regulate gene expression. PGC-1α induces the expression of ERRα itself, whereupon ERRα induces the expression of its target genes in the presence and in absence of PGC-1α. The MARA results from PGC-1α ChIP-Seq experiments already suggested such a mode of gene expression regulation by PGC-1α and ERRα, because ERRα activity was equally active in the promoters of primary and secondary genes (Manuscript 1, Figure 2). Previous work on cooperative regulation of gene expression by ERRα and PGC-1α often identified ERRα as an effector of PGC-1α but it was not revealed if ERRα also induced PGC-1α target genes without being coactivated by PGC-1α. We do not know why ERRα is not coactivated by PGC-1α on all of its target genes. The observation that the motif for the transcription factor specificity protein 1 (Sp1) is found more frequently in the ERRα peaks if they do not co-occur with PGC-1α tempts us to speculate. It can be carefully speculated that Sp1 might interact with ERRα, possibly forming a heterodimer and making PGC-1α dispensable for ERRα. This putative interaction however requires further investigation. It is important to note that PGC-1α can induce transcription factors which can also be active without being coactivated by PGC-1α. Therefore, it is very likely that this is not only true for ERRα. Furthermore, it is theoretically possible that PGC-1α induces the expression of some transcription factors but does not coactivate them at all. This would explain how PGC-1α indirectly regulates gene expression. Interestingly, when the ERRα ChIP-Seq data was explored by PCA to analyze the variance in the data the motif for Sp1 was identified in one component. The other component contained the motifs for ERRα and other nuclear receptors (Manuscript 2, Figure3). This again indicates that Sp1 might in a yet unknown way be involved in the regulation of gene expression by ERRα.

While the role for ERRα as an important mediator of PGC-1α mediated induction of metabolic genes is well established, it is not known which biological programs are regulated by PGC-1α and its predicted transcriptional binding partners. We have a biological validation that Fos, Jun, Atf3, Gtf2i, Nfe2l2 and Zfp143 are required for the induction of a subset of PGC-1α target genes. We also have found that Fos, Jun and Atf3, which are all possible components of the Activator protein 1 (AP-1) transcription complex, together with PGC-1α directly regulate the expression of 47 PGC-1α target genes (Manuscript 1, Figure 5) (Vesely et al., 2009). These genes are involved in response to hypoxia and mTOR (mammalian target of rapamycin) signaling pathways (Manuscript 1, Figure 5). Whether

this is true in skeletal muscle needs to be shown through *in vivo* experiments. However, it needs to be considered that AP-1 was shown to be involved in many biological processes like apoptosis, differentiation or growth (Vesely et al., 2009). In fact, Jun and Fos belong to the top 5 most cited transcription factors at all (Vaquerizas et al., 2009). AP-1 can be composed of different subunits and therefore either favor or suppress a biological process depending of which subunits AP-1 is composed. AP-1 has been found to have pro-apoptotic functions, but differently composed AP-1 can regulate cell survival (Hess et al., 2004). Interestingly, AP-1 has been described as a sensor of environmental processes, which subsequent to sensing induces changes in gene transcription. In the introduction of this thesis, this feature was attributed to PGC-1α (Wagner, 2001). Moreover, AP-1 can be induced by oxidative stress, and an overexpression of PGC-1α in muscle cells in our experiments clearly represents such a situation (Reuter et al., 2010). The fact that AP-1 can be regulated by cytokines raises the question whether in our PGC-1α ChIP-Seq experiments AP-1 suppresses the expression of immune response genes which is observed following PGC-1α overexpression (Manuskript1 Figure1) (Hess et al., 2004). Therefore, considering the current knowledge about AP-1, the possibility that AP-1 and PGC-1α cooperatively regulate gene expression is legitimate and not against all expectations. However, the complex biology of AP-1 calls for a profound investigation of the two transcription regulators.

Another protein which is regulated by oxidative stress is Nfe2l2, which was also found to regulate the expression of a subset of PGC-1α target genes in our experiments (Manuscript 1, Figure 4) (Reuter et al., 2010). Nfe2l2 is the key regulator of antioxidant genes and under normal circumstances, Nfe2l2 is bound by Keap1 which targets the protein for degradation (Kensler et al., 2007; Stepkowski and Kruszewski, 2011). Following oxidative stress, Keap1 is dissociated from Nfe2l2 rendering a transcriptionally active protein, which translocates to the nucleus and binds to DNA sequences called antioxidant response elements (AREs) in the promoters of antioxidant response genes to induce their expression (Stepkowski and Kruszewski, 2011). Therefore, the Nfe2l2 mRNA does not necessarily need to be induced in oxidative stress situations. In our PGC-1α ChIP-Seq experiments, the expression of Nfe2l2 is not induced, but this does not mean that Nfe2l2 is not active in cells overexpressing PGC-1α. Unfortunately, Nfe2l2 is also known as Nrf2 and therefore can be mistaken for Nuclear respiratory factor 2 (Nrf2 also known as GABPA-GA binding protein transcription factor alpha). The confusion is even greater because GABPA is coactivated by PGC-1α and for Nfe2l2 it has been speculated that it might form a regulatory loop with PGC-1α because the PGC-1α promoter contains ARE sequences (Baldelli et al., 2013). Because Nfe2l2 regulates antioxidant response and PGC-1α has been found to help the cell to deal with reactive oxygen species, it seems likely that PGC-1α indeed coactivates Nfe2l2 (St-Pierre et al., 2006).

Interestingly, AP-1 has been reported to control the response to oxidative stress through Nfe2l2 thereby connecting the two pathways to regulate oxidative stress response (Vaz et al., 2012). Indeed both Nfe2l2 and AP-1 regulate the expression of sulfiredoxin, an important antioxidant enzyme

(Soriano et al., 2009). Sulfiredoxin is required in oxidative stress when other antioxidant enzymes (peroxiredoxins) become hyperoxidated and inactive. Sulfiredoxin reverses this hyperoxidation and thus reactivates the peroxiredoxins (Soriano et al., 2009). It is peculiar that even though the expression of sulfiredoxin 1 (Srxn1) is induced by PGC-1α overexpression in our ChIP-Seq experiments, neither the knockdown of Nfe2l2 nor of the AP-1 components (Fos, Jun and Atf3) reduced the induction of Srxn1 by PGC-1α (Manuscript 1, Figure 4). The significance of the possible coactivation of Zfp143 and Gtf2i still needs to be further investigated.

Because the knockdown of Nfyc did not reduce the induction of the predicted PGC-1α target genes, one could argue that Nfyc is not coactivated by PGC-1α and that this prediction was wrong. However, this is not necessarily true. The Nfyc gene codes for the NF-YC subunit of the trimeric transcriptional complex NF-Y, which consists of the three subunits NF-YA, NF-YB and NF-YC (Dolfini et al., 2012). For the biological validation of our predictions in ChIP-Seq experiments, we have chosen to knock down Nfyc because the expression of this gene is strongly induced by PGC-1α. If the intracellular concentration of Nfyc is much higher than the concentration of Nfya or Nfyb, then the knockdown of Nfyc does not necessarily have to reduce the transcription of the entire NF-Y complex. A recent study investigated the binding of NF-Y to DNA in different cell lines and surprisingly found that around half of the NF-Y binding events were in DNA repeat regions (Fleming et al., 2013). Unlike common transcription factors, NF-Y was apparently able to bind to inactive or polycomb-repressed chromatin (Fleming et al., 2013). Because around half of PGC-1α peaks in our experiments is located in intergenic regions, it is possible that NF-Y recruits PGC-1α to these sites (Manuscript 1, Figure 1). To test this hypothesis, we would need to perform additional experiments. This could possibly be tested by combining ChIP with knockdown of Nfyc and followed by real-time PCR amplification of selected intergenic regions. Nevertheless, even if we assume that Nfyc was wrongly predicted as a mediator of PGC-1α gene expression regulation, it would be only one false positive prediction out of seven. Therefore, we can rely on our predictions and assume that for the most part the predicted transcriptional factors will be revealed as transcriptional partners for PGC-1α in future experiments.

5.3 Outlook

We have extensively studied how PGC-1α controls gene expression on a genome-wide scale and identified a set of transcription factors which are its potential binding partners and together with PGC-1α comprise a complex transcriptional network. However, the experiments were performed in cultured muscle cells, which have a low basal PGC-1α expression level. To have robust PGC-1α levels, we had to introduce tagged PGC-1α artificially by using adenoviral vectors. This was necessary because successful ChIP-Seq studies require well detectable levels of the protein of interest, many cells as starting material and a ChIP-grade antibody with as little as possible unspecific binding. If these requirements are not met, it gets even harder to distinguish the signal from noise or real binding events from unspecific binding. While the ChIP-Seq approach with cultured cells certainly has its advantages, it also clearly has some drawbacks. Biological processes like fiber type switch, angiogenesis, the development of neuromuscular junctions or generally adaptations to exercise, which are controlled by PGC-1α in a living muscle, cannot be studied in culture (Handschin, 2010). *In vivo* studies could not be performed because of the lack of good, ChIP-grade PGC-1α antibodies. Such studies would allow investigating the activity of PGC-1α before, during and after exercise, in different models of dystrophies, atrophies and other muscle disorders. Of course, in vivo studies would also facilitate it to study the role of skeletal muscle PGC-1α in systemic disorders like type II diabetes where the muscle, liver, pancreas, fat and other tissues interact. In addition, by precipitating endogenous PGC-1α it would be possible to study the protein at physiological levels and to include the different splice variant of PGC-1α in the study. Therefore, one of the next steps should be to perform ChIP-Seq studies of PGC-1α in a living muscle. Because obtaining a very good antibody is not a simple task, it should be considered to tag endogenous PGC-1α. For this purpose, one could decide to use a knock-in method like for example the endogenous tagging method described by Zhang and colleagues, which uses adeno-associated viruses to efficiently introduce the recombinant DNA into cells (Zhang et al., 2008).

Now that the PGC-1α ChIP-Seq is established, different posttranslational modifications of the PGC-1α protein might be introduced. This would allow detecting changes in PGC-1α recruitment to chromatin before and after the posttranslational modification was introduced. By analyzing the transcription factor motifs in the PGC-1α peaks it could be discovered which set of transcription factors is coactivated by PGC-1α after each posttranslational modification. If a gene ontology analysis is applied to genes adjacent to peaks, it would be possible to detect which biological pathways are regulated by PGC-1α following each posttranslational modification. In addition, the genome-wide occupation studies could be performed when PGC-1α is in presence of the inhibitory proteins $p160^{MBP}$ and RIP140. Thereby it would be possible to detect to which extent the function of PGC-1α as a coactivator is attenuated. Does PGC-1α become completely inactive when the inhibitory proteins are expressed or does it still coactivate a subset of its transcriptional partners?

With the PGC-1α and ERRα ChIP-Seq experiments we have generated large amounts of data. Although we have run different tools to analyze the data, the analysis is not complete. Not all

information has been extracted from this data at is very likely the future approaches and new tools will extract more information from this data and new knowledge about PGC-1α will be won. In future, the genomic annotations and gene ontology databases will be further updated, thereby allowing identification of new biological pathways which are not detectable now. Conversely, researchers could try to work in the opposite direction and create their own gene ontology groups. In other words, to search PGC-1α regulated genes and select these genes which carry out some known PGC-1α biological functions. For example, to extract PGC-1α regulated genes which are involved in ROS defense and search the adjacent peaks to identify which transcription might be involved in the PGC-1α-mediated regulation of ROS defense. Do these peaks harbor antioxidant response elements and if so, is the expression of the adjacent genes regulated by Nf2l2 or AP-1? PGC-1α has already previously been discussed as an inducer of hypoxia genes like VEGF in a pathway which did not involve the hypoxia inducible factor (HIF) (Arany et al., 2008). Does this regulation mainly depend on the transcriptional activity of the PGC-1α/ERRα tandem or are possibly other transcription factors involved (Shoag and Arany, 2010)?

Of course, it will be even more important to test the predictions that are made in this thesis for their biological significance. For example, do PGC-1α and AP-1 regulate response to hypoxia and mTOR signaling pathway, like it is predicted from our cell culture experiments (Manuscript 1, Figure 5)?

Similarly, it would be interesting to know how PGC-1α suppresses gene expression. It is evident, that this suppression is almost exclusively indirect, and therefore does not require that PGC-1α is physically present at the site of transcription (Manuscript 1, Figure 1). The suppressed genes include such genes which are involved in immune response and apoptosis (Manuscript 1, Figure 1). Interestingly, both Nfe2l2 and AP-1 have been shown to regulate cell survival following environmental stress situations (Hess et al., 2004; Kensler et al., 2007; Stepkowski and Kruszewski, 2011). Are these transcription factors responsible for the PGC-1α-mediated suppression of genes involved in apoptosis? Alternatively, does the small heterodimer partner (SHP) suppress the expression of these genes? SHP is a nuclear receptor which lacks a DNA binding domain and is known to directly bind to other nuclear receptors and inhibit their activity (Zhang et al., 2011). Interestingly, Nr0b2, the gene which codes for SHP, is barely expressed in cultured skeletal muscle cells treated with the control adenovirus, and becomes the most strongly induced gene when the cells are treated with the PGC-1α adenovirus. Thus it is possible that SHP is responsible for the suppression of gene expression by PGC-1α. In addition, the role of SHP might be to serve as an inhibitor of PGC-1α activity, thereby forming a negative feedback loop.

Nfe2l2 has recently been found to be required for mitochondrial biogenesis and suppression of pro-inflammatory genes in the lungs of mice, which are suffering from pneumonia (Athale et al., 2012). In the alveolar region of wild type mice the expression of mitochondrial biogenesis genes including PGC-1α was strongly induced by pneumonia. Interestingly, this induction was absent in Nfe2l2 knock-out mice (Athale et al., 2012). Although these experiments have been performed in lung tissue, it still

shows two important functions of Nfe2l2. First, it is able to suppress pro-inflammatory genes and might also be mediate the suppression of immune response genes by PGC-1α. Second, in lung tissue Nfe2l2 seems to be upstream of PGC-1α and possibly regulate its expression. This could also be true in our experiments in skeletal muscle cells. Nfe2l2 is released from Keap1 in environmental stress conditions and therefore might be available even before the transcription of PGC-1α is up-regulated. Possibly, it could even activate the PGC-1α protein or induce its expression. In this case Nfe2l2 would not only be coactivated by PGC-1α but might also regulate the abundance of active PGC-1α in the cell.

It is hard to explain why the half of all PGC-1α peaks is located in intergenic regions. One possible explanation is that is associated to enhancer regions, but it cannot be excluded that PGC-1α also has functions, which are beyond direct regulation of gene transcription. One possible way to investigate this would be to compare PGC-1α peaks to genome-wide histone modification studies or RNA polymerase II occupation. This might provide an explanation why PGC-1α occupies these distant locations.

Last, once the in vivo ChIP-Seq is established, it would be interesting to investigate the regulation of transcription by PGC-1α on a genome-wide scale in other tissues like liver, brain, heart or kidney. We would thereby discover which functions of PGC-1α are ubiquitous and which are tissue-specific. Additionally, the roles of the two remaining members of the PGC-1 family, PGC-1β and PRC, could be studied by ChIP-Seq.

In summary, this work has created large amounts of data and several predictions have been made. Therefore, these results can serve as a starting point for several projects in the future and will hopefully lead to the discovery not only of new facettes of regulation of transcription by PGC-1α but maybe even completely novel functions of PGC-1α.

5.4 References

Arany, Z., Foo, S.Y., Ma, Y., Ruas, J.L., Bommi-Reddy, A., Girnun, G., Cooper, M., Laznik, D., Chinsomboon, J., Rangwala, S.M., *et al.* (2008). HIF-independent regulation of VEGF and angiogenesis by the transcriptional coactivator PGC-1alpha. Nature *451*, 1008-1012.

Athale, J., Ulrich, A., Chou Macgarvey, N., Bartz, R.R., Welty-Wolf, K.E., Suliman, H.B., and Piantadosi, C.A. (2012). Nrf2 promotes alveolar mitochondrial biogenesis and resolution of lung injury in Staphylococcus aureus pneumonia in mice. Free Radic Biol Med *53*, 1584-1594.

Baldelli, S., Aquilano, K., and Ciriolo, M.R. (2013). Punctum on two different transcription factors regulated by PGC-1alpha: nuclear factor erythroid-derived 2-like 2 and nuclear respiratory factor 2. Biochim Biophys Acta *1830*, 4137-4146.

Bender, A.T., and Beavo, J.A. (2006). Cyclic nucleotide phosphodiesterases: molecular regulation to clinical use. Pharmacol Rev *58*, 488-520.

Charos, A.E., Reed, B.D., Raha, D., Szekely, A.M., Weissman, S.M., and Snyder, M. (2012). A highly integrated and complex PPARGC1A transcription factor binding network in HepG2 cells. Genome Res *22*, 1668-1679.

Dolfini, D., Gatta, R., and Mantovani, R. (2012). NF-Y and the transcriptional activation of CCAAT promoters. Crit Rev Biochem Mol Biol *47*, 29-49.

Eisele, P.S., Salatino, S., Sobek, J., Hottiger, M.O., and Handschin, C. (2013). The peroxisome proliferator-activated receptor gamma coactivator 1alpha/beta (PGC-1) coactivators repress the transcriptional activity of NF-kappaB in skeletal muscle cells. J Biol Chem *288*, 2246-2260.

Fleming, J.D., Pavesi, G., Benatti, P., Imbriano, C., Mantovani, R., and Struhl, K. (2013). NF-Y coassociates with FOS at promoters, enhancers, repetitive elements, and inactive chromatin regions, and is stereo-positioned with growth-controlling transcription factors. Genome Res *23*, 1195-1209.

Francis, S.H., Blount, M.A., and Corbin, J.D. (2011). Mammalian cyclic nucleotide phosphodiesterases: molecular mechanisms and physiological functions. Physiol Rev *91*, 651-690.

Furey, T.S. (2012). ChIP-seq and beyond: new and improved methodologies to detect and characterize protein-DNA interactions. Nat Rev Genet *13*, 840-852.

Handschin, C. (2010). Regulation of skeletal muscle cell plasticity by the peroxisome proliferator-activated receptor gamma coactivator 1alpha. J Recept Signal Transduct Res *30*, 376-384.

Handschin, C., and Spiegelman, B.M. (2006). Peroxisome proliferator-activated receptor gamma coactivator 1 coactivators, energy homeostasis, and metabolism. Endocr Rev *27*, 728-735.

Handschin, C., and Spiegelman, B.M. (2008). The role of exercise and PGC1alpha in inflammation and chronic disease. Nature *454*, 463-469.

Hess, J., Angel, P., and Schorpp-Kistner, M. (2004). AP-1 subunits: quarrel and harmony among siblings. J Cell Sci *117*, 5965-5973.

Kensler, T.W., Wakabayashi, N., and Biswal, S. (2007). Cell survival responses to environmental stresses via the Keap1-Nrf2-ARE pathway. Annu Rev Pharmacol Toxicol *47*, 89-116.

Lodish, H., Berk, A., Kaiser, C.A., Krieger, M., Bretscher, A., Ploegh, H., Amon, A., and Scott, M.P. (2012). Molecular Cell Biology, 7th edition edn (W.H. Freeman).

Mangelsdorf, D.J., Thummel, C., Beato, M., Herrlich, P., Schutz, G., Umesono, K., Blumberg, B., Kastner, P., Mark, M., Chambon, P., *et al.* (1995). The nuclear receptor superfamily: the second decade. Cell *83*, 835-839.

Michael, L.F., Wu, Z., Cheatham, R.B., Puigserver, P., Adelmant, G., Lehman, J.J., Kelly, D.P., and Spiegelman, B.M. (2001). Restoration of insulin-sensitive glucose transporter (GLUT4) gene expression in muscle cells by the transcriptional coactivator PGC-1. Proc Natl Acad Sci U S A *98*, 3820-3825.

Mootha, V.K., Handschin, C., Arlow, D., Xie, X., St Pierre, J., Sihag, S., Yang, W., Altshuler, D., Puigserver, P., Patterson, N., *et al.* (2004). Erralpha and Gabpa/b specify PGC-1alpha-dependent oxidative phosphorylation gene expression that is altered in diabetic muscle. Proc Natl Acad Sci U S A *101*, 6570-6575.

Omori, K., and Kotera, J. (2007). Overview of PDEs and their regulation. Circ Res *100*, 309-327.

Park, P.J. (2009). ChIP-seq: advantages and challenges of a maturing technology. Nat Rev Genet *10*, 669-680.

Puigserver, P., Rhee, J., Donovan, J., Walkey, C.J., Yoon, J.C., Oriente, F., Kitamura, Y., Altomonte, J., Dong, H., Accili, D.*, et al.* (2003). Insulin-regulated hepatic gluconeogenesis through FOXO1-PGC-1alpha interaction. Nature *423*, 550-555.

Puigserver, P., Wu, Z., Park, C.W., Graves, R., Wright, M., and Spiegelman, B.M. (1998). A cold-inducible coactivator of nuclear receptors linked to adaptive thermogenesis. Cell *92*, 829-839.

Reuter, S., Gupta, S.C., Chaturvedi, M.M., and Aggarwal, B.B. (2010). Oxidative stress, inflammation, and cancer: how are they linked? Free Radic Biol Med *49*, 1603-1616.

Schreiber, S.N., Emter, R., Hock, M.B., Knutti, D., Cardenas, J., Podvinec, M., Oakeley, E.J., and Kralli, A. (2004). The estrogen-related receptor alpha (ERRalpha) functions in PPARgamma coactivator 1alpha (PGC-1alpha)-induced mitochondrial biogenesis. Proc Natl Acad Sci U S A *101*, 6472-6477.

Shaulian, E. (2010). AP-1--The Jun proteins: Oncogenes or tumor suppressors in disguise? Cell Signal *22*, 894-899.

Shaulian, E., and Karin, M. (2002). AP-1 as a regulator of cell life and death. Nat Cell Biol *4*, E131-136.

Shoag, J., and Arany, Z. (2010). Regulation of hypoxia-inducible genes by PGC-1 alpha. Arterioscler Thromb Vasc Biol *30*, 662-666.

Soriano, F.X., Baxter, P., Murray, L.M., Sporn, M.B., Gillingwater, T.H., and Hardingham, G.E. (2009). Transcriptional regulation of the AP-1 and Nrf2 target gene sulfiredoxin. Mol Cells *27*, 279-282.

St-Pierre, J., Drori, S., Uldry, M., Silvaggi, J.M., Rhee, J., Jager, S., Handschin, C., Zheng, K., Lin, J., Yang, W.*, et al.* (2006). Suppression of reactive oxygen species and neurodegeneration by the PGC-1 transcriptional coactivators. Cell *127*, 397-408.

Stepkowski, T.M., and Kruszewski, M.K. (2011). Molecular cross-talk between the NRF2/KEAP1 signaling pathway, autophagy, and apoptosis. Free Radic Biol Med *50*, 1186-1195.

Tremblay, A.M., and Giguere, V. (2007). The NR3B subgroup: an ovERRview. Nucl Recept Signal *5*, e009.

Vaquerizas, J.M., Kummerfeld, S.K., Teichmann, S.A., and Luscombe, N.M. (2009). A census of human transcription factors: function, expression and evolution. Nat Rev Genet *10*, 252-263.

Vaz, M., Machireddy, N., Irving, A., Potteti, H.R., Chevalier, K., Kalvakolanu, D., and Reddy, S.P. (2012). Oxidant-induced cell death and Nrf2-dependent antioxidative response are controlled by Fra-1/AP-1. Mol Cell Biol *32*, 1694-1709.

Vesely, P.W., Staber, P.B., Hoefler, G., and Kenner, L. (2009). Translational regulation mechanisms of AP-1 proteins. Mutat Res *682*, 7-12.

Wagner, E.F. (2001). AP-1--Introductory remarks. Oncogene *20*, 2334-2335.

Zhang, X., Guo, C., Chen, Y., Shulha, H.P., Schnetz, M.P., LaFramboise, T., Bartels, C.F., Markowitz, S., Weng, Z., Scacheri, P.C.*, et al.* (2008). Epitope tagging of endogenous proteins for genome-wide ChIP-chip studies. Nat Methods *5*, 163-165.

Zhang, Y., Hagedorn, C.H., and Wang, L. (2011). Role of nuclear receptor SHP in metabolism and cancer. Biochim Biophys Acta *1812*, 893-908.

6 ACKNOWLEDGEMENTS

Doing a PhD might be compared to running in a race, because you have to give your best and you need to have the stamina. Last meters appear to be the toughest, but it feels good, once you have finished. That's at least how I expect it to be once I have completed it. Unlike in a race, where you are on your own, during the PhD you get the support and assistance from your supervisor, colleagues and friends. This makes your life easier, helps you to deal with troubles and allows you to attain your goals. Therefore, I would like to use this opportunity to thank to these people, who helped me to finish my thesis.

First of all, I would like to thank Prof. Christoph Handschin for supervising my thesis. Without him giving me a chance to join his lab, this thesis would not have been possible. He planned with me the thesis, considered my suggestions and was always open to try new approaches. During regular mini-meetings and lab meetings, he offered intellectual and technical support. I am very grateful, that even though he supervises many people, I always could knock on his door, and he would take the time to discuss with me any issue. I also appreciate that Christoph trusts his people and that he always gave us enough freedom to schedule our own work and helped us to learn to work independently.

It is a pleasure to thank the entire Handschin lab, the current and the former members. In addition to having had productive scientific discussions, we also organized the moving of the lab, Christmas party and celebrated birthdays. Of course I am grateful to Silvia Salatino and her second supervisor Prof. Erik van Nimwegen for their great contribution in our common projects. I thank Martine Christe, who unfortunately passed away, and Markus Beer for offering a helping hand for time-consuming experiments. I was very glad I could profit from Markus' great mechanical and improvisational skills. My colleagues Petra Eisele and Silvia Salatino shared the lab 778 with me, and I would like to thank them not only for the scientific and moral support but also for the time we have spent outside the lab. It was a pleasure to go sledging with them, swimming in the Rhein and Aare or just simply for a beer. I thank Marianne Liechti and Jny Wittker for their support in general and for the nice occasional chats we had.

There are of course many nice and helpful people outside the Handschin lab and the Biozentrum. In particular I would like to thank Manuel Kohler, Ina Nissen and Christian Beisel for the sequencing of our samples and Philippe Demougin for his support with the expression arrays.

I owe my deepest gratitude to my parents, my girlfriend Branka, especially for her enormous patience, my sister Ivana and my firends outside the lab. Talking to them often made me realize that any troubles with my project actually aren't so bad.

Last but not least it is an honor for me that Prof. Markus Rüegg and Prof. Martin Spiess agreed to join my thesis committee or to chair my doctoral exam.

Basel, October 2013 Mario Barešić